



<https://theses.gla.ac.uk/>

Theses Digitisation:

<https://www.gla.ac.uk/myglasgow/research/enlighten/theses/digitisation/>

This is a digitised version of the original print thesis.

Copyright and moral rights for this work are retained by the author

A copy can be downloaded for personal non-commercial research or study,
without prior permission or charge

This work cannot be reproduced or quoted extensively from without first
obtaining permission in writing from the author

The content must not be changed in any way or sold commercially in any
format or medium without the formal permission of the author

When referring to this work, full bibliographic details including the author,
title, awarding institution and date of the thesis must be given

Enlighten: Theses

<https://theses.gla.ac.uk/>
research-enlighten@glasgow.ac.uk

The Monoaminergic
Control of
Gamma Motoneurones

By

Anil Sahal

BSc. (Honours) Physiology

**A thesis submitted to the University of Glasgow
for the degree of Doctor of Philosophy in the
Faculty of Medicine**

September 2001

**Division of Neuroscience and Biomedical
Systems**

Institute of Biomedical and Life Sciences

University of Glasgow

ProQuest Number: 10647854

All rights reserved

INFORMATION TO ALL USERS

The quality of this reproduction is dependent upon the quality of the copy submitted.

In the unlikely event that the author did not send a complete manuscript and there are missing pages, these will be noted. Also, if material had to be removed, a note will indicate the deletion.



ProQuest 10647854

Published by ProQuest LLC (2017). Copyright of the Dissertation is held by the Author.

All rights reserved.

This work is protected against unauthorized copying under Title 17, United States Code
Microform Edition © ProQuest LLC.

ProQuest LLC.
789 East Eisenhower Parkway
P.O. Box 1346
Ann Arbor, MI 48106 – 1346

GLASGOW
UNIVERSITY
LIBRARY:

12687

COPY 2

Index

Index	i
List of figures	iv
List of tables	vi
Acknowledgments	vii
Publications	x
Abstract	xi
1 Introduction	1
1.1 Structure of γ -motoneurons	3
1.2 Monoamines	10
1.3 Serotonergic and noradrenergic receptors in the spinal cord	11
1.4 Synaptic versus volume transmission	12
1.5 The effects of noradrenaline and serotonin in spinal reflex pathways	13
1.5.1 <i>Systemically applied monoamines</i>	14
1.5.2 <i>Group I afferent pathways</i>	15
1.5.3 <i>Group II afferent pathways</i>	15
1.6 The neuromodulatory effects of noradrenaline and serotonin on γ -motoneurons	16
1.6.1 <i>Noradrenaline</i>	16
1.6.2 <i>Serotonin</i>	17
1.7 Central origin of noradrenergic axons projecting to the spinal cord; locus coeruleus and its afferent connections	18
1.8 Location of locus coeruleus	18
1.9 Dopaminergic inputs to the locus coeruleus	20
1.10 Noradrenergic inputs to the locus coeruleus	20
1.11 Serotonergic inputs to the locus coeruleus	21
1.12 Adrenergic inputs into the locus coeruleus	22
1.13 Projections to the spinal cord	22
1.14 Origins of descending noradrenergic projections	28
1.15 Central origin of serotonergic axons projecting to the spinal cord; the raphe nuclei and its afferent connections	33
1.16 Nucleus raphe obscurus	34
1.17 Nucleus raphe pallidus	34
1.18 Raphe magnus	35
1.19 Raphe – spinal neurones	36

1.20	Co-localisation of other peptides with serotonergic neurones	37
1.21	The role of the raphe and the locus coeruleus in motor control	41
1.21.1	<i>The locus coeruleus</i>	41
1.21.2	<i>The raphe</i>	43
1.22	Opiates and γ -motoneurone activity	45
1.23	The link between the locus coeruleus and effects of potent opiates	46
2	Methods	50
2.1	Preparation of γ -motoneurone	50
2.2	Labelling	53
2.3	Confocal microscopy	54
2.4	Analysis	55
2.5	Counting varicosities	55
2.6	Construction of the contour diagrams	58
2.7	Construction of stick diagrams	59
2.8	Preparative surgery for experiments on the effects of fentanyl	59
2.8.1	<i>Selection and care</i>	59
2.8.2	<i>Anaesthesia</i>	59
2.8.3	<i>Perioperative temperature regulation</i>	60
2.8.4	<i>Formation of tracheostomy</i>	60
2.8.5	<i>Femoral arterial and venous cannulation</i>	60
2.8.6	<i>Laminectomy</i>	61
2.8.7	<i>Preparation of the spinal cord for recording</i>	61
2.8.8	<i>Tests of γ-activity before fentanyl administration</i>	64
2.8.9	<i>Fentanyl administration</i>	64
2.8.10	<i>Preparation of gas mixtures</i>	64
2.8.11	<i>Administration of gas mixtures</i>	65
3	Results	66
3.1	Serotonergic immunoreactive fibres	68
3.2	Dopamine β -hydroxylase immunoreactive fibres	71
3.3	Appositions	74
3.3.1	<i>Cell bodies</i>	74
3.3.2	<i>Dendrites</i>	80
3.4	Varicosities in the surround of dendrites	86
3.5	Spines, beads and thread-like processes	88
3.6	The effects of fentanyl	89

3.7	The effects of reflexes on blood pressure, ventral and dorsal root and muscle nerve activity	91
3.7.1	<i>Pinna reflex</i>	92
3.7.2	<i>Pharyngeal reflex</i>	93
3.7.3	<i>Clamping tracheal cannula</i>	94
3.8	The effects of apnoea on ventral and dorsal root and muscle nerve activity	94
4	Discussion	96
4.1	Appositions and synaptic contacts	96
4.2	Comparison of density and distribution of serotonergic and noradrenergic varicosities	97
4.2.1	<i>Somata</i>	97
4.2.2	<i>Dendrites</i>	98
4.3	Comparison of distribution and density of contacts of serotonergic fibres on α - and γ -motoneurones	101
4.4	Comparison with noradrenergic contacts on α -motoneurones	102
4.5	Possible explanation for richer monoaminergic innervation of γ -motoneurones compared with premotor interneurones with inputs from group II afferents	102
4.6	Is fusimotion contributing to integrated responses?	103
4.7	Opiate-induced rigidity	104
4.8	Parallels between the sequence of events after onset of apnoea in opiate anaesthesia and the defence reaction	105
4.8.1	<i>The switch from quiescence to activity</i>	108
4.9	Possible pathways involved in excitation of γ -motoneurones in opiate-induced rigidity	109
5	References	111

List of Figures

Figure 1	Camera Lucida drawing of γ -motoneurone	5
Figure 2	Camera Lucida drawing of γ -motoneurone from serial sections	6
Figure 3	Camera Lucida drawing of α -motoneurone	6
Figure 4	Chemical structures of serotonin and noradrenaline	10
Figure 5	Typical location of locus coeruleus in the rat	19
Figure 6	Summary of DBH immunoreactivity at spinal cord levels	25
Figure 7A&B	Summary of retrogradely labelled cells following injection of DBH into different spinal cord levels	30
Figure 7C&D	Summary of retrogradely labelled cells following injection of DBH into different spinal cord levels	31
Figure 8	Schematic drawing comparing spinal projections from the ventral and medial portions of the medullary reticular formations	38
Figure 9	Schematic diagrams showing mechanism of arousal by orexin/hypocretin	42
Figure 10	Positive feedback circuit diagram between group II afferents and γ -motoneurones	49
Figure 11	Illustration of identification and labelling of γ -motoneurones	52
Figure 12	Diagrammatic representation of α - and γ -motoneurones innervation of the left longissimus caudae	62
Figure 13	Example of responses from γ -motoneurone 1	67
Figure 14	Serotonergic axons in the vicinity of γ -motoneurone 1	69
Figure 15	Serotonergic appositions on γ -motoneurone 1	70
Figure 16	Noradrenergic axons in the vicinity of γ -motoneurone 1	72
Figure 17	Noradrenergic appositions on γ -motoneurone 1	73
Figure 18	Distribution of serotonergic and DBH immunoreactive varicosities in apposition to soma and proximal dendrites of γ -motoneurone 1 and 2	75
Figure 19	Projected confocal images of all eight γ -motoneurones	78
Figure 20	Examples of appositions of serotonergic and noradrenergic varicosities on γ -motoneurone 1	82
Figure 21	Comparison of the density of appositions of serotonergic and DBH immunoreactive fibres with soma and dendrites at different distances from the somata	84
Figure 22	Montage of five pseudocolour projected confocal images of γ -motoneurone	85

Figure 23	Distribution of serotonergic and noradrenergic varicosities in a 5 μ m shell around soma and proximal dendrites of γ -motoneurons 1 and 2	86
Figure 24	Comparison of densities of serotonergic and noradrenergic immunoreactive varicosities in the immediate surround of dendrites and then in apposition with distance from soma	88
Figure 25	The effects of fentanyl on end tidal CO ₂ , blood pressure, electromyographic and neural activity in the ventral root, dorsal root and muscle nerve	89
Figure 26	Traces taken from a typical fentanyl experiment	91
Figure 27	Apnoea appears to be necessary for the γ -motoneurone surge	94
Figure 28	Suggested mechanism for the initial phase of the opiate response after the onset of apnoea	109

List of Tables

Table 1	Comparison of morphology of α - and γ -motoneurones	9
Table 2	Summary of the locations of all the raphe nuclei with respect to their classification by Dahlström and Fuxe	39
Table 3	Raphe nuclei in the medulla oblongata; projections to the spinal cord	40
Table 4	Comparison of densities of serotonergic and noradrenergic appositions on somata and dendrites of eight γ -motoneurones	77
Table 5	Comparison of distribution of contacts between noradrenergic fibres and γ -, α - and premotor group II interneurones	100

Acknowledgements

I am deeply indebted to my supervisor, Dr. M.H. Gladden. My years of research under her care have been a pleasure from beginning to end. Her dedication, clear insight and hard work have been an inspiration to me. She has given me so much time in the preparation of this thesis, far beyond the call of duty, for which I am grateful. I will miss our many chats about science, life and weight loss and I shall remember these times under her care as fruitful and satisfying years and, of course, with great fondness.

I am grateful to Dr J. D. Morrison on several counts. His sense of justice and fair play allowed me to commence this course of research despite the various obstacles placed in my way. His advice was always true and honest and his office door was always open for a cup of tea and a chat. Every department in every University needs a 'Dr Morrison' to make those clutching the purse strings or those with desire for change for changes sake, think carefully before they act! Thanks for everything, Dr Morrison.

Thanks to Professor Rosenberg who also took it upon himself to help overcome my 'obstacles' when starting this Ph.D. I always felt secure knowing he was standing by my side. When Professor Rosenberg and Dr Morrison got together, they were a force to be reckoned with! Thank you Professor Rosenberg.

Special thanks to Professor Elzbieta Jankowska in allowing me to work with her and witness her at work! Her single minded and determined approach to science is a true inspiration and if I could aspire to a fraction of her great abilities I'd be a happy person. May your work continue to be fruitful for many years to come!

Thanks go to Dr D. J. Maxwell. His skills with a confocal microscope, ability to explain its workings to me and draw conclusions from its images were a marvel. I

particularly enjoyed working on the paper with Dr Maxwell as his numerous digressions were always informative and gave me great insight to other areas of science.

Much of this work could not have been attempted without the technical assistance of Robert Kerr and David Russell. No amount of tissue processing was beyond them, their knowledge was 'text book' and they always performed it with a smile. Thanks chaps, I couldn't have done it without you.

Special thanks must go to my wife, Joanne. Throughout these years she has been a pillar of strength, even when times were not so good. Her sense of humour and willingness to listen to my ideas was a great tonic after a hard day. On a practical level, Jo, put her proof reading skills to the test on the text of this thesis and I probably wouldn't have got it finished on time if it weren't for her dedication, often into the wee small hours of the morning. Thanks Jo and all my love.

Thanks go to my fellow PhDers, Sarah Wheeler and Claire Tochel. Sarah was always a willing listener and often gave her advice (usually too much advice) but it made the visits to her dark and dingy lab all the more fun. Her scientific abilities never ceased to amaze me and I hope that a future employer will appreciate her skills. After Sarah 'flew the nest' of Glasgow University, Claire was always round the corner and willing to chat about anything and everything. She kept me sane and her tales of drunkenness always kept me amused. I shall never forgive her for finishing her Ph.D. first, though. To see her office empty when I visit always leaves me a little sad. I miss you both, my dear friends and the times we shared.

My thanks must extend to Kathryn Foye, Graeme Salmond and their son Luke who put me up in their lovely home while I was finishing off this thesis. A 5-day visit became a 14-day stay and some more. And yet they were always cheery, accommodating and provided a stable stress free environment to chill out in after a hard day in front of a PC. Thanks Kathryn, 'Ga' and Luke.

A huge debt of gratitude goes out to my beloved parents, Brij Bhooshan and Swarn Prabha Sahal. They've supported me in everything I've ever done, good or bad. Indeed, the investigations into fentanyl-induced muscle rigidity was inspired by a conversation with my Father who pointed this phenomenon out to me and witnessed it during his career as an anaesthetist. Thank you for believing in me, giving me your unconditional love and feeding me (Mum!). I sincerely dedicate this thesis to them both.

A special thanks to a special man - Jack Sandiford. Joanne's Grandpa and friend to me over the short time I knew him. He was always enthusiastic about my Ph.D. and various career moves-never once asking if I'd get a 'proper job' like so many others. It's rare to enjoy the company of somebody 50+ years ones senior, but I genuinely craved his company. Rest in peace, Jack - gone but never forgotten.

Publications

- Gladden, M.H., Maxwell, D.J., Sahal, A. & Jankowska, E. (2000). Coupling between serotonergic and noradrenergic neurones and gamma motoneurones in the cat. *Journal of Physiology*, **527.2** 213-223.
- Gladden, M.H. & Sahal, A. (2000). Gamma motoneurones, asphyxia and opiates. *J. Physiol.* **531.P**, 144P.
- Gladden, M.H., & Sahal, A. (2000). Gamma motoneurones, asphyxia and opiates. *Journal of Physiology*, **527.P**,136P.
- Gladden, M.H., Sahal, A.& Matsuzaki,H. (2000). Responses of γ -motoneurones to apnoea. *J. Physiol.* **531.P**, 144P.
- Macdougall, N., Dalrymple, D., Carrick, L., Oag, J.S., Sahal, A., & Gladden, M.H. (1999). The functional organisation of the caudal segments of the rat spinal cord. *Journal of Physiology*, **521.P**, 48P.
- Sahal, A., Maxwell, D.J., Jankowska, E. & Gladden, M.H. (1998) Relationship between noradrenaline and serotonin-immunoreactive axons and hindlimb γ -motoneurones. *Journal of Physiology*, **509.P**, 172P.

Abstract

1. The monoamines are known to modulate transmission from group II muscle afferents to γ -motoneurons in the cat. Noradrenaline has a suppressive effect whereas serotonin facilitates this transmission. The aim of this study was to determine whether γ -motoneurons are innervated by noradrenergic and serotonergic neurons.
2. Eight γ -motoneurons were investigated. These had been identified by their conduction velocity and labelled by ionophoretic microinjection of rhodamine-dextran intracellularly. 50 μ m thick sagittal sections of spinal cord containing these γ -motoneurons were cut and these were exposed to antibodies against serotonin and dopamine β -hydroxylase (DBH), the final enzyme involved in the conversion of dopamine into noradrenaline.
3. A three-colour confocal laser scanning microscope was used to examine the 50 μ m thick sections. Optical sections were gathered from the areas where the γ -motoneurons were identified. These optical sections were analysed to establish any appositions between serotonin- and DBH- immunoreactive fibres.
4. Serotonergic and noradrenergic varicosities formed appositions with the somata and dendrites of all the γ -motoneurons. Monoaminergic appositions on dendrites greatly outnumbered those on the somata. The mean densities for serotonin were 1.12 ± 0.11 appositions per 100 μ m² on the somata and 0.91 ± 0.07 per 100 μ m² for dendrites. These data were similar to those reported for α -motoneurons. The density of DBH appositions was consistently lower than for serotonin, with corresponding means 53% and 62% of those for serotonin on the somata and dendrites respectively.
5. For the two best labelled γ -motoneurons, the number of appositions on the dendrites was compared to the number of varicosities in a 5 μ m wide shell *around*

the dendrites. This comparison showed that the number of noradrenergic and serotonergic appositions was more than ten times greater than would be expected by chance alone. Thus it was concluded that the γ -motoneurons were innervated by serotonergic and noradrenergic axons.

6. High doses of potent opiates such as fentanyl are known to be responsible for muscular rigidity. This is particularly dangerous since fentanyl is routinely used as an anaesthetic agent and the rigidity often occurs in the crucial stage just prior to intubation and artificial ventilation. These procedures are much more difficult when muscle rigidity is present.
7. It has been shown that rigidity can be induced in anaesthetised rats by injecting opiates into the locus coeruleus, which is the main source of noradrenaline in the spinal cord. Opiates suppress noradrenergic release. Since noradrenaline has facilitatory effects on α -motoneurons, and γ -motoneurons should be disinhibited, it was argued that γ -motoneurons may be involved in the mechanism for opiate induced rigidity.
8. It was found that systemic injection of fentanyl into urethane anaesthetised rats produced a surge in the activity of γ -motoneurons supplying a caudal muscle. This surge preceded any EMG activity, thus suggesting that the excitation of the α -motoneurons was secondary to the excitation of the muscle spindles by the γ -motoneurons.
9. The depressive effect of fentanyl on the respiratory rhythm generator caused apnoea. The surge in the activity of γ -motoneurons occurred with a latency of about 50 seconds after the onset of apnoea caused by the administration of fentanyl or after stopping the ventilator.
10. It was postulated that the delay before the onset of the γ -activity was due to the accumulation of CO₂ and/or to progressive hypoxia. It was found that the surge in γ -motoneurone activity could not be induced by the administration of various gas mixtures (hypoxic, hypercapnoeic and hypoxic/hypercapnoeic) to the rat in the

presence of fentanyl. Also, if there was some residual rhythmic respiratory effort, the γ -surge did not occur. This suggested that the tonic activity of afferents normally activated rhythmically during respiration was responsible for the switch to rigidity. However, cutting the vagus bilaterally to abolish the input from lung stretch afferents had no effect on this phenomenon. It is therefore suggested that tonic activity of afferents from receptors in the chest wall and abdomen are important in initiating opiate induced rigidity. A mechanism for this phenomenon involving the locus coeruleus, the raphe nuclei and the periaqueductal grey matter in the brainstem is proposed.

1 Introduction

The output of γ -motoneurons can be modulated by the monoamines serotonin and noradrenaline, and by their precursors and agonists. Additionally, various types of interneurons are now known to respond to locally applied noradrenaline and serotonin (Jankowska *et al.*, 2000). Among these are intermediate zone interneurons that are premotor to γ -motoneurons. From this it can be deduced that the monoamines may not necessarily be acting *directly* on γ -motoneurons, but could be acting at different points in the various excitatory and inhibitory pathways that control them. These could be descending or spinal pathways, but monoamines have even been shown to have direct effects on muscle spindles (see Ellaway & Trott, 1975, and Bennett *et al.*, 1996).

However, noradrenaline (NA) and serotonin (5-HT) do indeed have actions at the level of γ -motoneurons. Serotonin was shown to excite γ -motoneurons, as did the precursor 5-hydroxytryptophan and agonist LSD (Ahlman *et al.*, 1971; Ellaway & Trott, 1975). The effects of noradrenaline and its related compounds are more complex. Systemic L-DOPA (which is a NA precursor) had a differential effect on the background discharges of dynamic and static γ -motoneurons in flexors and extensors. L-DOPA may therefore have been acting by increasing the output from noradrenergic axons (Grillner *et al.*, 1967; Bergmans & Grillner, 1968; Grillner, 1969). On the other hand clonidine (an α_2 -adrenoceptor agonist) was observed to diminish or stop background discharges of γ -motoneurons (Bennett *et al.*, 1996).

When γ -motoneurons were excited by stimulating group II muscle afferents, their activation was depressed by the ionophoretic application of NA and tizanidine (an α_2 -adrenoreceptor agonist). However, serotonin *enhanced* the resting activity of γ -motoneurons and facilitated their activation by group II muscle afferents (Jankowska *et al.*, 1998a). Nevertheless this does not indicate any *direct* monoaminergic innervation: the

affects of serotonin and noradrenaline could have been acting pre-synaptically. In addition, monoamines can also modulate the activity of neurones when they are released as far as 20 μm away from the cell. This is referred to as volume transmission (see Bunin & Wightman 1998). In fact in the lamprey, a primitive vertebrate, serotonergic fibres do not form synapses with motoneurones and so volume transmission must be their only mode of electrochemical modulation (see Jacobs & Azmitia 1992).

The aim of the work described in this thesis was to ascertain whether γ -motoneurones have a monoaminergic innervation. It is well known that the ventral horn of the spinal cord has a dense serotonergic and noradrenergic supply, so the problem was to prove that γ -motoneurones are *specifically innervated* by monoaminergic axons. During experiments reported by Jankowska *et al.* (1998), several γ -motoneurones were intracellularly labelled with rhodamine-dextran. The sections of spinal cord containing these γ -motoneurones were then processed to reveal the varicosities of noradrenergic and serotonergic axons in the immediate vicinity of the γ -motoneurones by immunofluorescence. These labelled sections were then viewed with a confocal microscope, which is able to accurately display very small areas of the sections with minimal interference from brightly fluorescing objects close to the areas of interest. This was useful in identifying the monoaminergic varicosities and defining their relation to the labelled cells.

Despite the high resolution, confocal microscopy alone is insufficient to confidently determine actual contacts between noradrenaline- and serotonin- containing varicosities and γ -motoneurones. This is mainly because it is impossible to be *certain* that there are no intervening cellular processes between the fluorescences of the varicosity and γ -motoneurone. Such processes *can* be readily identified by electron microscopy. However, to undertake the present kind of study with electron microscopy would be unrealistic since it would be prohibitively time-consuming. Detailed maps were constructed with confocal microscopy showing instances of close *apposition* of monoaminergic varicosities and γ -motoneurones. When the density of appositions was compared with the density of

varicosities in the immediate surround of the cells it could be shown that the expected density of the appositions was much higher than expected by chance.

The role of γ -motoneurons in rigidities is all but neglected. Lui *et al.*, (1989), reported that microinjection of opiates into the locus coeruleus produced rigidity in rats. This is an animal model for a serious anaesthetic problem: during induction of anaesthesia with potent opiates, severe rigidity can develop. The locus coeruleus is the main source of the noradrenergic innervation of the spinal cord. Since it was known that serotonin and noradrenaline had opposite effects on γ -motoneurons but both had facilitatory effects on α -motoneurons, it was postulated that γ -motoneurons would be disinhibited by the suppression of the release of noradrenaline by opiates. As will be shown, administration of strong opiates to anaesthetised rats did, indeed, elicit a surge in γ -motoneurone activity, which preceded any changes in the electromyograph.

1.1 The Structure of γ -motoneurons

γ -motoneurons, of which there are 'static' and 'dynamic' varieties, innervate the intrafusal fibres of the muscle spindle. Their function is to alter the mechanical properties of the intrafusal fibres and thus increase or decrease the sensitivity of the spindle to muscle stretch. γ -motoneurone stimulation will cause the intrafusal fibres to contract (become 'stiffer') which allows even minute changes in muscle length to be detectable by the central nervous system (CNS). Conversely, a decrease in γ -motoneurone stimulation causes a commensurate relaxation of the intrafusal fibre making them more elastic and so less sensitive to changes in muscle length.

Several studies have elucidated the structure of γ -motoneurons and compared them with α -motoneurons, since α -motoneurons have been studied much more extensively. Westbury (1982) used the horseradish peroxidase (HRP) method to intracellularly label seven γ -motoneurons in the cat lumbosacral spinal cord. The γ -motoneurons were identified by the slow conduction velocity of their axons.

Westbury noted that although γ -motoneurone cell body diameters were much smaller than those of α -motoneurones, their dendritic trees covered a similar area to the dendritic trees of α -motoneurones (compare figure 1, 2 and 3). However, the dendritic trees were considerably less complex and exhibited less branching. γ -motoneurones had fewer main dendrites and these branched much less often than those of the α -motoneurones. The branching of the primary dendrites was also observed closer to the cell body, and the γ -motoneurones had many fewer peripheral branches. From this, Westbury inferred that there were thus fewer possibilities for synaptic input to the γ -motoneurone dendrites compared with the α -motoneurone. The surface areas of the somata were also considerably smaller. Westbury's estimate of the γ -motoneurone surface area was on average only one quarter that of the α -motoneurone. The smallest γ -motoneurone he analysed had about one tenth of the surface area of his labelled α -motoneurones and so, if synapses cover the whole of the neurone and they occupy similar areas of contact, then γ -motoneurones receive many fewer synaptic contacts than α -motoneurones. Westbury suggested that this could be offset to some degree by the greater sensitivity of γ -motoneurones to injected current (Westbury 1982). An additional consideration was that, whereas the dendritic trees of α -motoneurones were well distributed over a considerable rostro-caudal length of the spinal cord, the γ -motoneurones had dendritic trees that were much more restricted to a transverse 'slice' of spinal cord. In the transverse plane α - and γ -motoneurones were similar in dendritic distribution.

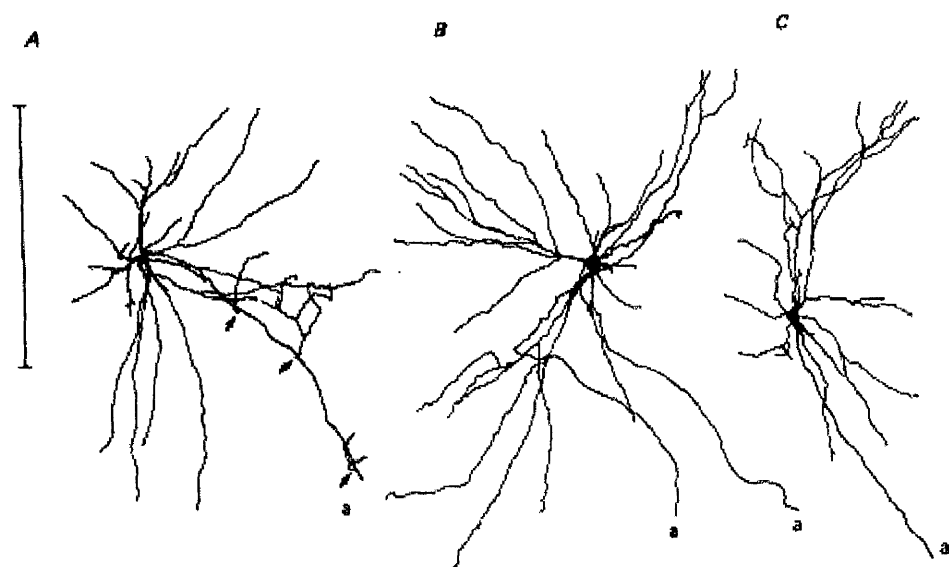


Figure 1. Camera Lucida drawings of γ -motoneurons by Westbury (1982). The arrows indicate recurrent collaterals and 'a' indicates the axon. (scale bar = 1mm)

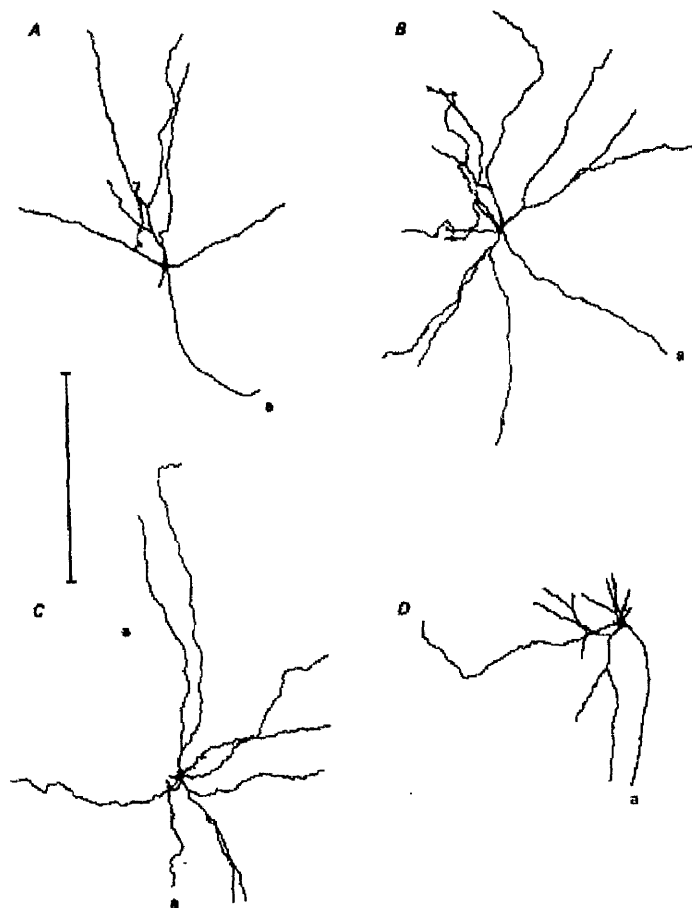


Figure 2. Camera Lucida drawings of γ -motoneurons, reconstructed from serial sections (Westbury 1982). These drawings were displayed as if projected onto the transverse plane of the spinal cord. (scale bar = 1mm)

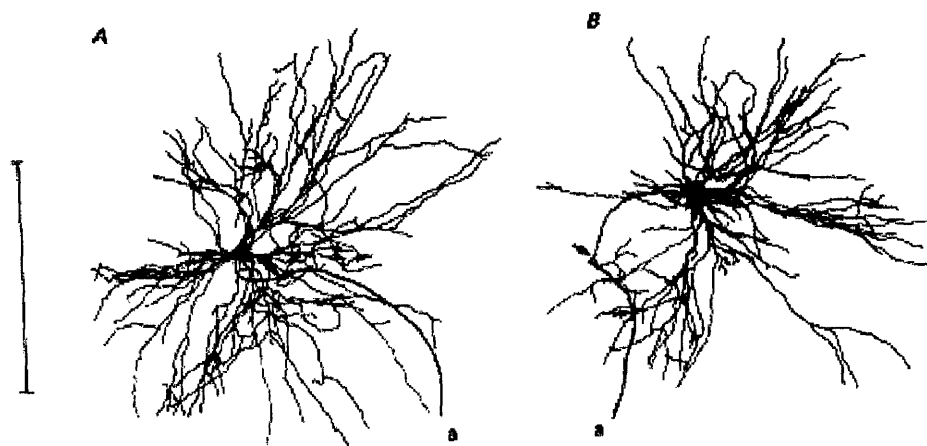


Figure 3. Camera Lucida drawings of two α -motoneurons by Westbury (1982). "a" indicates the axon; arrows indicate the origin of axon collaterals. Notice the clear morphological differences between the α -motoneurons and the γ -motoneurons (see table 1). (scale bar = 1mm).

Ulfake and Cullheim (1981) carried out a quantitative light microscopic study of the dendrites of cat spinal γ -motoneurons after intracellular HRP injection. They found that the cell bodies of the γ -motoneurons were all located within lamina IX of Rexed. They reported that the somata and first order dendrites showed 'smooth contours' and the first order dendrites radiated from the soma in various directions. They described the dendrites as long and slender and usually having an oblique course in the sagittal plane. The dendrites extended in various directions up to 1.5mm from the soma. They noted that dendritic branching was sparse and even saw unbranched dendrites occasionally. They found that the number of dendritic end branches, the combined dendritic length, the membrane surface area and the volume of the entire dendrite correlated positively with the diameter of the *parent* dendrite. When compared with α -motoneurons, the γ -motoneurons had smaller values for mean soma diameter and mean diameter of the first order dendrites. They also had fewer first-order dendrites. The γ -motoneurons had fewer branching points and larger values for combined dendritic length. One similarity they found between α - and γ -motoneurons was that the relation between the diameter of the first-order dendrite and the surface area of the entire dendrite was almost identical.

Moschovakis *et al.*, (1991) made a very detailed HRP study of 60 fully reconstructed dendritic trees belonging to eight γ -motoneurons in the cat spinal cord. They compared their data with measurements from 79 reconstructed dendrites belonging to seven-documented α -motoneurons. Their results concurred with previously published data that suggested that the soma dimensions and total membrane area of the γ -motoneurons were smaller than that of the α -motoneurons. In addition, they found that although γ -motoneurone dendrites were, on average, slightly but significantly longer than those of the α -motoneurons, γ -motoneurons had smaller diameter stem dendrites, less membrane surface area and less profuse branching. The dendrites also tended to branch closer to, and terminate further from the soma, as first described by Westbury (1982). These differences were even evident when subsets of

dendrites with similar stem diameters were compared. They concluded that although some anatomical distinctions suggested that γ - and α -motoneurons were qualitatively and quantitatively different, there were no abrupt *morphometric* discontinuities between each motoneurone group.

Destombes *et al.*, (1992) also made a comparison between α - and γ -motoneurons, but in particular investigated whether they could be identified as α - or γ -motoneurons on the basis of ultrastructural features rather than by size alone. The peroneus brevis and peroneus tertius muscles of the cat were injected with HRP and motoneurons labelled by retrograde axonal transport were examined by electron microscopy. They found that in both nuclei the cell body diameter distribution was bimodal (range 28-84 μ m with a trough at 15 μ m). They sampled 25 motoneurons included intermediate (range 40-60 μ m) as well as large (presumed α) and small (presumed γ) neurons. The aim was to establish whether cells in the intermediate group could be assigned to α - or γ -motoneurone groups with confidence by identifying additional ultrastructural criteria.

All the examined motoneurons fell into two categories, on the basis of three criteria: (a) bouton types present on the membrane, (b) percentage of membrane length covered by synapses, and (c) the aspect of the nucleolus. Fourteen motoneurons with cell body diameter 55-84 μ m were contacted by all types of bouton (mainly S-type with spherical vesicles, F-type with flattened vesicles and C-type with subsynaptic cistern); the synaptic covering of the somatic membrane was over 40% and the nucleus contained a vacuolated nucleolus. These were considered to be α -motoneurons. Eleven motoneurons had only S-type and F-type boutons, a synaptic covering of fewer than 30%, a compact nucleolus and a cell body diameter of the range of 28 to 50 μ m. These were considered to be γ -motoneurons. Destombes *et al.* (1992) observed no other combination of the three criteria. Thus motoneurons, could be assigned to the α - or γ - group by these new criteria and not just according to their soma diameters (see table 1).

Table 1. Comparison of the morphology of α - and γ -motoneurones

	α-motoneurone	γ-motoneurone
Soma diameter and shape	55-84 μ m*	28-50 μ m *, Smooth contours #
Direction of Branching	Rostro-caudal and sagittal [⊗]	Sagittal [⊗]
Branching complexity	'more complex' [⊗]	-Less profuse branching [°] -Simple-less branching [⊗] -Longer than α - motoneurone [°] -Long and slender #
Dendrite Characteristics		-Terminate further from soma than α -motoneurone [°] -Branch closer to soma [°] -Smaller diameter stem dendrite. [°] -1 st order dendrites radiate in various directions #
Bouton type present	S-type, F-type, C-type *	S-type, F-type *
Percentage of membrane length covered by synapses	> 40% *	< 30% *
Aspect of nucleolus	Vacuolated *	Compact *

*Destombes et al. (1992)

[°] Moschovakis et al. (1991)

[⊗] Westbury (1982)

#Ulfake et al. (1981)

1.2 The Monoamines

The monoamines (sometimes referred to as the biogenic amines) consist of a subgroup of small molecular neurotransmitters/neuromodulators. Among the monoamines are adrenaline, dopamine and noradrenaline (known collectively as the *catecholamines*). These are all synthesised from the amino acid tyrosine. They are present in distinct cell groups in the central and peripheral nervous system. Neurones containing adrenaline, dopamine and noradrenaline are said to be adrenergic, dopaminergic and noradrenergic respectively. The other monoamines, 5-hydroxytryptamine (serotonin) and histamine, are formed from tryptophane and histidine respectively. Serotonin-containing cells are described as serotonergic. Figure 4 shows the chemical structure of serotonin and noradrenaline.

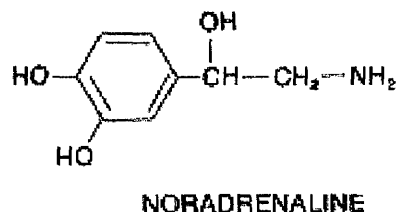
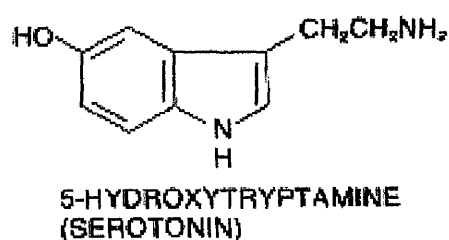


Figure 4. Chemical structures of serotonin and noradrenaline.

The synaptic effects of the monoamines are complex.

- They cause slow changes of the membrane potential via intracellular second messengers.
- There are several types of receptor for each monoamine and for serotonin.
- Their effects can sometimes be the same, and sometimes opposite.
- The receptors are differentially distributed in cell membranes.

- The effects of serotonin and noradrenaline depend on the type and location of their receptors.
- Their receptors have seven transmembrane segments and are G-protein coupled.

Four types of serotonin receptor are present in the CNS (5-HT₁, 5-HT₂, 5-HT₃ and 5-HT₄) including various subtypes including for example CNS (5-HT_{1A}, 5-HT_{2B}, 5-HT_{3C} and 5-HT_{4D}). The 5-HT₃ receptor is the exception since it has four transmembrane segments and acts on ligand-gated channels to mediate rapid excitation. The rest act by the adenylate cyclase or phospholipase C transduction system by opening or closing K⁺ channels (see Stone 1995).

Both α - and β -receptors for noradrenaline occur in the CNS. In general, α_1 -adrenoceptors are present post-synaptically and α_2 -adrenoceptors are present pre-synaptically.

1.3 Serotonergic and noradrenergic receptors in the spinal cord

Several types of serotonin receptors have been found in the CNS. For example, 5-HT_{1A} and 5-HT_{1B} are present in high density in the dorsal raphe and substantia nigra of rat brain (Pazos & Palacios 1985) and 5-HT₂ is concentrated in the cortex, hippocampus and striatum of rat brain (Pazos *et al* 1985) with differing and partly opposing effects. Thus a monoamine cannot be described as “excitatory” or “inhibitory” as their action depends upon the post-synaptic receptor on which they act.

Noradrenaline binding sites in the CNS are α_1 -adrenoceptors which are G-protein coupled (G_q), and act via the activation of phospholipases A₂, C and D. α_2 -adrenoceptors, which are also G-protein coupled receptors (G_i and G_o), act in the CNS as presynaptic inhibitors of transmitter release by: inhibition of adenylate

cyclase; increasing the conductance of K^+ ; activation of phospholipases A2 and C; closure of N-type calcium channels. α_1 -, α_2 - and β -adrenoceptors have been shown to exist in the rat spinal cord (Simmons & Jones, 1988) and cat spinal cord (Giroux *et al.*, 1999).

1.4 Synaptic versus volume transmission

The concept of synaptic transmission of information via neurotransmitters and neuromodulators is well established and researched in the literature. The exocytotic release of a neurotransmitter or modulator, which then diffuses across the synaptic cleft, binds to post synaptic receptors and activates the receptor, allows rapid communication between neurones and the orderly flow of information. However there is evidence for another mode of transmission of information between neurones. This is termed volume transmission (Fuxe & Agnati 1991). Volume transmission does not rely upon synapses and may occur over distances of micrometers rather than the nanometer distances of transmission across the synaptic cleft. Volume transmission has profound consequences for the interpretation of neural processing in the brain and spinal cord since it allows the regulation of excitability of different species of neurones from a remote source. In one form of volume transmission the axons ramify in an area, releasing transmitter *en passant*, as with sympathetic innervation in the peripheral nervous system. However, there can be leakage of transmitter from synapses and thus the transmitter could affect the same neurone at some distance from the release site, and also neighbouring neurones of the same type, providing the appropriate receptors are present. Effectively this is autocrine and paracrine transmission respectively.

*In the present investigation it was important to establish whether monoaminergic axons were affecting γ -motoneurones **en passant** or whether there were direct contacts. If direct contacts could not be found this would imply a non-specific interaction between the monoaminergic innervation and γ -motoneurones via volume transmission.*

Volume communication is only feasible if neurotransmitters/modulators reach their receptors at sufficiently high concentrations and if receptors are located extrasynaptically. In the case of serotonin it has been shown that leakage from the synaptic cleft can reach targets in physiologically effective concentrations (Bunin & Wightman 1998). Early research with carbon fibre microelectrodes showed that serotonin could be detected following release elicited by electrical stimulation (O'Connor & Kruk 1992) and advances in techniques led to real-time measurements of concentration changes (Bunin *et al.*, 1998). Two processes would limit the spread of serotonin, the rate of diffusion (which would depend on the concentration gradient and the conformation of the intercellular spaces) and the uptake into surrounding cells. In the substantia nigra, the half-life of serotonin following release (determined from voltammetrical measurements under conditions where uptake is unsaturated) was found to be 200ms (Bunin and Wightman 1998). In this time it could diffuse up to 20µm from its origin and thus potentially interact with extracellular structures.

An example of volume transmission in serotonergic pathways is in the dorsal raphe in the medulla. In this area, cells have release sites which are apparently both synaptic and non-synaptic although the latter predominates (Chazal & Ralston, 1987). Ultrastructural studies of the 5-HT₁ receptor (the predominant receptor in the dorsal raphe) have revealed extensive extrasynaptic localisation for these receptors (Charzal & Ralston 1987). This evidence supports a role for volume transmission, at least in the dorsal raphe.

There is also evidence that noradrenaline released from axons originating in the locus coeruleus can act by volume transmission (Vizi 1980). Recently it has been shown that activation of N-methyl-D-aspartate (NMDA) receptors can reduce the reuptake of monoamines in the release sites. Transporters for monoamine reuptake are confined to the release sites on monoaminergic axons rather than being present on the membranes of glia, as is the case with gamma-aminobutyric acid (GABA) for example. Activation of NMDA receptors enhances the release of nitric oxide, which

then diffuses to the monoaminergic release sites and inhibits the transporters that allow reuptake of the monoamine (see Kiss and Vizi 2001).

1.5 The effects of noradrenaline and serotonin in spinal reflex pathways

In reflex pathways monoamines are acting as neuromodulators. Neuromodulation may be defined as the alteration of synaptic or cellular properties when a substance released from one neurone affects another 'target' neurone (Kupfermann 1979). Thus, the neuromodulator does not elicit inhibitory or excitatory post synaptic potentials (IPSPs and EPSPs), but has a slower more prolonged action causing prolonged membrane potential shifts which may, for example, alter the probability of neurotransmitter release and action potential generation in a neurone.

1.5.1 Systemically applied monoamines

Serotonin and noradrenaline do not cross the blood brain barrier, thus their spinal effects were first studied by giving precursors systemically. 5-hydroxytryptophan (5-HTP) was used as a precursor for serotonin and L-DOPA as the precursor for noradrenaline. Although L-DOPA is also a precursor for dopamine, it was shown that its effects in the spinal cord were due to noradrenaline rather than to dopamine (Anden *et al.*, 1966a, Jurna and Lundberg 1966). The effects of monoamines on spinal reflexes were found to be complex. L-DOPA and 5-HTP potently depressed short latency reflexes of high threshold muscle, skin and joint afferents in flexor reflex afferent (FRA) pathways while simultaneously facilitating long-latency, long duration actions of these afferents (Anden *et al.*, 1966b Carlsson *et al.*, 1963). However there were little or no effects on monosynaptic reflexes and on Ia reciprocal inhibition. Both 5-HTP and L-DOPA induce locomotion in spinal cats. In these cats the connection between the α -motoneurons and the raphe is, of course, severed. The special importance of the raphe nuclei in locomotion was shown by Veasey *et al.*, (1995) who found that the activity of the serotonergic cells in the pallidus and obscurus nuclei was directly related to the rate of locomotion in conscious cats.

Monoamines also have an important direct effect on α -motoneurons. Plateau potentials can be initiated by trains of impulses in Ia afferents or by muscle stretch in the presence of either 5-HTP (Hultborn *et al.*, 1975, Hounsgaard *et al.*, 1984) or L-DOPA (Conway *et al.*, 1988).

Very recently a greater insight into the effects of monoamines in group I and group II reflex pathways has been provided by studies in which noradrenaline and serotonin were applied locally to interneurons in these pathways. (Jankowska *et al.*, 2000).

1.5.2 Group I afferent pathways

As stated above, it was thought that serotonin and noradrenaline had no or very weak effects on transmission in group I spinal pathways. However, recently the effects of noradrenaline and serotonin have been tested on transmission to Ia inhibitory interneurons, Ib inhibitory interneurons and interneurons mediating Ia non-reciprocal inhibition. In all cases there was facilitation (Jankowska *et al.* 2000). It was suggested that the monoamines would enhance the responses of the interneurons to fast stretches and increases in tension and so increase the efficiency of these disynaptic pathways during movements.

1.5.3 Group II afferent pathways

In contrast to group I pathways, the modulatory effects of monoamines in group II afferent pathways were found to be much more varied. Transmission from group II afferents to intermediate zone interneurons (which are premotor to α - and γ -motoneurons) was most often facilitated by serotonin and depressed by noradrenaline. This was the case even when they were co-excited by Ia afferents (Jankowska *et al.* 2000). However, transmission from these afferents to dorsal horn group II interneurons was depressed by serotonin and usually facilitated by noradrenaline. It has been suggested that this differentiation gives the monoaminergic systems a more versatile role in controlling movement (Jankowska 2001).

1.6 The neuromodulatory effects of noradrenaline and serotonin on γ -motoneurons

1.6.1 Noradrenaline

The effects of noradrenaline and the α_2 agonists, tizanidine and clonidine, upon γ -motoneurons in the cat were demonstrated by Jankowska *et al.* (1998). Two types of response from γ -motoneurone were used to test the effects of noradrenaline and the two agonists; those responses elicited by electrical stimulation of the group II afferents in the muscle nerve (and therefore synaptically) and the tonic, spontaneous background discharges of the γ -motoneurons. Noradrenaline and/or tizanidine were iontophoresed from micropipettes placed close to γ -motoneurons. In order to evoke synaptic responses attributable to the group II afferents, muscle nerve fibres were stimulated at intensities submaximal for group II afferents (3-5 times threshold) since any stronger stimuli could excite group III afferents in addition. Also double stimuli were used rather than single, to produce temporal summation in the group II afferents. The responses of the γ -motoneurone were recorded by electrodes, which were positioned close to the micropipette.

On application of noradrenaline, the excitation of γ -motoneurons by group II afferents was found to be far less effective. This effect peaked 1-2 minutes after application. A similar depression was evoked when the α_2 agonist, tizanidine was applied to the γ -motoneurone. The decrease in the number of group II muscle afferent-evoked responses was associated with considerable increases in the latencies of their responses. Clonidine, applied systemically (intravenously), had a depressive effect on both the spontaneous, background discharges of the γ -motoneurons and the group II muscle afferent evoked discharges. However, it was noted that the locally applied noradrenaline and tizanidine *strongly* depressed the group II muscle afferent evoked γ -motoneurone responses, but only weakly, and inconsistently affected their spontaneous, background activity. On the other hand, the systemically administered

clonidine had a similarly strong effect upon both types of γ -motoneurone discharge. Jankowska *et al.*, (1998) postulated that this may be due to the systemically-applied clonidine having influence over both the γ -motoneurons *and* any neurones presynaptic to them whilst noradrenaline or tizanidine, ionophoretically applied close to the γ -motoneurone could not affect neurones outside the motor nuclei. They suggested the depressive effects of the activation of γ -motoneurons by group II afferents may occur at the level of these motoneurons or of neurones presynaptic to them, whereas the depression of tonic discharges of γ -motoneurons was primarily due to modulatory actions of monoamines earlier in the neural pathways.

1.6.2 Serotonin

Jankowska *et al* (1998) repeated their experiment with serotonin instead of noradrenaline or its agonists. They found it had the opposite effect to noradrenaline and its agonists. Serotonin increased the background discharges and evoked responses by group II afferents. This facilitation was sufficiently potent to cause γ -motoneurons to respond to one-third or even one-half of the stimuli after 0.5-2.0 minutes of ionophoresis when they had failed to respond before.

1.7 The Central Origin of Noradrenergic Axons projecting to the Spinal Cord; the Locus Coeruleus its afferent connections

The locus coeruleus (LC) is located in the dorsomedial region of the pons, close to the floor of the fourth ventricle. The locus coeruleus is the main source of noradrenergic axons for the entire brain and spinal cord in contrast to the multiple sources of serotonergic axons, the raphe nuclei, as described later (1.15). A striking feature of the LC is the discrepancy between the extensive efferent projections and the very restricted nature of its afferent innervation (Oyamada *et al.* 1998). Although the efferent projections include much of the neuroaxis, the afferent innervation is dominated by projections from two regions of the rostral medulla, the nucleus paragigantocellularis and the nucleus prepositus hypoglossi (Aston-Jones *et al.* 1986). A third small but important input is from the hypothalamus (see Kilduff and Peyron 2000). Recently it has been shown that dendrites of neurones in the core of the locus coeruleus extend to a shell region allowing more extensive interaction (Shipley *et al.* 1996). The manner in which the locus coeruleus processes afferent inputs is interesting. It is associated with a great diversity of somatic and autonomic functions, often as a consequence of its control of arousal (Foote *et al.* 1983). In contrast, under *in vitro* slice preparations, the nucleus is composed of largely electrophysiologically homogenous neurones. These exhibit an endogenously generated rhythm of discharge (Williams *et al.* 1984).

1.8 Location of the Locus Coeruleus

The most detailed anatomical information about the locus coeruleus is derived from studies of the rat. The locus coeruleus is delineated in the ventrolateral corner of the basal central grey of the fourth ventricle approximately 1.2mm posterior to the lambda, where noradrenaline containing cell bodies are packed (figure 5). A mass of noradrenaline somata extends in the rostral direction forming the prominence of the locus coeruleus. Ventrally, a distinct number of noradrenaline cells are distributed continuously with the locus coeruleus in the underlying reticular formation and are designated as subcoeruleus.

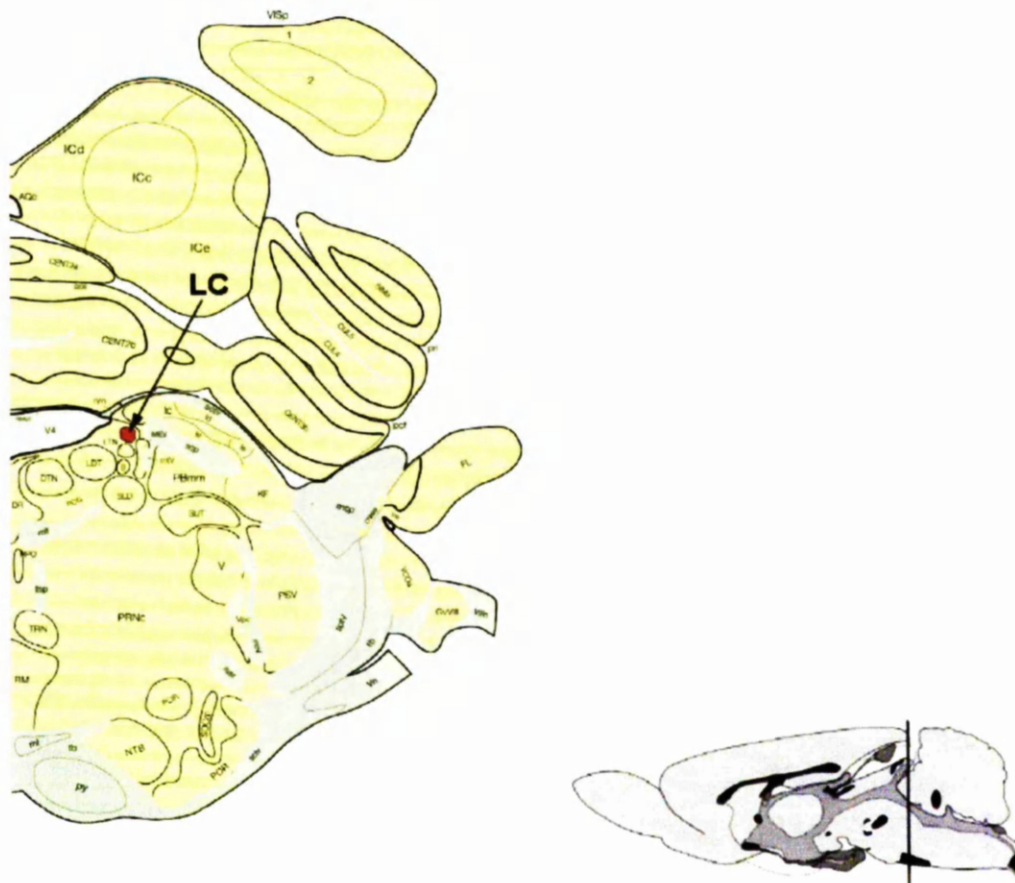


Figure 5. The diagram on the left shows the typical location of the locus coeruleus (LC) in the rat (red). The diagram on the right shows the relative position from where the section was taken. (Taken from Swanson 1998).

Thick dendrites of locus coeruleus noradrenergic neurones extend a distance of 0.5mm in a ventromediorostral direction. These occupy the lateral part of the basal central grey ventromedial prominence of the locus coeruleus where medium to small sized non-aminergic cells are densely present. Grey matter occupied by a plexus of noradrenergic dendrites is designated as the locus coeruleus dendrite area. The dendrite plexus extends in the dorsolateral direction for a short distance in the ventromedial parabrachial nucleus.

Extranuclear dendrites of the locus coeruleus have been described by many authors. Aston-Jones *et al.*, (1986) argued that the innervation of the dendritic area is insufficient to yield excitation in locus coeruleus neurones, based on their electrophysiological data. However, as already mentioned, the locus coeruleus also has an additional dendritic area outside the cytoarchitectonic territory. Maeda *et al.* (1989a) have described the presence of aminergic terminals forming synaptic junctions with noradrenergic neurones in *both* dendritic areas of the locus coeruleus.

1.9 Dopaminergic inputs to the Locus Coeruleus

Dopamine (DA) containing varicose fibres have been described as being very dense and almost exclusive to the locus coeruleus, in both somatic and dendritic areas. Retrograde labelling from the locus coeruleus occurred almost exclusively in the A13 catecholamine group of the hypothalamus (Skagerberg *et al.* 1982). Mesencephalic dopaminergic neurones such as substantia nigra (A9) the ventral tegmental area (A10) and retrorubral nucleus (A8) did not become labelled.

1.10 Noradrenergic Inputs to the Locus Coeruleus

The noradrenergic inputs to the locus coeruleus can be difficult to ascertain due to the intrinsic noradrenaline of the locus coeruleus. Thus a retrograde tracer and isolation experiments with monoamine oxidase histochemistry were employed by Maeda *et al.* (1989a). They concluded that noradrenergic fibres terminate mainly in the area where the somata are concentrated, and adjacent to the dendritic area. Tracer, injected into the somatic area, labelled medullary noradrenergic cells almost exclusively within the A2 group (the nucleus commissuralis and tractus solitarius), in which double-labelled cells were densely distributed from the most caudal part in the cervical cord to the area postrema level predominantly on the ipsilateral side. When the injection site was limited to the dendritic area, there was a significant decrease in the labelled A2 cells. Other tracer labelled noradrenergic cells injected in the locus

coeruleus region were situated in the locus coeruleus complex and subcoeruleus, A4, A5 and A7 groups. Some noradrenergic cells in the contralateral locus coeruleus were also labelled.

Isolation of the region containing the locus coeruleus complex showed a distinct number of MAO-positive terminals intact in both somatic and dendritic areas of the locus coeruleus. These represent input from the locus coeruleus complex including recurrent terminals of the locus coeruleus itself (Maeda *et al.* 1989a). Sixty per cent of the MAO-positive terminals were connected with noradrenergic neurones of the locus coeruleus; the remainder were in synaptic contact with non-amine neurones of the locus coeruleus. The area of target dendrites of the amine-amine contact was found to be relatively large, over $1\mu\text{m}$ in diameter. This may imply that the intrinsic noradrenergic interaction within the locus coeruleus is performed through terminal contact with the proximal portion of the dendrite and somata of the noradrenergic neurones and is relatively powerful.

1.11 Serotonergic Inputs to the Locus Coeruleus

5-HT 1R terminal fibres are relatively dense in both the somatic and dendritic regions of the locus coeruleus (Maeda *et al.* 1989a). Terminal boutons and target dendrites were found to be small ($>1\mu\text{m}$ in diameter). The majority of MAO-B positive aminergic contacts were composed of small terminals and dendrites with a $1\mu\text{m}$ diameter. Most MAO-A and B positive aminergic terminals were less than $1\mu\text{m}$ in diameter and almost exclusively terminated on small non-aminergic (MAO negative) dendrites $>1\mu\text{m}$ in diameter. This implied that most of the serotonergic inputs to the somatic and dendritic locus coeruleus regions terminated on non-aminergic neurones. The origins of the serotonergic inputs to the locus coeruleus were concentrated in the mesencephalic serotonergic cell groups. Few serotonergic inputs originated from the nucleus raphe magnus. Tracer, injected into the dendritic area exclusively labelled the dorsal raphe region, while there was widely distributed labelling in the mesencephalic region. Tracer injected into the somatic region of the

locus coeruleus labelled serotonergic cells of the nucleus raphe medianus and its adjacent reticular formation and lemniscus medialis (Maeda *et al.* 1989a).

1.12 Adrenergic inputs to the Locus Coeruleus

Adrenergic neurone terminals were found in high density in the somatic locus coeruleus area and moderately in the dendritic area (Maeda *et al.* 1991). Boutons were mostly (60%) large, over 1µm in diameter and 80% showed typical asymmetrical synapses. Target dendrites were also large. Adrenergic neurones directly innervated noradrenergic neurones of the locus coeruleus at the proximal part of the dendrites (Maeda *et al.* 1991). Some varicosities made supplemental synapses with small spines by which they appeared to be penetrated, and some very large ones had irregular shapes due to plural synapses with separate dendrites. This implies a powerful influence from adrenergic inputs. The cells of origin were traced to an area roughly corresponding to the nucleus paragigantocelluris. Small numbers of adrenergic cells gave rise to axons innervating the dendritic area of the locus coeruleus. Adrenergic effects are predominantly inhibitory on locus coeruleus neurones.

1.13 Projections to the Spinal Cord

Many studies of the noradrenergic projections to the spinal cord have been performed using degeneration methods and or combined lesions with various histochemical staining methods (Commissiong *et al.* 1978). The conclusions Commissiong *et al.* (1978) drew from their studies were based on staining pattern changes after lesions. These conclusions were that all noradrenergic cell groups of the pons and medulla sent descending fibres to the spinal cord. But loss of staining after lesions must be interpreted with caution because sectioning fibres will initiate their degeneration and hence cause loss of staining.

HRP studies identified large numbers of spinally projecting cells within the brainstem regions known to contain noradrenergic neurones. Comparisons of HRP labelled neurones and histochemically identified neurones also suggested that all noradrenergic cell groups in the brainstem contribute descending projections to the spinal cord. However, it is difficult to know if the HRP labelled neurones are in fact noradrenergic. In a study by Westlund *et al.* (1983), immunocytochemical techniques were used to identify noradrenergic terminations in the rat spinal cord and noradrenergic cells in the brainstem which project to the spinal cord. The immunocytochemical localisation of dopamine β -hydroxylase (DBH), the final enzyme in the synthesis of noradrenaline (DBH converts dopamine into noradrenaline), was used as a means of identifying noradrenergic neurones and fibres. Firstly, Westlund *et al.* (1983) identified noradrenergic fibres and varicosities in the spinal cord. Then, two immunocytochemical axonal tracing techniques were used to identify the sources of the NA fibres in the spinal cord. The origins of the descending noradrenergic inputs were identified by using the retrograde transport of an antibody to DBH. This relies on the ability of noradrenergic systems to take up and transport DBH antibody retrogradely. Then they used a double-labelling technique (retrograde HRP from spinal cord combined with DBH immunocytochemical localisation) to confirm the findings of the retrograde DBH antibody study. From their findings they concluded that pontine noradrenergic cell groups were the sole source of descending noradrenergic projections and spinal cord terminations.

An extensive network of noradrenergic fibres was found throughout the spinal grey matter at all levels of the cord. Many large, darkly stained varicosities were observed along the labelled fibres as they coursed over the entire grey matter. Labelled fibres and varicosities were connected in specific regions: in the superficial layers of the dorsal horn; in the ventral horn around 'large' motoneurones and around the central canal. Heavy immunocytochemical staining of fibres and varicosities was seen in the intermediolateral spinal grey matter, the thoracic spinal cord and in the corresponding region in the sacral spinal cord.

The pattern of noradrenergic terminals stained immunocytochemically for DBH at various levels in the spinal cord is summarised figure 6.

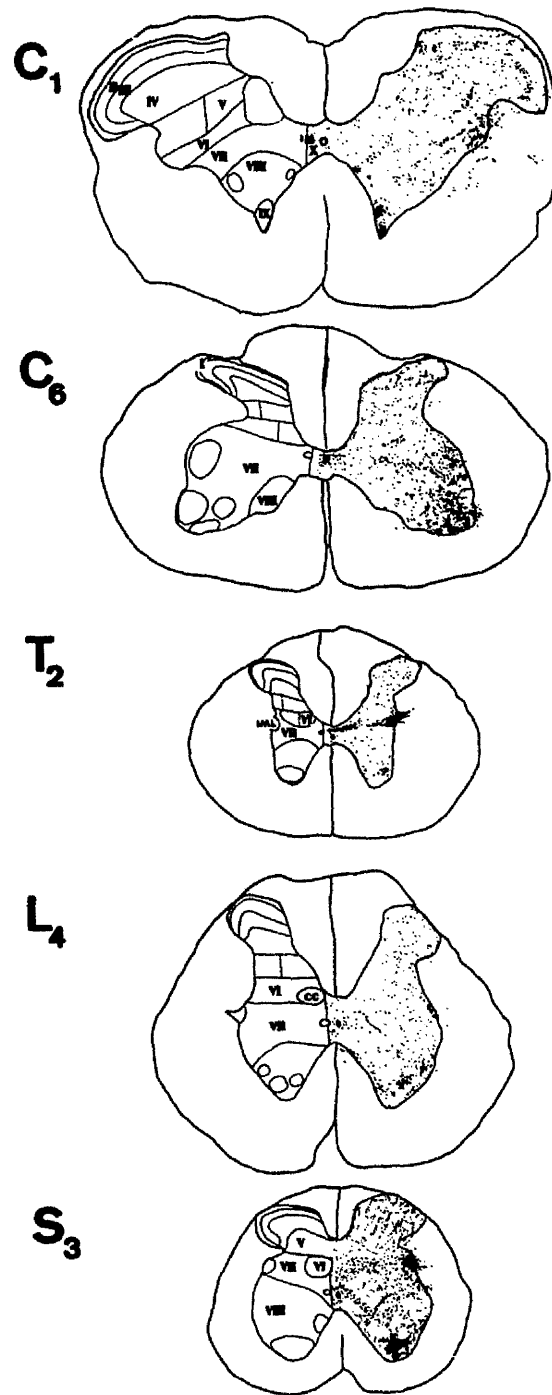


Figure 6. Summary of dopamine- β -hydroxylase immunoreactivity spinal cord levels C1, C8, T2, L4 and S3. Rexed's laminae are shown on the left and the immunoreactivity on the right. From Westlund et al. (1983).

In the spinal dorsal horn, lamina I and outer portions of lamina II were heavily labelled with immunoreactive fibres and varicosities. The fibres and terminals formed a fine meshwork radiating through laminae I and II, perpendicular to the laminar borders, as well as forming T-shaped branches in the dorsal horn.

In the cervical and lumbar ventral horn, networks of DBH-immunoreactive fibres and terminal varicosities were concentrated in regions containing large cells which Westlund *et al.* (1983) assumed to be α -motoneurons. They noted that the varicose terminals appeared to surround the somata of some of the putative α -motoneurons, in a 'corona-like' distribution. Heavily stained varicosities were seen in the intermediolateral grey matter of the spinal cord at both thoracic and sacral levels. In the upper thoracic levels, DBH labelled fibres extended in a band toward the central canal into the region of the central autonomic and intercalated nuclei, as well as into the lateral white matter. Large, darkly stained fibres and varicosities were concentrated in the region of the cells of origin of the parasympathetic preganglionic fibres in the sacral intermediolateral cell column.

Rajaofetra *et al.*, (1992) used a more definitive immunocytochemical technique to eliminate a methodological inconsistency in the detection of dopamine- β -hydroxylase as a marker for noradrenergic axons projecting to the spinal cord. DBH is also present as the final enzyme in the biosynthetic pathway of adrenaline as well as noradrenaline. Thus, structures cannot be unequivocally identified as noradrenergic using DBH as a marker. Consequently, Rajaofetra *et al.* (1992) used an antiserum raised against noradrenaline to identify and describe the distribution of noradrenergic innervation in the rat spinal cord. They confirmed the findings of Westlund *et al.*, (1983). Noradrenaline-immunoreactive (NA-IR) fibres and their terminals were distributed along the entire length of the spinal cord grey matter. These were concentrated in layers equivalent to the laminae of Rexed. These included the ventral horn 'motoneurone' areas. At the cervical level thin varicose fibres were dispersed throughout the ventral horn, with distinct accumulations around clusters of motoneurons, especially the external group. At the thoracic level, NA-IR fibres

were concentrated around internal and external groups of motoneurons. At the lumbar level the NA-IR fibres were described as ‘whorls around the internal and external groups of motoneurons’. Additionally, some radial fibres were seen to invade the white matter at the periphery of the ventral horn.

At the sacral level NA-IR fibres were particularly concentrated in the external groups of motoneurons (in the lateral or Onuf’s nucleus and the dorsolateral column). Rajaofetra *et al.* (1992) further scrutinised their vibratome sections, this time with electron microscopy. They found that the NA-IR fibres appeared *larger* than in the dorsal horn. They had large varicosities of diameter greater than 1µm and having synaptic contacts with large and medium sized dendrites. In some cases they observed that several NA-IR varicosities filled with vesicles were *not* in contact with synaptic densities. They appeared to be intermingled with non-immunoreactive varicosities, none of which appeared synaptic.

Rajaofetra *et al.*’s (1992) conclusions concerning the ventral horn innervation by NA-IR fibres were: NA-IR fibres and terminals were found accumulated in the motoneurone areas of the ventral horn. The incidence of synapses was much higher than in the dorsal horn; these synapses were principally axodendritic and upon large and medium sized dendrites, some of which were likely to belong to α-motoneurons. Axosomatic synapses on motoneurone somata were present but were less common. They suggested that the purpose of this innervation may be to stimulate the activity of at least a group of motoneurons. This stimulation may be by direct innervation (axodendritic and axosomatic synapses) or may involve interneurons since many of the axodendritic synapses they found could, potentially, involve interneurons.

1.14 Origins of descending noradrenergic projections

Using the DBH antibody transport method in the rat, Westlund *et al.*, (1983) demonstrated that the cells of origin of the noradrenergic fibres in the spinal cord could be revealed following uptake and retrograde transport of DBH antibody from injection sites in the grey matter at different levels of the spinal cord. These DBH-immunoreactive neurones were located in regions known to contain noradrenergic cells, including the locus coeruleus, nucleus subcoeruleus, the medial and lateral parabrachial nuclei, the Kölliker-Fuse nucleus and the region dorsal and lateral to the superior olivary nucleus. No labelled neurones were found in other regions of the brainstem. However the most densely stained brainstem region corresponded to the locus coeruleus in the dorsolateral pontine tegmentum (A6 cell group of Dalström and Fuxe). The spinally projecting immunoreactive cells were scattered throughout the rostrocaudal extent of the nucleus, but were concentrated in the caudal and ventral parts of the locus coeruleus. In the locus coeruleus, the proximal dendrites and the perikarya of the labelled cells were aligned, accentuating the curved ventral and lateral borders of the locus coeruleus. Throughout the remainder of the rostral locus coeruleus, the labelled perikarya and dendrites were most often orientated in a dorsomedial-ventrolateral direction. Some of the dendrites were seen to extend beyond the borders of the locus coeruleus. At the rostral most portions of the locus coeruleus, through levels of the caudal inferior colliculus, only occasional retrogradely labelled neurones were observed.

Caudal to the locus coeruleus, neurones in the dorsolateral pons were observed to be retrogradely labelled with DBH antiserum at levels rostral to the genu of the facial nerve. This region of the pontine tegmentum had all its labelled neurones located lateral and ventrolateral to the fourth ventricle. These were included by Westlund *et al.*, (1983) in the population of the locus coeruleus (A6 cell group).

Ventral to the locus coeruleus, a population of labelled perikarya was observed in the nucleus subcoeruleus. The noradrenergic cells of the subcoeruleus form a major

portion of the A7 cell group of Dalström and Fuxe. The retrogradely labelled neurones extend from the ventral edge of the locus coeruleus to the ventrolateral border of the brainstem and were concentrated in the midpontine levels. The labelled cells were 11-23 μ m in diameter and fusiform or multipolar in shape. The fusiform cells were located in the ventrolateral part of the subcoeruleus and lateral to the ventrolateral nucleus of the lateral lemniscus.

Neurones in the other portions of the A7 cell group that were retrogradely labelled from the spinal cord included cells in the medial and lateral parabrachial nuclei and Kölliker-Fuse nucleus. The neurones of the medial and lateral parabrachial nuclei were 13-20 μ m in diameter and fusiform shaped, similar to those located ventrally in the subcoeruleus. The cells of the Kölliker-Fuse nucleus, in the lateral pons, were morphologically distinct from labelled cells in other areas of the pons. The cells of the Kölliker-Fuse nucleus were multipolar with a prominent nucleus and were 18-25 μ m in diameter. Another pontine region that Westlund *et al.*, (1983) found contained DBH antiserum labelled cells was the part of the ventrolateral reticular formation immediately lateral and dorsolateral to the superior olivary nucleus (A5 cell group). These cells were mainly fusiform in shape, 14-24 μ m in diameter and distributed in an arc over the dorsolateral surface of the superior olivary nucleus.

Westlund *et al.*, (1983) quantitatively analysed their data to determine the numbers of DBH-immunoreactive neurones in the various pontine nuclei that projected to the spinal cord. They found that 86% were localised in the locus coeruleus and subcoeruleus, almost equally divided between them. The region lateral and dorso-lateral to the superior olivary and facial nuclei (A5 cell group) contained 5-10% of the spinally projecting noradrenergic neurones, with the remainder distributed in the Kölliker-Fuse nucleus and parabrachial nucleus. The distribution of DBH antiserum labelled neurones in the pontine nuclei are shown in figure 7. Note that the majority of DBH labelled axons in the lumbosacral region (figure 7C) are derived from the locus coeruleus.

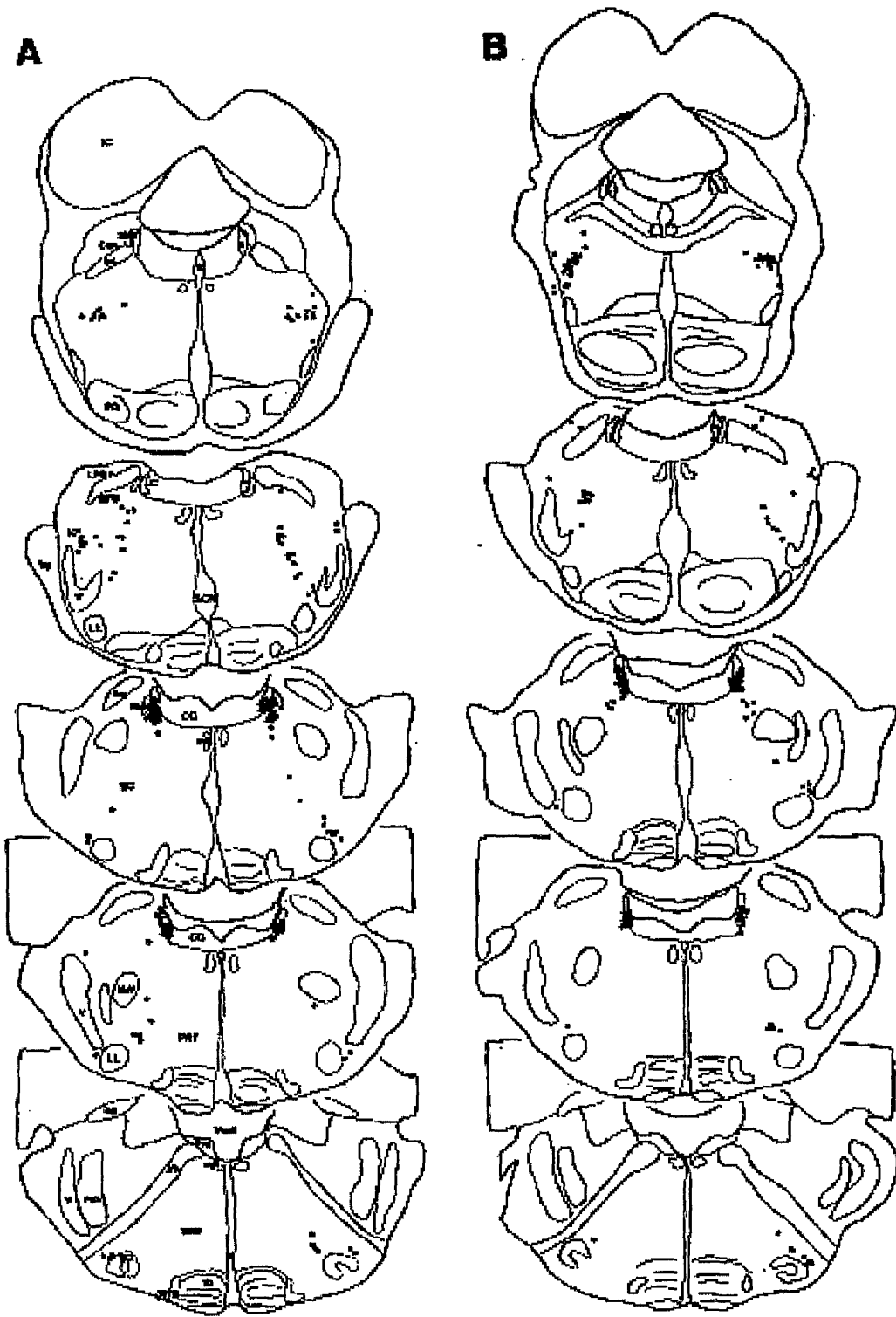


Figure 7A and B. Summary of retrogradely labelled cells after injection of DBH antibody into different spinal cord levels. A: cervical; B: thoracic; (continued)

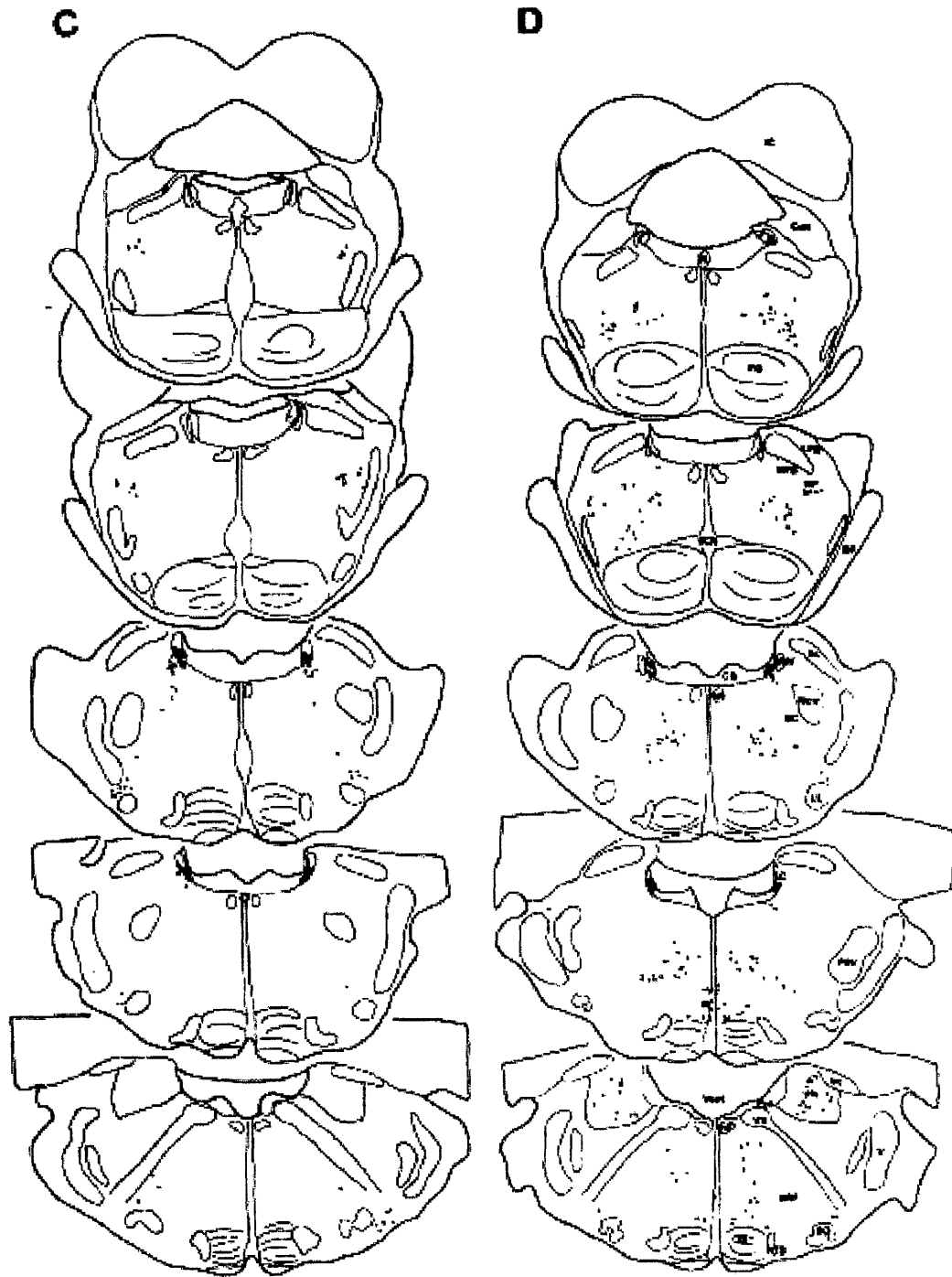


Figure 7C and D (continued). C lumbar and sacral enlargement; D: summary of the distribution of HRP-labelled cells after injection into the sacral spinal cord for comparison. From Westlund et al., (1983).

In a total of 14 experiments, no obvious differences were observed by Westlund *et al.*, (1983) in the distribution of the labelled cells, regardless of whether the injection was made into the cervical (figure 7A), thoracic (figure 7B) or lumbosacral (figure.7C) spinal cord. In figure 7D the distribution pattern of the neurones labelled retrogradely with HRP injections into the sacral spinal cord levels has been included for comparison.

1.15 The Central Origin of Serotonergic Axons projecting to the Spinal Cord: the Raphe nuclei and its afferent connections

The raphe nuclei are groups of large cells mainly located in the midline of the brain stem, most of which contain the neuromodulator serotonin. This group of cells can be divided into rostral and caudal regions based on the early developmental appearance of the myelencephalic and mesencephalic groups. The rostral group gives rise to ascending projections whereas the projections of the caudal group extend to the spinal cord.

The caudal group consists of three nuclei: nucleus raphe obscurus (NRO), nucleus raphe magnus (NRM) and nucleus raphe pallidus (NRP) (Jacobs *et al.* 1984 Parent *et al.* 1981). They project to the spinal cord mainly through the dorsal half of the lateral funiculus (NRM), or via the ventral and ventrolateral funiculi (NRP, NRO).

The caudal group of raphe nuclei has been the subject of much research since these cells can influence a variety of spinal cord functions. For example, the raphe magnus is well known to modulate sensory transmission in the dorsal horn (Oliveras *et al.* 1975, see Basbaum *et al.* 1976), while the two more caudally placed nuclei are involved in regulating both autonomic and motor systems in the spinal cord. Many of the raphe-spinal effects are mediated by serotonin since a very large fraction of the raphe-spinal neurones are serotonergic. But recent evidence shows that peptidergic neurotransmitters such as substance P, thyrotropin-releasing hormone, leucine and methionine, somastatin and certain amino acids are also present in the neurones of the raphe nuclei and are co-localised with serotonin within neurones.

1.16 Nucleus Raphe Obscurus

The nucleus raphe obscurus (NRO) lies in a symmetrical paramedian cluster that extends from the caudal border of the pons to the cervical spinal cord. The projections to the spinal cord are distributed in the central grey matter ventral to the aqueduct on the medial border of the ventral horn. The majority of these projections are associated with fibres of the medial longitudinal fasciculus (the descending fibres of which influence the function of motoneurons) and the tectospinal tract.

The serotonin-containing neurones of the raphe obscurus are clustered around the midline and extend from the level of the pyramidal decussation caudally, where they flank the decussating fibres to the rostral pole of the inferior olive. Longitudinally, the cells occupy approximately the middle third of the medulla and are situated in the dorsal part of the tegmentum. Ventrally the group fuses with the dorsal division of the raphe pallidus. This boundary frequently appears arbitrary and indistinct. However, in a favourable section, the raphe obscurus is less densely packed and thinner than the subjacent raphe pallidus. The cells of the raphe obscurus are between 11-18 μ m in diameter with dendrites which project mainly in the dorso-ventral direction. This dendritic orientation helps distinguish the raphe obscurus from the more isotropic raphe pallidus.

1.17 Nucleus Raphe Pallidus

The nucleus raphe pallidus (NRP) is a column of cells that occupy the ventral third of the mid-sagittal plane. This extends from the level of the decussation of the pyramidal tract to the rostral pole of the inferior olive. The dorsal border is continuously fused with the NRO. In transverse section, the raphe pallidus appears to have an hourglass shape, although the 'chambers' are unequal, with the constricted segment lying in the midline between the inferior olivary nuclei. The dorsal portion is larger and has an almond shaped cross section; the ventral portion lies along the ventral midline adjacent to the medial margin of the pyramidal tracts. The dorsal

division is broader and more densely packed than the NRO. The cells of the dorsal division are arranged primarily in two paramedian sheets along the raphe, with some cells actually within the raphe, and others mingled among the fibre bundles of the medial lemniscus. A small number of individual serotonergic neurones are found lying laterally, along the border between the inferior olive and the pyramidal tract. The individual cells of the dorsal division are multipolar neurones between 15-21 μ m in diameter, and with long dendrites extending into the nucleus reticularis gigantocellularis; in transverse sections the dendrites appear to have a medio-lateral orientation. The cells of the central division have a diameter between 14-22 μ m and are tightly clustered. They appear to have few dendrites, most abutting the ventral surface of the medulla. In sagittal sections, the cells of both divisions have striking axonal and dendritic extensions in a caudo-ventral to rostro-dorsal direction.

1.18 Raphe Magnus

It should be noted that the majority of serotonergic neurones in this nuclear group are located *outside* the confines of the raphe. Laterally to the inferior olive, the nucleus reticularis paragigantocellularis is continuous with a group of serotonergic cells that are scattered through the nucleus reticularis paragigantocellularis. This group is roughly quadrilateral in cross section, and extends rostrally above the nuclei of the trapezoid body and superior olive. Raphe magnus cells are loosely packed and, unlike other raphe nuclei, there is no clustering of the cells in the midline. Ventrally the nucleus is bounded by the pyramidal tract and trapezoid body, and it does not extend dorsally above the middle tegmentum. Cells extend laterally almost as far as the medial edges of the nuclei of the trapezoid body. The individual cell diameters are 14-23 μ m with tortuous dendrites extending almost exclusively in the mediolateral direction.

1.19 Raphe-Spinal Neurones

The first attempt to demonstrate that raphe neurones project to the spinal cord was made by Brodal *et al.*, (1960) in the cat. The technique they employed was mapping of cells that showed retrograde chromatolysis after transverse lesions were made in the spinal cord. After lesions were made in the spinal cord, retrograde changes were observed in the nuclei raphe pallidus, obscurus, magnus and pontis. The raphe magnus and the rostral portion of the raphe pallidus showed the greatest number of cells with lesion changes. No other raphe nuclei showed chromatolysis. When lesions were restricted to the dorsal part of the lateral funiculus, chromatic cells were observed in the nuclei raphe magnus, pallidus and obscurus which implies that some raphe-spinal axons descend in this part of the spinal cord white matter. The most chromatolysis was observed after cervical lesions were made but some cells with retrograde changes were observed after lesions were made at the first thoracic level, which implies that the raphe-spinal neurones project to levels below the cervical cord.

Other techniques have also been employed by Kausz (1991) to elucidate the distribution of raphe neurones and cells of the medullary reticular formation to the thoracic, lumbar and sacral segments of the feline spinal cord. She used the retrograde transport of HRP alone or in combination with nuclear yellow. Injections were made unilaterally in three major areas: the medial and lateral portions of the intermediate grey matter and the lateral funiculus.

She observed that the entire thoracic, lumbar and sacral spinal cord received projections from the medullary raphe nuclei. The number of labelled raphe neurones was much larger after sacral injections than after thoracic injections. An intensive reciprocal connection seemed to exist between the spinal sacral segments and higher brain regions. Kausz (1991) found that the thoracic and upper lumbar segments receive raphe-spinal fibres from all bulbar raphe nuclei coursing ipsilaterally. However, descending raphe-spinal fibres terminate *bilaterally* in the lower lumbar and sacral segments. She speculated that sacrally descending raphe-spinal fibres do

so not only via the lateral funiculus, but also through the central grey matter alongside the central canal. This is because labelled neurones could be detected in only the raphe nuclei when the HRP injection was preceded by an extensive bilateral destruction of the lateral and anterior funiculi. Figure 8 indicates the serotonergic pathways to the spinal cord (Kausz 1991). Note that the spinal projections descending in the central grey matter are ipsilateral, whereas those descending with reticulospinal axons project bilaterally in the lower lumbar and sacral parts of the spinal cord. Table 2 summarises the location and classification of all the raphe nuclei and Table 3 summarises the connections of those projecting to the spinal cord.

1.20 Co-localisation of other peptides with serotonergic neurones

Serotonin has been shown to exist with other neuro-active peptides in medullary raphe axons. In a study performed on the cat by Bowker *et al.* (1987) the number of medullary cells containing multiple neurotransmitters, particularly in conjunction with serotonin, was determined. They found that a very large proportion of the raphe neurones projecting to the spinal cord were purely serotonergic (80%) in each nuclei. More than 85% of the descending raphe-spinal neurones in the raphe pallidus and raphe obscurus were serotonergic, whereas 75% of the neurones from the raphe magnus contained serotonin.

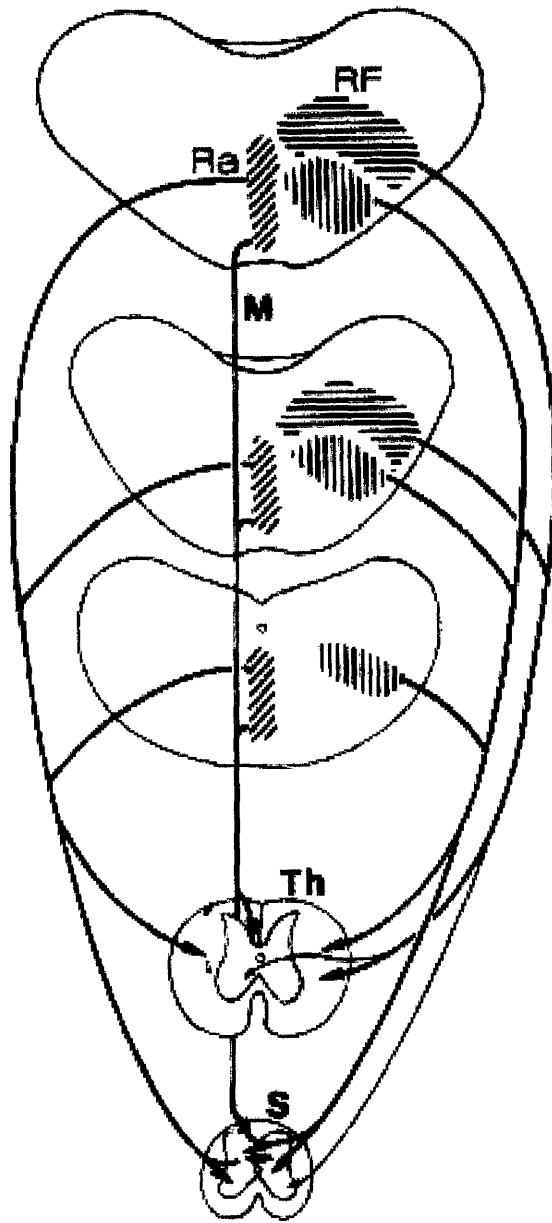


Figure 8. A schematic drawing comparing the spinal projections from the raphe and from the ventral and medial portions of the medullary reticular formation (RF, vertically hatched). Note that the raphe nuclei project to the entire length of the cord. The projections to the thoracic segments (Th) are ipsilateral and the projections to the sacral segments (S) are bilateral. M shows the raphe-spinal fibres which descend through the grey matter alongside the central canal and are ipsilateral. (from Krauz 1991).

Table 2 Summary of the location of all the raphe nuclei with respect to their classification by Dahlström & Fuxe (1964)

Dahlström & Fuxe Classification (1964)	Anatomical Location	Spinal Cord Projection	Axon location (Funiculus) **	Percentage of 60,300 5-HT containing Cells*
B1	NRP [#] & adjacent area	All levels	Ventral lateral	7938 (13%)
B2	NRO [#]	All levels	Ventral	2314 (4%)
B3	NRM [#] & around medial lemniscus & nucleus Paragigantocellularis lateralis	All levels	Dorsal lateral	2368 (4%)
B5	Nucleus Raphe Pontis	Cervical only		276 (0.5%)
B7	In PAG especially NR dorsalis and adjacent areas	Cervical only		
B9	Medial lemniscus & mesencephalic Reticular formation	Cervical only		
B4	Beneath IV ventricle close to vestibular & abducens nuclei	None		
B6	Beneath IV ventricle in pons	None		
B8	Median raphe nucleus & adjacent areas	None		

Dahlström & Fuxe (rat)

[#] 73% of 5-HT containing cells project to spinal cord of rat (Bowker *et al.*, 1987)

*Only 47,000 5-HT containing cells in the cat were in raphe nuclei (Wiklund *et al.*, 1981)

**Basbaum & Fields.1979 (rat & cat)

Table 3 Raphe Nuclei in the medulla oblongata: Projections to Spinal Cord

Nucleus	Axon Location (funiculus)	Termination in Rexed laminae	Spinal Cord Level	Additional Comments
NRP	Ventral lateral some in dorsal lateral	IV→X+I X*		Also sacral parasympathetic nuclei
NRO	Ventral & ventral lateral	IV→X+I X*		
NRM	Dorso-lateral mainly (few in ventral lateral & ventral)	I, II, V-VII	Cervical and lumbar	Caudal part projects to IV-X

Data from Willis, 1984.

*These serotonin-containing axons descend in the ventral part of the ventral lateral funiculus and in the ventral funiculus. They cross at the cord level.

1.21 The Role of the Raphe and Locus Coeruleus in Motor Control

1.21.1 The Locus Coeruleus

There is evidence that the locus coeruleus plays an important role in motor control. During rapid-eye-movement (REM) sleep noradrenergic and serotonergic neurones in the brainstem are inactive and this coincides with sleep paralysis. The only loss of muscle tone comparable to that of REM sleep is in people with narcolepsy. Cataplexy (a symptom of narcolepsy) is the loss of muscle tone, whilst the subject is fully awake and alert (see Siegal 2000). It is usually triggered by sudden emotionally significant stimuli such as anger or laughter (Aldrich 1990). The electroencephalogram (EEG) is activated during cataplexy as in wakefulness and REM sleep (Aldrich 1990).

The neurones of the locus coeruleus have been shown to be tonically active during both quiet and active waking (Aston-Jones & Bloom 1981). Neuronal activity of the locus coeruleus is reduced during non-REM sleep and they cease discharging for some time during REM sleep. Wu *et al.*, (1999) reported that locus coeruleus neurones ceased their discharge throughout cataplexy periods in canine narcoleptics. They found that the discharge rates were as low or lower than during REM sleep. The administration of cataplexy-inducing drugs (prazosin- α_1 antagonist and physostigmine-cholinesterase inhibitor) decreased the locus coeruleus discharge rate. They stated that their results were consistent with the hypothesis that activity in the locus coeruleus contributes to the maintenance of muscle tone during waking and a decrease in locus coeruleus discharge plays an important role in the loss of muscle tone during cataplexy and REM sleep. Recently it has been proposed that the circuitry responsible for the regulation of sleep involves an excitatory input from the hypothalamus to the locus coeruleus (see Kilduff & Peyron 2000 and figure 9). The peptide transmitters involved are hypocretins.

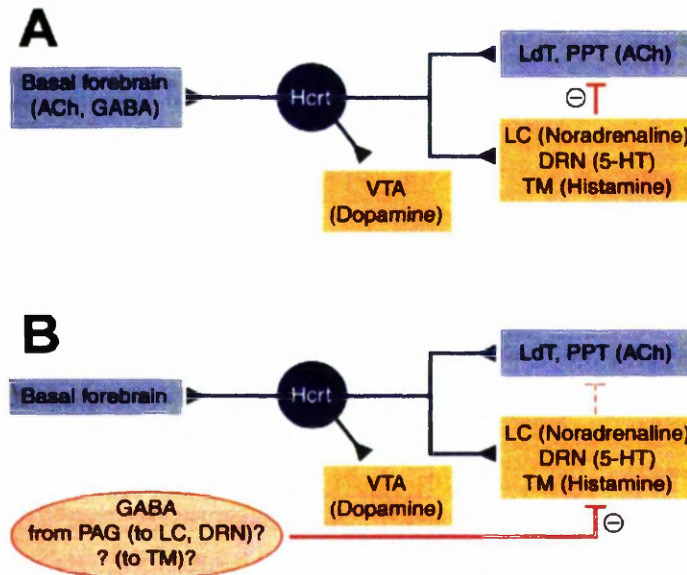


Figure 9. A shows the postulated mechanism by which hypocretin (Hcrt)/orexin cells might produce arousal through excitation of the 'wake-active' monoaminergic populations in the tuberomammillary nucleus (TM), locus coeruleus (LC), dorsal raphe nuclei (DRN) and ventral tegmental area (VTA). B. During REM sleep excitatory input from the Hcrt/orexin cells to cholinergic cells would facilitate cortical desynchrony, but the excitatory effects onto monoaminergic cell groups might be blocked by GABA-mediated inhibition from the periaqueductal grey (PAG), since GABA levels are high in both the LC and DRN during this state. The absence of excitatory input from the Hcrt/orexin cells onto the monoaminergic cells would result in a reduction of their activity and thus in a net disinhibition of the 'REM-on' groups in the basal forebrain (LdT) and pons (PPT), thereby promoting REM sleep.

One of the major afferent inputs to the locus coeruleus, the nucleus paragigantocellularis, is known to be involved in, amongst other things, cardiorespiratory control (Oyamada *et al.* 1998). Of particular interest is the established fact that locus coeruleus neurones discharge at an increased frequency in response to systemic hypercapnoea (Elam *et al.* 1981). Recently it was found that focal tissue acidosis in the vicinity of the locus coeruleus is followed by a large increase in respiratory motor output (phrenic nerve). This may suggest that locus coeruleus neurones function as respiratory chemoreceptors (Coates *et al.* 1993).

Oyamada *et al.* (1998) used an *in vitro* brainstem-spinal cord preparation of the neonatal rat to investigate the influence of the locus coeruleus chemosensitivity on naturally occurring afferent inputs. This preparation had sufficient synaptic circuitry to sustain a rhythmic respiratory motor output and responsiveness to bath-applied

changes in pH for several hours. Their aim was to determine how the activity of locus coeruleus neurones was modified in response to bath-applied hypercapnoeic acidosis, and to identify the relationship of this response to the acidosis-induced increase in respiratory motor output on phrenic root nerves. They had three major findings: the activity of the locus coeruleus neurones was synaptically modulated at the frequency of respiratory rhythm; increasing CO₂ concentration weakened or removed an inhibitory component of this modulation which contributed significantly to the overall excitatory response of the locus coeruleus neurones to hypercapnoeic acidosis; the membrane potential response of locus coeruleus neurones to hypercapnoeic acidosis was retained following suppression of their synaptic input.

1.21.2 The Raphe

The raphe have been shown to have wide and varied effects on several physiological systems ranging from the cardiovascular and gastrointestinal system to somatomotor control and in sleep (see above and figure 9). They are thought to be important in integrating autonomic and somatomotor responses (see Lovick 1997).

As is well known, stimulation of the nucleus raphe magnus in conscious animals produces profound analgesia (Oliveras *et al.*, 1975). These authors showed that the behavioural response to strong pinches of all four limbs and tail were suppressed and there was an increased threshold for the jaw-opening reflex as evoked by tooth pulp stimulation (a pure source of nociceptive input to the CNS).

Jacobs & Fornal (1993) recorded from cells in the nucleus raphe pallidus and obscurus in conscious cats. They showed that single cells could be active in multiple activities as diverse as locomotion and feeding. This supports the concept of an integrative role for these nuclei.

Phrenic nerve activity could be increased for more than an hour following a ten minute period of electrical stimulation applied to the nucleus raphe obscurus

(Milhorn 1986). This raphe-induced hyperpnoea appeared to be mediated by serotonin since the effect could be blocked by pretreatment with methysergide.

Stimulation of the nucleus raphe obscurus has also been found to increase feline gastric motility (Hornby *et al.*, 1990) and to increase pancreatic endocrine secretion (Krowicki & Hornby 1995). These effects were shown to be vagally mediated via a projection from the caudal raphe to the dorsal vagal motoneurons.

After stimulation of the nucleus raphe magnus or nucleus raphe obscurus an electrical stimulation of the dorsolateral periaqueductal grey matter produced a long lasting depression of the cardiovascular and respiratory components of the 'defence' response (Schenberg & Lovick 1995).

The ventral horn of the spinal cord receives extensive raphe projections and yet stimulation of the raphe does not produce any obvious motor activity (Oliveras *et al.* 1975). In the rat, stimulation of the nucleus raphe obscurus produces a serotonergically mediated facilitation of the excitability of lumbar motoneurons via 5-HT₁ receptors (Roberts *et al.* 1988). However ionophoretic application of serotonin or stimulation of the nucleus raphe obscurus did *not* depolarise the motoneurons sufficiently to induce firing. It was suggested by Jacobs & Fornal, (1993) that serotonin may prime the motor output by bring motoneurons closer to threshold in anticipation of motor activity. Thus the raphe acts as a modulator of the levels of excitability in motor pathways but does not initiate movement.

As mentioned previously, the neurones of the raphe obscurus and pallidus are active during locomotion (Jacobs & Fornal 1993). Locomotion in the high decerebrate cat is initiated by stimulating a subthalamic centre (Shik *et al.* 1966) and in chronic spinal cats by the administration of noradrenergic agonists such as clonidine, but not by serotonergic agonists. The serotonergic system in spinal cats lengthens the step cycle whereas the serotonergic system increases the extensor power (Barbeau & Rossignol, 1991 and see Rossignol *et al.* 2001).

1.22 Opiates and Rigidity

High doses of potent opiates, such as fentanyl and alfentanil, are in general use as anaesthetic agents and are especially valuable during cardiac surgery and neurosurgery, as they provide cardiovascular/pulmonary stability and good analgesia (Stanley *et al.* 1979). Opioids appear to produce their physiological effects by binding to at least three types of opioid receptors: μ -; κ -; δ - receptors. The μ_1 -receptor is postulated to mediate analgesia (Pasternak 1993) whereas the μ_2 -receptor is thought to play a role in respiratory depression. Unfortunately opiates are also commonly responsible for muscular rigidity leading to the so-called 'wooden chest' phenomenon where chest wall compliance is greatly decreased because of the muscular rigidity (Scanman 1983). The μ_1 receptor has been implicated (Neguss *et al.* 1993) in this phenomenon. The rigidity appears to occur mainly during the critical phase of anaesthetic induction, when the patient is about to be intubated prior to artificial positive pressure ventilation and so decreased chest wall compliance is potentially life -threatening. Also during the rigidity, increased central venous and pulmonary artery pressure have been noted. Benthuisen *et al.*, (1986) investigated the haemodynamic, metabolic, electrocardiographic (ECG) and electromyographic (EMG) characteristics of alfentanil-induced rigidity. They demonstrated a general increase in EMG activity as well as clinically recognisable rigidity in patients anaesthetised with alfentanil. This was first noted in the upper body (sternocleidomastoid, deltoid, biceps and forearm) and soon spread to the rest of the musculature. Otherwise there was no regular pattern of muscle activation. The mean onset time of rigidity with alfentanil was forty-seven seconds from the beginning of administration. The rigidity and increased EMG activity could be provoked or *increased* by stimulation of the patient by, for example, passive movement of an extremity, manipulation of the mask or by loud auditory stimuli.

Benthuisen *et al.*, (1986) reported that, clinically, the rigidity was often explosive in onset with subjects assuming typical postures - flexion of the upper extremity at the

fingers, wrists and elbows; extension at the toes, ankles knees and hips; rigid immobility of the head with atlanto-occipital flexion of the chin onto the chest, and severe rigidity of the abdominal and chest wall musculature. The atlanto-occipital flexion made intubation difficult. Two of their patients made ineffective inspiratory efforts after 2-3 minutes of apnoea when rigidity was present. Muscle relaxants completely eliminated all clinical as well as EMG evidence of rigidity.

Benthuisen *et al.*, (1986) showed that the rigidity was central in origin by applying a tourniquet to a limb, to temporarily cut off its blood supply, before administering the opiate. They found that the rigidity developed in the limb that was isolated from any direct action of the narcotic by a tourniquet. In addition, rigidity in the limb persisted when it was abolished from the rest of the body by neuromuscular blocking agents. This unequivocally established that a centrally mediated mechanism is responsible for opiate-induced rigidity.

1.23 The link between the Locus Coeruleus and the effects of potent opiates.

Lui *et al.* (1989) first showed that opiate induced rigidity occurred in non-anaesthetised rats as in humans, establishing an animal model. Using anaesthetised rats and together with careful control of respiration, body temperature and end-tidal CO₂, Lui *et al.* (1989) administered fentanyl (50-100µg/kg) systemically which consistently produced increased electromyographic activity in the gastrocnemius and abdominal rectus muscles. In attempting to elucidate the mechanism for this type of rigidity, Lui *et al.* (1989) injected fentanyl into the locus coeruleus and found this also induced rigidity. There was a discernible increase in electromyographic activity in the gastrocnemius and abdominal rectus muscle. The effect was significantly antagonised or at least reduced by prior electrolytic lesions of the locus coeruleus *or* with pretreatment with the α_1 -adrenoceptor blocker, prazosin. Thus they speculated that induction of muscular rigidity by fentanyl might involve coeruleospinal noradrenergic fibres to motoneurons of the spinal cord.

Lui *et al.* (1990) extended this work by reproducing the fentanyl-induced rigidity in the rat gastrocnemius and extensor caudal lateralis muscles after microinjection of opiate into the locus coeruleus. The EMG activity was greater in the caudal muscles. Again this effect was antagonised by the α_1 -adrenoceptor, prazosin, but the α_2 -adrenoceptor blocker, yohimbine, failed to antagonise the fentanyl-induced rigidity. They thus concluded that the coeruleospinal noradrenergic pathway might be directly involved in the elicitation of muscular rigidity by fentanyl, possibly via α_1 -adrenoceptors.

A major obstacle Lui *et al.* (1990) had to overcome was to explain how α -motoneurons could become excited when fentanyl was injected into the locus coeruleus. Opiates are known to strongly *inhibit* the noradrenergic cells projecting to the spinal cord from the locus coeruleus (Guyenet 1980), and this would therefore have to *disinhibit* the α -motoneurons into greater activity. There are three lines of evidence suggesting that α -motoneurons are *not* disinhibited by this route. Firstly, most reports state that noradrenaline facilitates α -motoneurons rather than inhibiting them, although Engberg & Marshall, (1971) reported a hyperpolarisation and depression of responses. Secondly, according to Pompeiano (1995) the coeruleo-spinal system normally depresses the activity of Renshaw cells via a pathway involving the pontine reticular formation. Hence, inhibiting the coeruleo-spinal system would release the Renshaw cells from this inhibition and thus suppress any tonic activity of α -motoneurons. Thirdly, naloxone increases monosynaptic reflexes suggesting that opioids have a direct suppressive effect on α -motoneurons (see Duggan *et al.* 1984). Lui *et al.* (1995) tried to address this issue by proposing a role for the excitatory transmitter, glutamate, which they found co-localised with the noradrenaline containing neurones of the cat locus coeruleus. However, they did not explain how the glutamate would be released if the neurones were themselves inhibited. An alternative explanation, which was not considered by Lui *et al.* (1990) is that the γ -motoneurons could be disinhibited and excite the α -motoneurons via the spindle afferents. γ -motoneurons are known to be inhibited by ionophoretically

applied noradrenaline (Jankowska *et al* 1998). Activity of γ -motoneurons would then excite muscle spindle afferents, which in turn would excite α -motoneurons. The excitation of γ -motoneurons could be enhanced by a disinhibition of the group II interneurons in the intermediate zone (see figure 10). These are also inhibited by noradrenaline (see section 1.5.3). Thus a positive feedback pathway could be released involving γ -motoneurons and group II interneurons. The diagram shows three routes by which opiate-induced rigidity could result from the over-excitation of α -motoneurons by spindle afferents via the positive feedback loop between group II afferents and γ -motoneurons:

- Opiates may antagonise the facilitation of α -motoneurons by noradrenaline thereby reducing the efficacy of the positive feedback loop between group Ia afferents and α -motoneurons-this would allow α excitation from other sources.
- Noradrenaline could depress γ -motoneurons and opiates would antagonise this depression.
- The interneurons impinging on the γ -motoneurons could be excitatory.

Positive feed-back in pathways from group II afferents

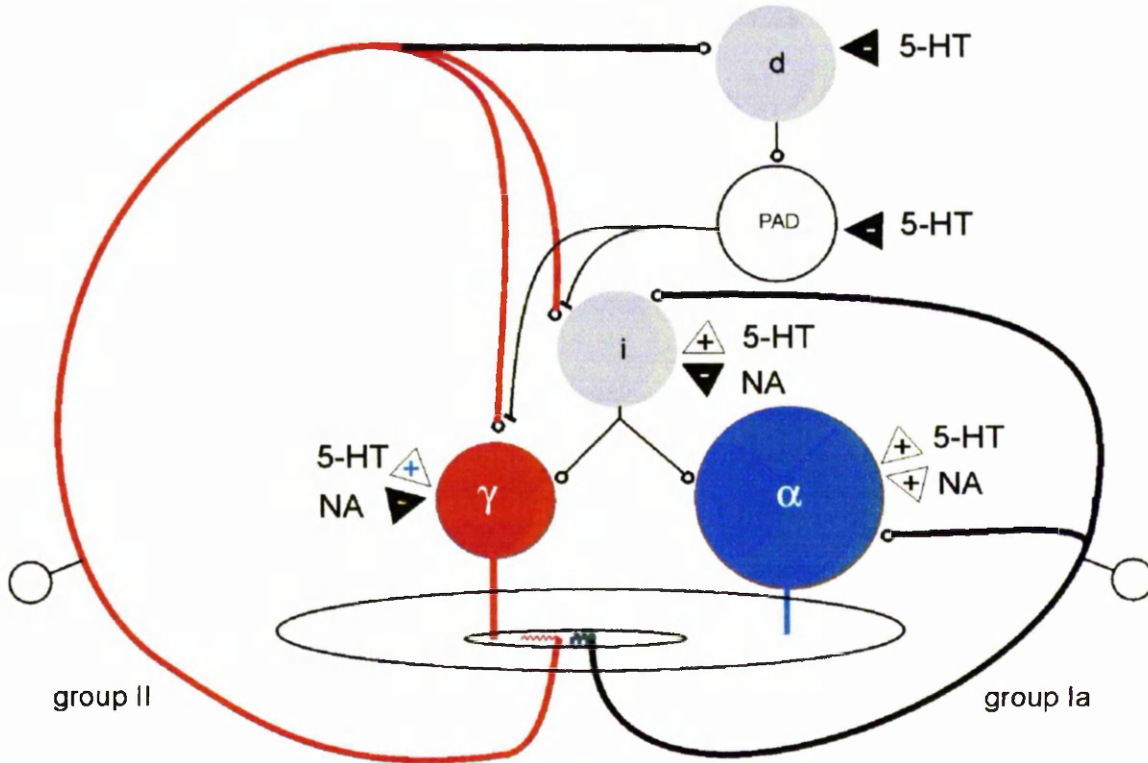


Figure 10. A simplified diagram showing the connections in the circuit of positive feedback between group II afferents and γ -motoneurone. The circles represent different populations of spinal neurones: γ -motoneurone (red) and α -motoneurone (blue) innervating muscle spindles and extrafusal fibres respectively. Two first order interneurons are shown in grey, in the pathways from group II afferents, in the intermediate and dorsal zone of the spinal cord (i and d respectively). The white neurone is a last order interneurone mediating primary afferent depolarisation (PAD). The thick black and red lines represent the primary and secondary muscle spindle afferents and their intraspinal collaterals. Thin lines represent axons of the interneurons. Small circles indicate terminals of the afferent and excitatory interneurons. Triangles represent sites of release of serotonin and noradrenaline; their excitatory and inhibitory actions are indicated by + and -.

2 METHODS

The experiments in which the γ -motoneurons were identified, labelled and gathered were performed by Professor E. Jankowska and Dr. M.H. Gladden in the Department of Physiology, University of Göteborg, Sweden.

2.1 Preparation of γ -motoneurons

A total of eight hindlimb γ -motoneurons were labelled in two deeply anaesthetised cats. The cats were anaesthetised with sodium pentobarbital in a dose of $45\mu\text{g kg}^{-1}$ body weight administered intraperitoneally. This induction agent was supplemented with $5\mu\text{g kg}^{-1}$ body weight hour^{-1} of α -chloralose administered intravenously. During the recording phase of the experiments, the animals were paralysed with an initial dose of $0.4\mu\text{g}$ of pancuronium bromide intravenously (Pavulon) and supplemented by similar doses every 2-3 hours. The animals were sacrificed with an overdose of intravenous sodium pentobarbital and formalin perfusion. Tests were performed regularly and frequently to ensure that the animal's pupils remained constricted to the same extent throughout the experiments. It was fastidiously ensured that the animals did not respond to any stimuli with an increase in either blood pressure or heart rate following the administration of pancuronium bromide. Their blood pressure was maintained above 100mm Hg, and the end tidal CO_2 at or close to 4%. This was achieved by adjusting the volume of the artificial respiration and by a continuous infusion of a bicarbonate buffer solution (5g glucose and 0.84g NaHCO_3 in 100ml of water). The core temperature was maintained between 37 and 38°C, and the temperature in the hindlimb oil pool between 33 and 36°C by means of a heating lamp. A number of hindlimb nerves were dissected and stimulated in a mineral oil pool (separate muscle branches of the sciatic nerve: posterior biceps and semitendinosus, PBST; anterior biceps and semimembranosus, ABSM; medial gastrocnemius, MG; lateral gastrocnemius and soleus, LGS; plantaris, Pl; flexor digitorum longus, FDL; deep peroneal, DP, (including anterior tibial, TA, and extensor digitorum longus, EDL). A laminectomy was

performed to expose the spinal cord from L4 to the sacral segments, the dura was opened. The L7 and sacral dorsal roots were reflected to provide access to the lateral funiculus at the L7 and S1 levels.

The γ -motoneurons were searched for in the L7 segment and in the rostral part of the S1 segment. Their responses were first recorded extracellularly. Antidromic responses were identified by the following criteria: (i) constant latencies of the responses evoked by near threshold and stronger stimuli, and by the first and later stimuli in a train, (ii) latencies exceeding the latencies of activation of α -motoneurons by 1.5 - 9.2ms and compatible with conduction velocities of 16-49ms⁻¹, (iii) stimulus thresholds exceeding the thresholds of activation for α -motoneurons (2-13 times the thresholds of group Ia afferents in a given muscle nerve), (iv) collision with synaptically or 'spontaneously' evoked responses at an appropriate critical interval (twice the latency of the antidromic responses plus about 0.7ms, as illustrated in upper and middle traces of figure. 11.

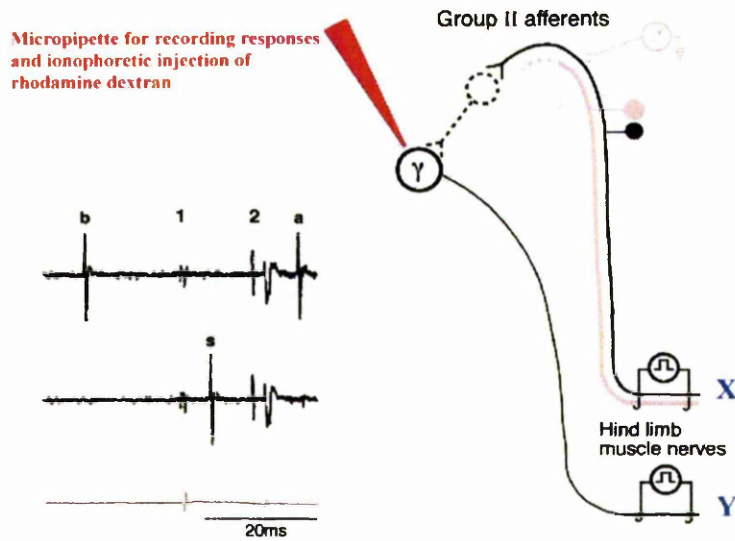


Figure 11 illustrates how γ -motoneurons were identified and labelled. X and Y are stimulating electrodes on hindlimb muscle nerves. Electrode Y is on the nerve of the muscle innervated by the γ -motoneurone. The top trace shows four important events. 'b' indicates a spontaneous background spike in the γ -motoneurone. 1 indicates when nerve Y was stimulated and 2 shows when nerve X was stimulated. In order to ensure that spikes initiated in γ -motoneurons via the reflex pathway collided with spikes propagating antidromically, stimulation for the long reflex pathway (X) had to be applied before stimulation for the shorter antidromic route (Y). 'a' indicates the antidromic γ spike recorded by the micropipette. The middle trace shows that when a spike occurs in the γ -motoneurone, activated via the reflex route (activated from electrode X), there is no antidromic spike because the reflexly induced spike has collided and cancelled out the antidromic spike. This is confirmation that the synaptic and antidromic spike occurred in the same γ -motoneurone. The bottom trace is the recording from the dorsal roots and indicated when the volleys arrived at that point.

2.2 Labelling

The neurones were labelled by ionophoretically injecting rhodamine-dextran intracellularly from glass microelectrodes containing a 2% solution of tetramethylrhodamine-dextran (3000 MW, anionic, lysine fixable; Molecular Probes Inc. D-3308) in saline (pH 6; tips of about 2.5 μ m; resistance 13-18M Ω) following the procedure of Carr *et al.*, (1994). Rhodamine was injected by passing constant positive current of 5nA, totally of 20-56nA min. Animals were perfused with fixative through the descending aorta. Initially they were perfused with a rinsing solution which consisted of 200ml of 0.1M phosphate buffered saline (PBS) and subsequently with a fixative solution which consisted of 2:1 of 4% paraformaldehyde in PBS at pH 7.4. Segments of spinal cord 5 and 6.5mm long containing the labelled neurones were removed and placed in the same fixative for up to 8 hours. Sections (50 μ M) were cut in the sagittal plane with a Vibratome, collected in serial order, mounted in Vectashield (Vector Laboratories, Peterborough, UK) and examined with a fluorescence microscope to identify labelled neurones.

Short series of sections containing labelled neurones were processed for immunocytochemistry in serial order. Initially sections were preincubated in 10% normal donkey serum in PBS for 30 minutes. They were then transferred to a solution containing a mixture of rat anti-serotonin (5-HT) antiserum (1:200; Affiniti Research Products Ltd.) and rabbit anti-dopamine β -hydroxylase (DBH) antiserum (1:500; Affiniti Research Products Ltd.) in a standard diluting solution consisting of PBS with 5% normal donkey serum and 0.3% Triton X-100, and incubated at room temperature for 48 hours. Sections were washed in PBS and placed in a solution containing secondary antisera which consisted of Fluorescein (FITC)-donkey anti-rabbit (1:100) and cyanine 5.18 (Cy-5)-donkey anti-rat (1:100) for 1h at room temperature. These were obtained from Jackson Immunochemicals and were diluted in the standard solution. Finally, sections were washed again in PBS and mounted in Vectashield (Vector Laboratories, Peterborough, UK) and stored at -20 $^{\circ}$ C.

2.3 Confocal Microscopy

Conventional fluorescence microscopy relies upon the excitation light illuminating a large area in the x, y plane allowing the simultaneous measurement of the fluorescence emission for all points in the focal plane. Fluorescence also unavoidably excites an extended volume *above* and *below* the focal plane. This additional signal is not confined to the focal plane and blurs the image at the faceplate of the camera. This is not desirable and the out-of-focus blur degrades the contrast and distorts any attempts at quantitative measurement. Confocal microscopy focuses the excitation light onto one or more discrete points in the specimen. The laser still excites fluorescence in a cone of tissue above and below the plane of focus, but it does not cause blurring because of a physical barrier preventing this signal from impinging upon the detector. The desired in-focus fluorescence from the focal point, passes through a very small aperture in the image plane. The illumination and detection points are thus co-aligned or “confocal”. A single optical section is generated by scanning the confocal point in the x, y plane to build up an image. A series of optical sections are collected at different focus levels to constitute a three-dimensional image. The main advantage of confocal microscopy, in quantitative fluorescence measurements of physiological parameters, arises from a well-defined 3-D volume (voxel) that is sampled to form each 2-D picture element (pixel). During the point-to-point sampling the volume probed is always asymmetrical (being three to four times longer in the z-axis). To minimise the z-axis dimension, a high power objective lens is required. Optical probe dimensions are usually given in terms of full width at half maximum height in a given direction along one of the orthogonal axes. Point scanning confocal instruments can achieve a probe size of 0.2 μ m, 0.2 μ m and 0.6 μ m in the x, y, and z-axis respectively with a high numerical aperture oil immersion lens.

Sections were examined with a three-channel confocal laser scanning microscope (BioRad MRC1024). Series of images were gathered sequentially from single optical sections at 0.5 or 1 μ m intervals (11-30 planes per series) by using the 488, 568 and 647nm laser lines to excite FITC, rhodamine-dextran and Cy-5 respectively. In control experiments, where primary antisera were omitted, there was no evidence of specific immunoreactions for serotonin or DBH. The majority of images were obtained by using a times 60 oil-immersion

lens (Numerical Aperture of 1.4), however large structures such as cell bodies were examined with a times 20 dry lens and, occasionally, large dendrites were examined with a times 40 oil-immersion lens (Numerical Aperture of 1.3). After the confocal examination was completed, the dendritic trees of the neurones were reconstructed with the Lucivid/NeuroLucida reconstruction program (MicroBrightField, Inc., Colchester, Vermont). The locations of structures examined with the confocal microscope were identified from the reconstructions and the sites of the appositions related to the distances from the soma.

2.4 Analysis

Series of images from single optical sections were combined, by using Confocal Assist (Version 3.10). Confocal images of the γ -motoneurone were visualised consecutively and images from all relevant optical sections could then be superimposed, creating a projected image. Chains of immunoreactive varicosities and inter-varicosity portions of axons could be clearly distinguished, some of which surrounded the γ -motoneurone.

2.5 Counting Varicosities

Each noradrenergic and serotonergic profile in the vicinity of the γ -motoneurone was followed, frame by frame, in order to find any appositions between noradrenergic or serotonergic immunoreactive varicosities and the motoneurone membrane. Varicosities were taken to be in apposition with the γ -motoneurone when there were no intervening pixels between them and/or when there was an overlap between their contours. This lateral resolution with the times 60 lens would be about $0.17\mu\text{m}$ (theoretical resolution at λ of 500nm). Dendrites were almost always orientated obliquely to the plane of the optical sections so estimates of appositions were made from lateral relationships. Occasionally a dendrite could be seen to pass *into* the plane of the sections (z-axis). Care was taken not to repeatedly count these same varicosity in successive confocal sections. This could be avoided because the diameter of the varicosity could clearly be seen to increase to a maximum (at which point it was counted) and then decrease to a much smaller diameter, corresponding to the inter-varicosity dendrite. The varicosities were classified into three

categories: small (s), which were less than 1.5 μm in diameter; medium (m), which were between 1.5 and 3 μm in diameter, and large (l), which were 3 μm or over in diameter. These three categories were marked on a printed copy of the projected image of the optical sections (a “contour” diagram) in which they were noted by using different symbols (see 2.6 Construction of Contour Diagrams). The smallest varicosities were distinguished from any background fluorescence. Invariably, any artefacts caused by insufficient washing of the immunocytochemical stains produced very small points of immunofluorescence, which could have been mistaken for a varicosity. However these could be distinguished from true ‘s’ varicosities because they only appeared in one place for one confocal frame. Fluorescence which was accepted as a type ‘s’ varicosity was present in more than one confocal frame and in the same location.

The serotonergic and noradrenergic appositions with the γ -motoneurone *may* have been occurring by chance. In order to check this hypothesis the number of varicosities within a 5 μm wide shell around the γ -motoneurone were counted and marked upon the contour diagram of the cell. These data were used to calculate the density of varicosities in the *immediate vicinity* of the cells. If the appositions on the surface of the dendrites occurred by chance, the dendrite surface would act as a barrier to the course of the axons. If the varicosities could be freely distributed in the volume of space occupied by the dendrite, then the density of varicosities should be the same as for the surround. The number of appositions was therefore expressed as if distributed in the volume *occupied* by the dendrite (i.e. as a density/ μ^3 rather than density/ μ^2), and compared with the density of the varicosities in the immediate surround. It could then be seen if the number of apposing varicosities was a reflection of the density of those in the vicinity of the γ -motoneurone (chance occurrences), or if the γ -motoneurones were being *preferentially* targeted by monoaminergic axons. These data also allowed the quantification of the density of monoaminergic innervation in the immediate vicinity of the motoneurones.

The surface areas of the analysed parts of somata of all 8 neurones (excluding the surfaces cut by the vibratome) were calculated from the formulae for the surface areas of the corresponding 3-dimensional geometric shapes, or combinations of geometric shapes. Many of the complex shapes of the γ -motoneurone somata could be accurately represented with geometric shapes such as equivalent cylinder, segment of a sphere cut by a single plane, or by two parallel planes. Allowances were also made for the area covered by the bases of dendrites arising from the cells. By relating the number of appositions to total areas calculated, the density of the appositions was expressed as the number of appositions per $100\mu\text{m}^2$.

In some cases, parts of the somata were damaged by the sectioning. In order to estimate the total number of appositions per cell, the area of the surface of the somata as calculated above was first related to the surface of an equivalent sphere. This had a radius equal to the mean radius of the soma; the number of appositions that had actually been observed were increased by the same factor. The densities were thus extrapolated to the surface area of the equivalent sphere. This allowed a comparison with values of total numbers of appositions per soma cited for α -motoneurones (Alvarez *et al.* 1998).

Monoaminergic appositions with proximal dendrites (within a distance of $100\mu\text{m}$ from the soma) were identified in the sections containing the soma for all the γ -motoneurones. Appositions with more distal parts of the dendrites could sometimes be analysed in the same sections but usually required a reconstruction of the dendritic tree from several sections using the NeuroLucida reconstruction program. The distances along the segments of dendrites analysed were evaluated from these reconstructions. However, the distribution of the appositions as a function of the distance was only analysed for the two most strongly labelled motoneurones cell 1 and cell 2. The segments of dendrites selected for analysis were those that were fairly long in one plane. The total length of the analysed segments amounted to $7159\mu\text{m}$.

For the two most strongly labelled γ -motoneurons (cell 1 and 2), dendritic segments were analysed in four allocated compartments, divided by radial distance from the soma, rather than by path length. These were distances of 0-100, 100-200, 200-300 and >300 μm from the soma. The average density (appositions per 100 μm^2) of appositions on all suitable dendritic segments in these compartments was calculated from the total numbers of appositions. The total lengths and the average diameter of dendritic segments in each compartment were also measured in order to calculate the total surface areas. The segments of dendrites analysed belonging to the two neurons with the best labelled dendritic trees are indicated by stippling (see figure 21). The densities for individual segments of dendrite were also calculated. The number of appositions with dendrites was calculated per 100 μm length. This allowed a comparison to be made with data from group II premotor interneurons (Maxwell *et al.* 2000). The total number of appositions with dendrites was estimated by multiplying the value for unit length by the mean minimal and maximal total dendritic length of γ -motoneurons reported previously (Moschovakis *et al.* 1991). This allowed comparison with data for α -motoneurons (Alvarez *et al.* 1998). Data are presented as means \pm S.E.M. Statistical significance was determined at $P < 0.05$ using Student's t test.

2.6 Construction of the Contour Diagrams

In order to collate the information obtained whilst counting varicosities (such as varicosity size and location) a 'contour diagram' of the two best-labelled γ -motoneurons, cell 1 and cell 2 (both supplying medial gastrocnemius) was produced. This was essentially an outline drawing of the projected image of the cell. Initially the whole confocal file for each cell was projected in the Confocal Assist program. This was saved as a '.TIF' file to allow importation into the Corel 8 Graphics package. Once imported, the image was magnified to a convenient size (usually times 8) and the 'Bezier' tool selected from the menu. The image was then carefully outlined, with attention being taken to follow all undulations and irregularities in the γ -motoneurone outline. The outline was selected and pasted onto

a new background (without the original γ -motoneurone TIF file). This could then be printed and used as a convenient template on which to mark the location and size of apposing and close range serotonergic and noradrenergic varicosities.

2.7 Construction of stick diagrams

‘Stick’ diagrams of the γ -motoneurone somata and dendritic trees were constructed in order to allow the location and orientation of the segments of dendrites in the confocal images to be accurately ascribed to each γ -motoneurone. Successive vibratome sections of the spinal cord were viewed under light microscopy. The attached Neurolucida system was then used to draw the outline of the soma and any portions of dendrite. Once every vibratome section was processed in this way, the Neurolucida files were superimposed to recreate a two-dimensional rendering of the γ -motoneurone three-dimensional structure including its associated dendrite tree.

2.8 Preparative surgery for experiments on the effects of fentanyl

2.8.1 Selection and Care

Male Sprague Dawley rats weighing between 250-570g were selected. They were kept in a darkened, quiet room to avoid stressing them in any way prior to anaesthesia. They were given free access to food and water.

2.8.2 Anaesthesia

Each rat was anaesthetised with intraperitoneally injected urethane at a dose of 170mg per 100g body mass. Depth of anaesthesia was regularly and frequently checked by use of the flexion-withdrawal and corneal reflexes. Since rats vary in their response to urethane, approximately three quarters of the dose was given first. This immobilised the rats, but usually a withdrawal and a corneal reflex were still present. Fractions of the remainder of the dose were then given intraperitoneally until the reflexes were abolished. Usually the rats did not require more than the measured dose. If the reflexes were still present it was

preferable to allow longer for the anaesthetic to take effect. Animals given additional urethane invariably became too deeply anaesthetised to elicit physiological responses.

2.8.3 Perioperative Temperature Regulation

The body temperature of the rat was maintained at 37°C by placing it on a thermostatically controlled heating blanket.

2.8.4 Formation of Tracheostomy

A pretracheal midline incision was made through the skin. The skin was retracted and the muscles covering the trachea were separated by means of blunt dissection, exposing a section of trachea approximately 7-10mm in length. A white cotton thread was passed behind and around the trachea with forceps. An incision was made between two cartilaginous rings, rostral to the thread and an appropriately sized, plastic cannula was slipped in through this incision and tied into position by means of the thread. The incision was then closed by means of Michel suture clips.

2.8.5 Femoral Arterial and Venous Cannulation

The right femoral artery was cannulated by separating it from the femoral nerve and vein over the upper part of the thigh. Two lengths of suture thread were passed under the artery at the lower and upper ends of the free artery section. The lower thread was tightened, ligaturing the artery securely. An artery cannulation clip was applied above the second thread thus isolating a small section of artery from the systemic circulation. A small incision was cut between the ligature and artery clip and a pink Portex luer nylon cannula, filled with heparinised saline, and bubble-free, was inserted into the artery and pushed 1-1.5 centimetres toward the heart. The upper suture thread was then tied securely around the cannula, fixing it in place, and the artery clip was removed. The cannula was then connected to an in-house produced pressure transducer, which had been calibrated previously, and the output displayed on an oscilloscope and recorded.

The right femoral vein was also cannulated by a cannula filled with physiological saline. A three-way tap was connected to this, which allowed intravenous access as required.

2.8.6 Laminectomy

The purpose of the laminectomy was to expose the spinal cord in the lower lumbar and sacral regions without damage to the cord or its spinal roots and with minimal blood loss.

A midline skin incision was made over the vertebral column from about L3 to S3. The skin was freed from the fascia by blunt dissection and then two parallel incisions were made either side of the dorsal processes, approximately the same length as the skin incision. The transversospinalis muscles were carefully removed. The laminectomy was performed by opening the joints between the vertebrae while gripping the spinous process of the more proximal vertebra with forceps. The spinous process was removed and then the laminae of the vertebral arch with bone nibblers. This procedure was repeated for each vertebra. The cord and cauda equina was then covered with a saline soaked swab.

A muscle nerve branch, which supplied the most rostral slip of the longissimus caudae muscle, was then dissected free. A pool of liquid paraffin over the exposed cord was enclosed by a strip of X-ray film and attached to the skin with Michel clips.

2.8.7 Preparation of the spinal cord for recording

The dura over the exposed cauda equina was cut, and the muscle nerve, and the corresponding dorsal and ventral roots were raised up in the paraffin over recording electrodes for recording in continuity (see figure 12).

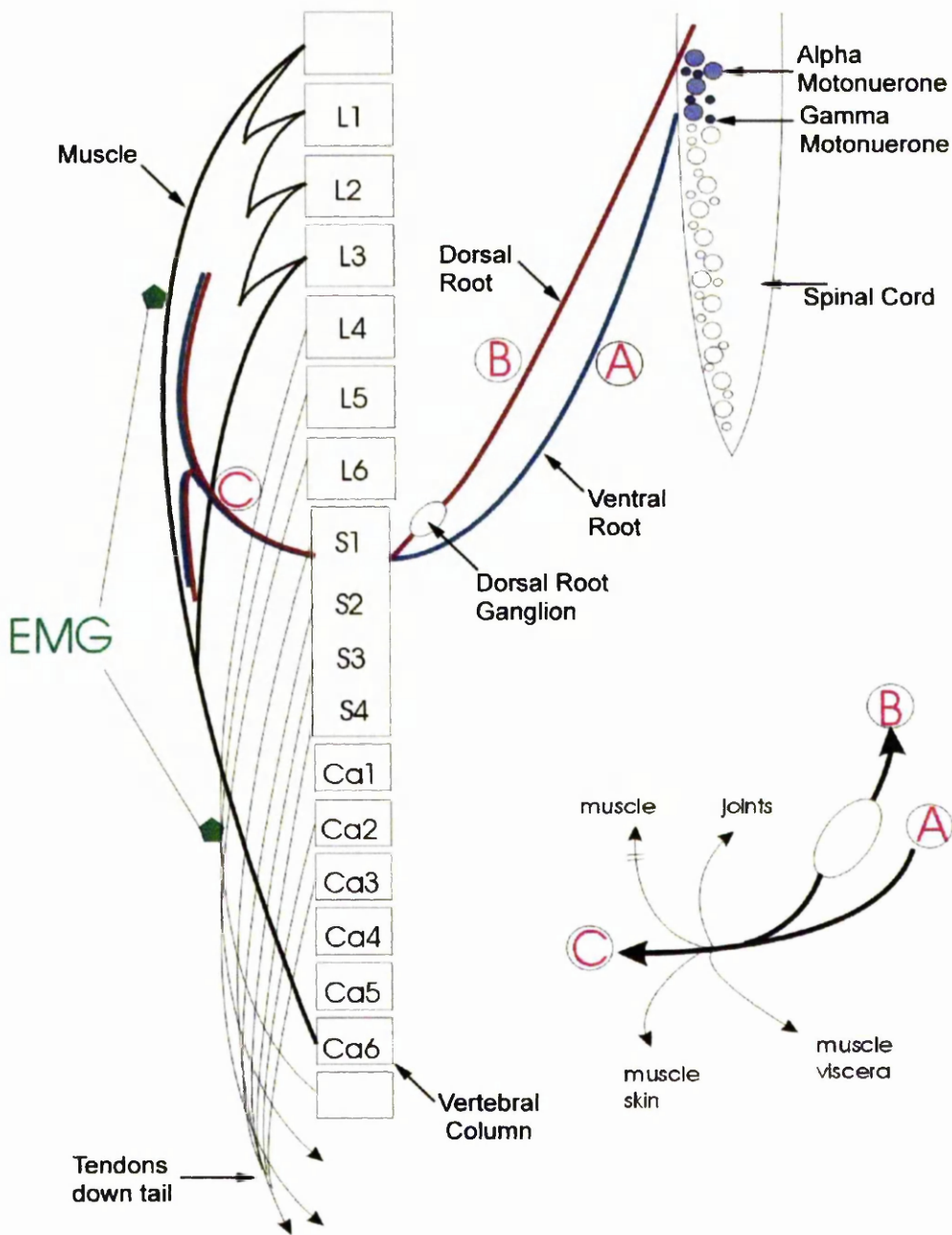


Figure 12. The caudal end of the spinal cord on the upper right shows diagrammatically, α -motoneurons and γ -motoneurons which supply the whole of the left longissimus caudae muscle in the ventral horn. The ventral and dorsal roots are indicated. Slips of this muscle are shown on the upper left with their origins at various lumbar vertebrae and their slips inserting toward the tail vertebrae. A and B show where platinum recording electrodes were placed on the ventral and dorsal roots, and C shows the point at where the recording was made from the muscle nerve on the ipsilateral side.. EMG recordings were made from the surface of the muscle as indicated by the green hexagons. The inset to the bottom right shows diagrammatically the relation of the nerve supply of the muscle slip with that of the surrounding tissues.

Electromyographic (EMG) electrodes were placed on the surface of the muscle slip on either side of the nerve entry. A thread was tied to the tendon of the slip (without cutting the tendon) for stretching the muscle in order to excite muscle afferents. Recordings from these four sources (electrodes on the S1 dorsal and ventral roots, muscle nerve and the EMG) were amplified and filtered using a Neurolog System (Digitimer Ltd.), digitised with a PCM-8 VCR Recorder Adaptor (Medical Systems Corp., NY), and stored on magnetic tape. Also recorded simultaneously were the tidal volume (CS5T, G.M.Inst. Ltd), F_{ET, CO_2} (fraction, end tidal carbon dioxide) and F_{ET, O_2} (fraction end tidal oxygen) (Normocap, Datex 200 *oxy*) and the blood pressure. The stored data was analysed off-line with Spike 3 software (Cambridge Electronic Design, Ltd.).

α -activity was detected a) from the presence of any spikes in the nerve branch with a conduction velocity $>20\text{m s}^{-1}$ (established by spike-triggered averaging between the nerve branch and corresponding ventral root), b) by EMG recording from the surface of the muscle slip, and c) by monitoring dorsal root and muscle afferents: the muscle shortening due to muscle contraction diminished or stopped on-going afferent activity. Reduction in afferent activity recorded in the nerve branch supplying the most rostral slip of the longissimus caudae muscle could indicate contraction in neighbouring slips which are arranged in parallel to it. Spikes recorded from the muscle nerve branch were accepted as occurring in γ -axons if the initial deflection of the spike was in the opposite direction to simultaneously recorded afferent spikes, and if the conduction velocity, measured by spike-triggered averaging in the ventral root, was $<20\text{m s}^{-1}$. However, extracellularly-recorded γ -spikes recorded in rat peripheral nerves are very small. It was frequently not possible to discriminate probable spikes from noise. Since no, or very little tonic afferent activity was recorded in the muscle branch when the tail was placed straight, the sudden onset of afferent activity without any change in muscle length, together with some definite γ -spikes (in that they were smaller than afferent spikes, preceded afferent spikes, and had an initial deflection contrary to that of afferent spikes) was taken to indicate the presence of unrecordable γ -activity. In such cases the variations in afferent activity could be assumed to indicate fluctuations in γ -output.

2.8.8 Tests of γ -activity before fentanyl administration

The pinna reflex (Sherrington, 1917; Granit *et al.* 1952) was elicited by gently stroking the walls of the external auditory meatus with a soft flexible plastic probe. Pharyngeal stimulation was by means of a blunt glass probe, which was slid through the mouth. Another test was simply to occlude the airway by clamping the tube leading to the tracheal cannula with Spencer Wells forceps.

2.8.9 Fentanyl administration

Fentanyl citrate (Sublimaze, 50 μ g ml⁻¹, Janssen-Cilag Ltd., High Wycombe, U.K.) was injected slowly intravenously in doses of 30-90 μ g kg⁻¹ body weight. Additional increments were sometimes necessary to keep the rats apnoeic, since fentanyl was metabolised quite quickly.

2.8.10 Preparation of Gas Mixtures

Three gas mixtures were used in the experimental protocol. These were a hypoxic mixture, a hypercapnoeic mixture and a hypoxic/hypercapnoeic mixture. The hypoxic mixture was made by placing a small volume of 100% oxygen (BOC Gases) into an empty, small animal, Douglas bag. 100% nitrogen (BOC Gases 100% oxygen free) was then added to the bag, incrementally. Care was taken to allow the gas to fully mix and a small quantity of it was purged through the connecting tubing to ensure that a gas mixture from the bag, and not a pure gas from the source cylinder, was being analysed. Regular checks of the gaseous composition were made by piping small quantities of the Douglas bag gas into the Normocap Datex 200 *oxy*. The oxygen content was adjusted to 10%. The connecting tubing was then firmly clamped closed to prevent leakage. To produce a hypercapnoeic mixture, carbon dioxide was added to a Douglas bag containing atmospheric air and the same equilibrating and testing process was repeated as before. The correct hypercapnoeic mixture was obtained when the carbon dioxide level was at 5%. The hypoxic/hypercapnoeic mixture was made by first producing a hypoxic mixture as

described previously, and then adding carbon dioxide until 5% of this was present in the hypoxic mixture.

2.8.11 Administration of Gases

The gas mixtures were administered to the animal by slipping the end of the connecting silastic tubing onto the inlet valve of the small animal ventilator (Harvard Apparatus Rodent Respirator 680). The tubing was sufficiently small to allow a gas tight fit over the inlet valve. The clamp was quickly released in order to prevent any discontinuity in gas flow to the animal.

After using the gas mixture, the reintroduction of atmospheric air to the animal was achieved by removing the connecting tube from the ventilator inlet valve.

3 Results

A total of eleven γ -motoneurons were ionophoretically injected with rhodamine-dextran. Eight of these were successfully labelled, three in the first cat and five in the second.

These eight γ -motoneurons innervated muscle spindles of flexor digitorum longus (FDL) (γ -motoneurons number 7 & 8), lateral gastrocnemius/soleus (LGS) (γ -motoneurone number 6), medial gastrocnemius (MG) (no. 1-5, see Table 3). Their axons conducted at 23-34 ms^{-1} (see Table 1) which is within the range for γ -motoneurons. Group II afferents provided input to all of these neurones. Two neurones (cells 2 and 3, Table 1) were excited by group II afferents at latencies compatible with monosynaptically evoked actions, while the remaining neurones were excited and/or inhibited at longer latencies.

Records from the two neurones, which were most extensively studied (cells 1 and 2), are shown below, in Fig. 13 A-D. Fig. 13A and C illustrate the collision technique (as described in Methods) used to prove that the antidromically evoked spike potentials occur in the same γ -motoneurone as spikes evoked synaptically or occurring spontaneously.

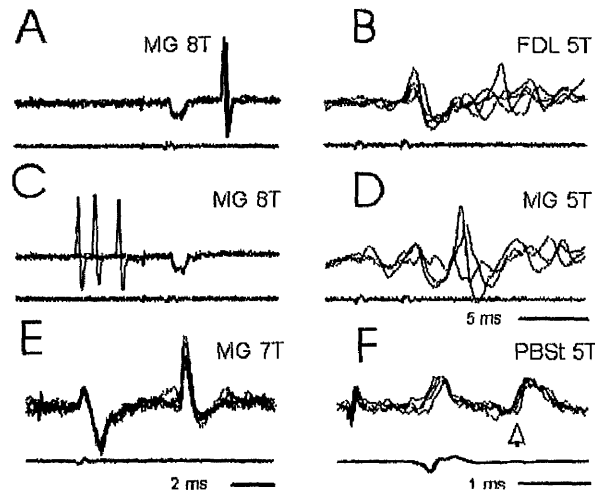


Figure 13. Examples of responses of γ -motoneurone number 1. In each case the upper record is from a γ -motoneurone (extra- or intracellularly); the lower record is from the spinal root, showing the timing of the arrival of the Ia volley, and in some cases also the stimulus artefact. A and C records just before penetration of the neurone illustrating collision of antidromically evoked responses (in A) by background discharges. In C three background spikes occurred during the critical period for collision (records superimposed and each time no antidromic spike was elicited). B and D: PSP's evoked polysynaptically by double stimuli applied to the flexor digitorum longus (B) and medial gastrocnemius nerves (D) at a strength sufficient to recruit group II muscle afferents. E and F: antidromically evoked blocked spikes (E) and monosynaptically evoked EPSPs (arrow, F) γ -motoneurone number 2. Time calibrations: 5 ms for A-D, 2 ms for E and 1 ms for F. Stimulus strength is indicated as a multiple of T, threshold strength for exciting Ia afferents.

The antidromically propagated spike (i.e. travelling toward the soma) seen in A was blocked in C on three occasions by orthodromically propagating discharges (away from the soma) 'background' spikes. This indicates all the spikes were recorded from the same γ -motoneurone. After penetrating cell number one, double stimulus pulses, at short intervals, were applied to the FDL and MG muscle nerves (Figure 15 B and D) at strengths sufficient to recruit group II muscle afferents. Double pulses were employed to increase the probability of recording responses. The latencies of the PSPs evoked by these stimuli indicated that polysynaptic pathways were involved since a monosynaptic pathway would have had a much shorter latency (Gladden *et al.* 1998) for estimates of latencies too short for disynaptic transmission). The intracellular records shown in figure 15 E and F were from γ -motoneurone number 18. Figure 15E shows the blocked antidromically propagated spike recorded when the MG muscle nerve was stimulated. In figure 13F, stimulation of the hamstring nerve at group II muscle strength elicited EPSPs (indicated by arrow) at

latencies which are too short for an interneurone to be interposed in the pathway. These responses, and those of the other labelled cells, were representative of the responses shown by the whole population of 76 γ -motoneurones and already reported (Gladden *et al.* 1998).

3.1 Serotonergic immunoreactive fibres

Serotonergic immunoreactive fibres were abundant in the ventral horns in both cats. The serotonergic immunoreactive fibres appeared to course through the sections in definite strings. These were punctuated by bead-like swellings, or varicosities. The varicosities were separated into three size ranges. Figure 14 shows the background immunoreactivity and examples of varicosities in the three chosen ranges. (See Methods section 2.5). Serotonergic appositions with a labelled γ -motoneurone are illustrated in figure 15.

α -motoneurones frequently have a 'corona' of serotonergic immunoreactive fibres surrounding their somata. For example, Westlund *et al.*, (1983) reported this arrangement associated with 'large motoneurones' (presumably α -motoneurones). This was not observed for any of the γ -motoneurones labelled in this study.

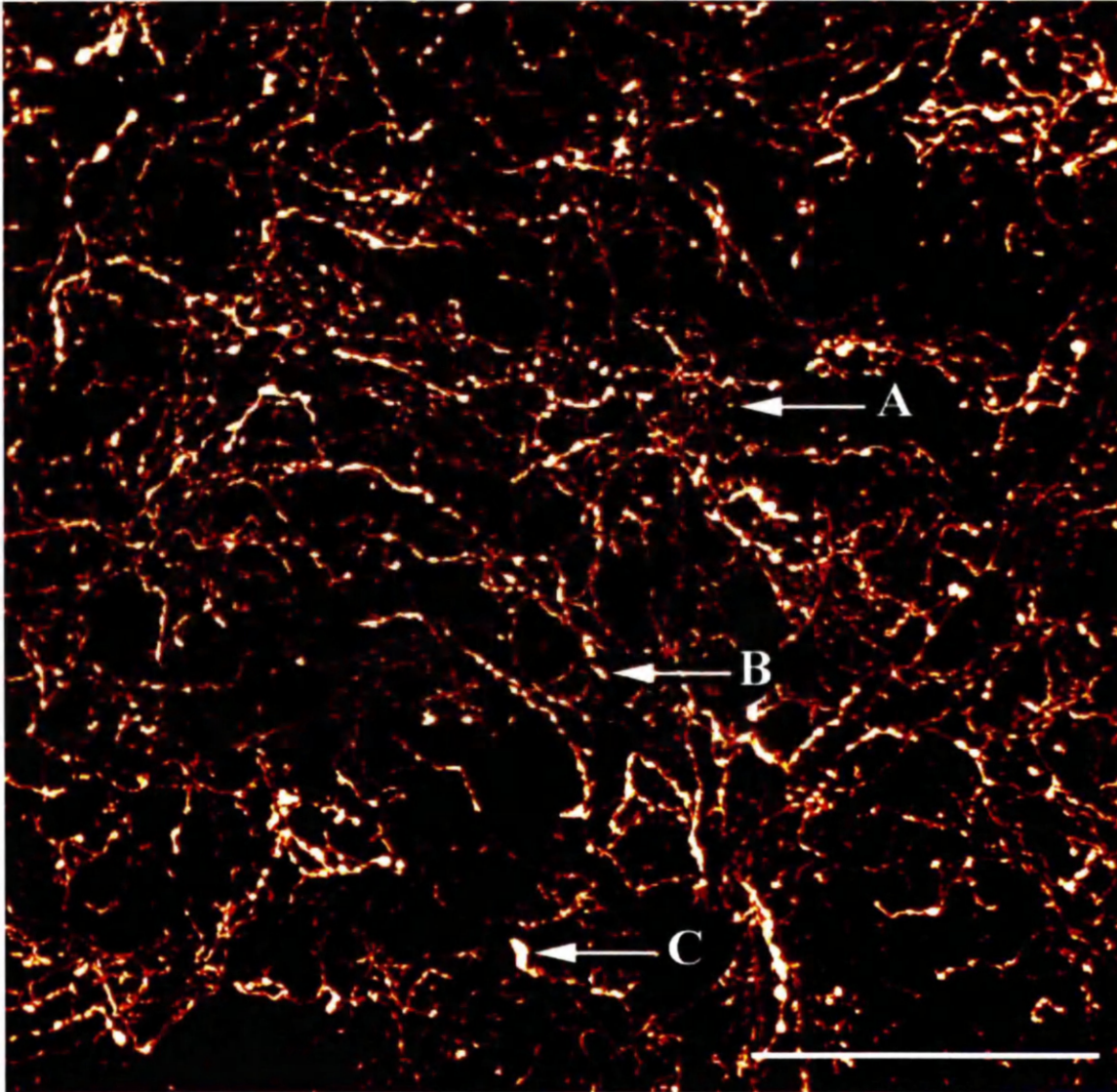


Figure 14. A projected pseudocolour confocal image of typical serotonergic axons present in the vicinity of γ -motoneurons. The arrows indicate varicosities on serotonergic axons. A: small varicosity, B: medium sized varicosity and C: large varicosity. The varicosities are sometimes seen to be connected by segments of axon. The density is much greater than for noradrenergic axons and varicosities (see figure 17). Scale bar = 150 μ m.

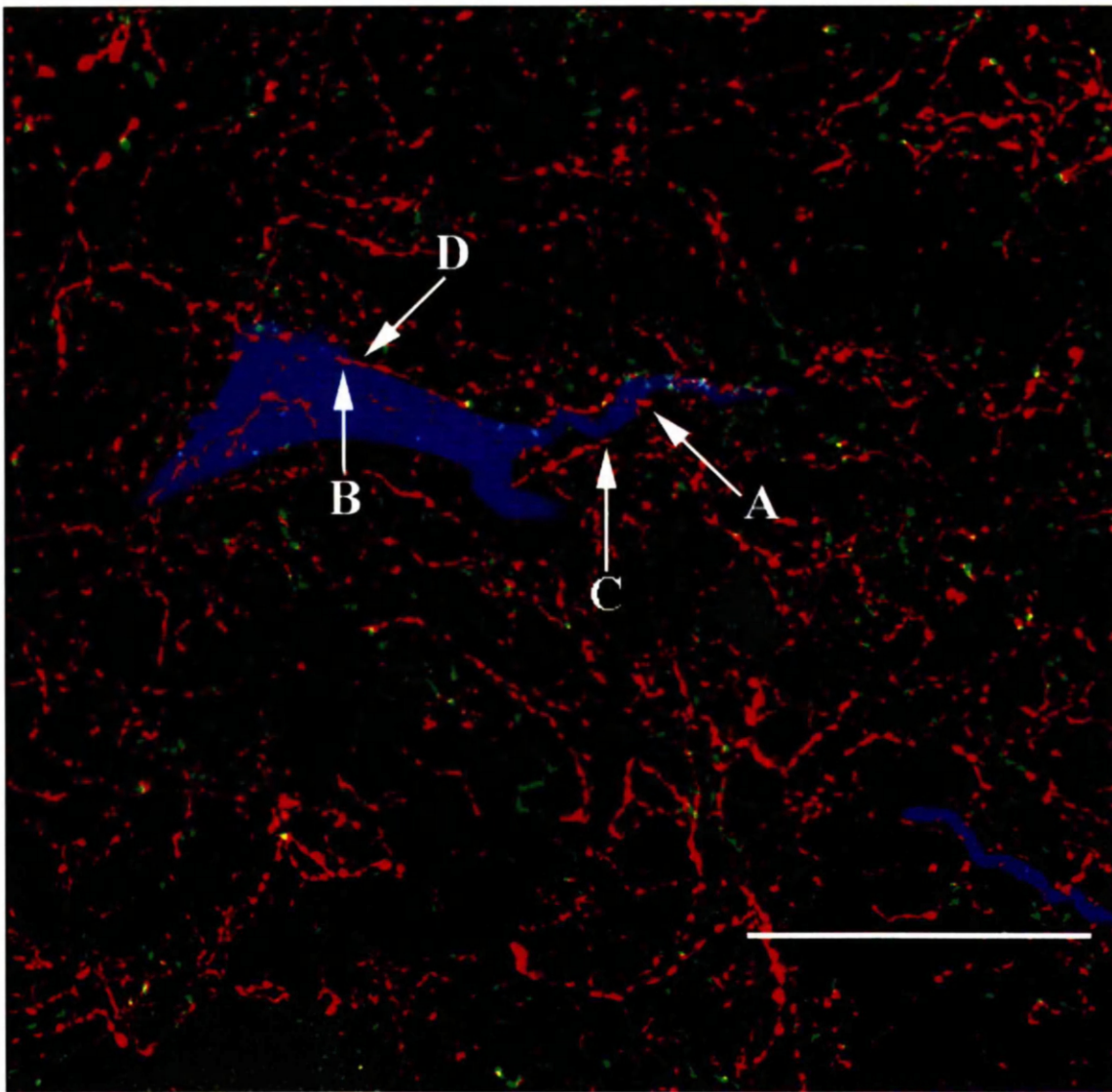


Figure 15. Serotonergic appositions with part of γ -motoneurone 1. A projected, pseudocolour confocal image of a γ -motoneurone (blue) surrounded by serotonergic axons and varicosities (red) and noradrenergic axons and varicosities (green). A: large varicosity which can be seen making an apposition with a proximal dendrite. B: varicosity which is part of a string of such varicosities making an apposition with the soma of the γ -motoneurone. C: varicosity which is coming into close proximity to a proximal dendrite but intervening pixels indicate that it is not in apposition. This varicosity is within $5\mu\text{m}$ of the soma. D indicates a section of inter-varicosity axon. Scale bar = $150\mu\text{m}$.

3.2 Dopamine β -hydroxylase immunoreactive fibres

Figure 16 shows DBH-immunoreactive varicosities in the vicinity of a γ -motoneurone, in fact the same area of the ventral horn as for figure 14. The same colouring as for figure 15 has been chosen to facilitate comparison with background serotonergic immunoreactivity. DBH immunoreactive axons can be seen coursing through the section, but their paths are generally less distinct than the serotonergic immunoreactive axons and it was generally difficult to follow their paths for any distance. The DBH immunoreactive varicosities were separated into the same three size categories as for the serotonergic immunoreactive fibres (see figure 14).

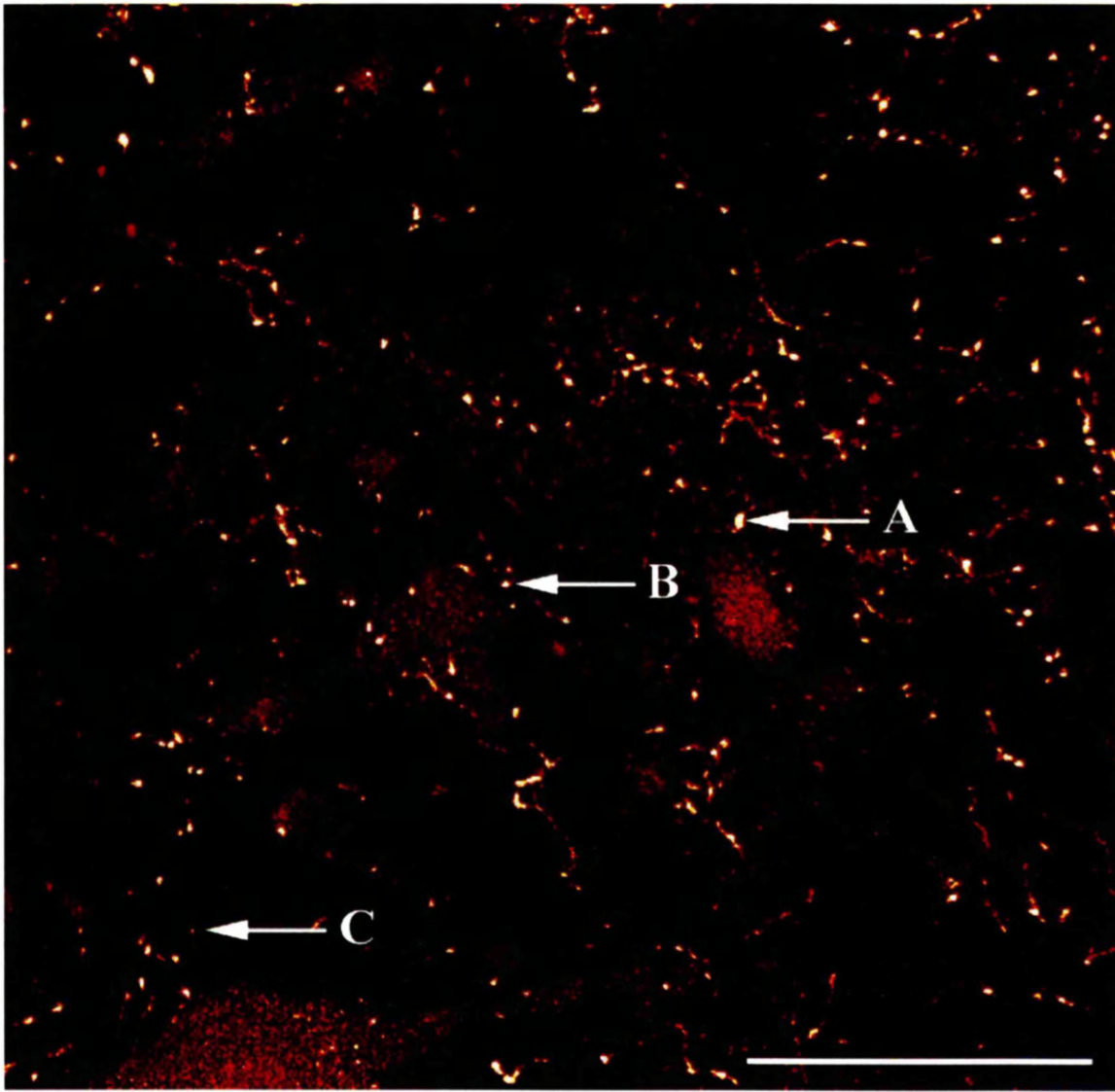


Figure 16. A projected pseudocolour confocal image of typical noradrenergic axons in the vicinity of a γ -motoneurone. The density of axons can be seen to be generally less than for serotonergic axons. A: large varicosity B: medium varicosity and C: small noradrenergic varicosity. Few inter-varicosity segments of axon can be seen in this image and this is typical for noradrenaline. Scale bar=150 μ m.

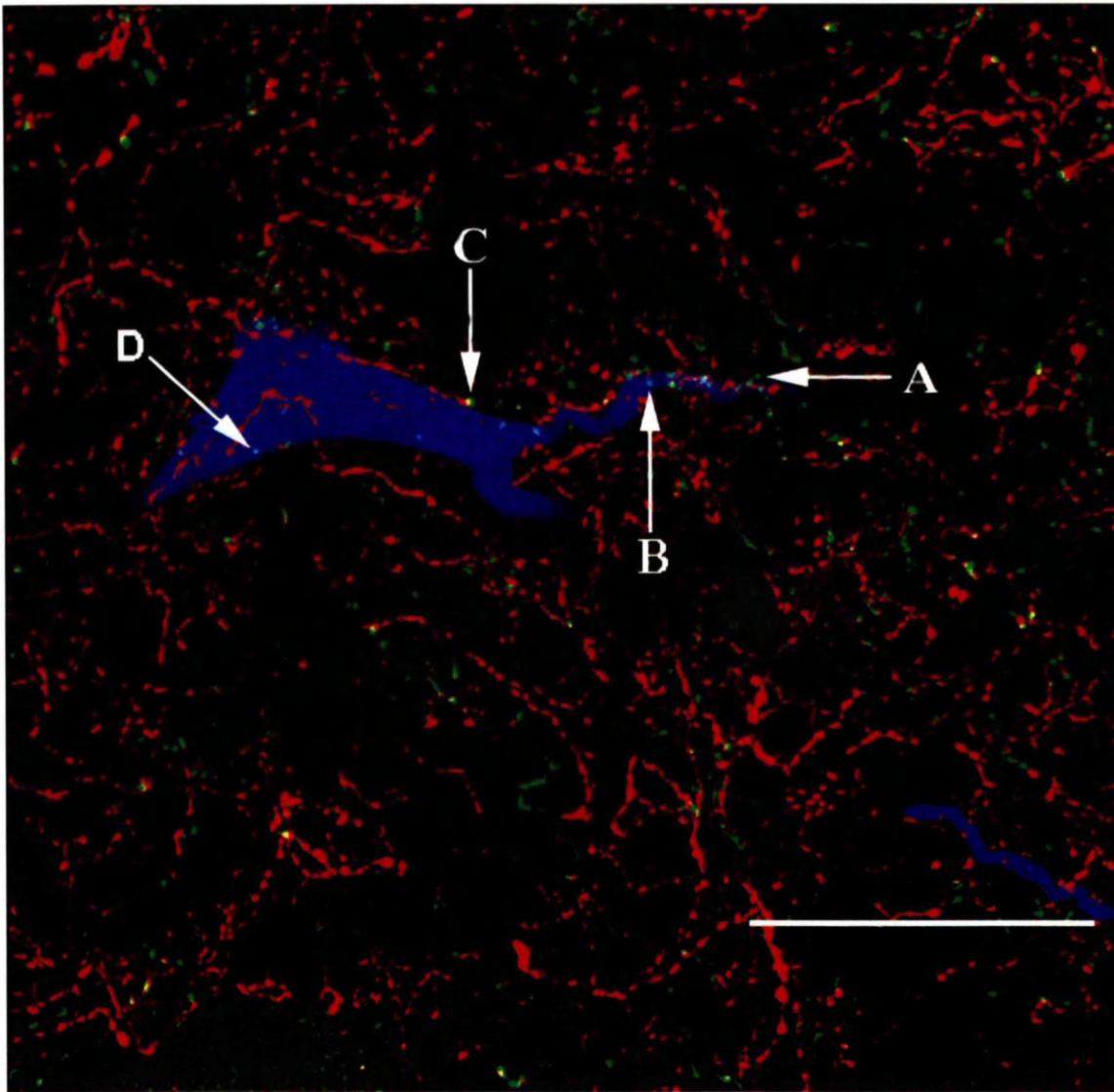


Figure 17. Noradrenergic appositions with part of γ -motoneurone number 1. A projected, pseudocolour confocal image of a γ -motoneurone (blue) surrounded by noradrenergic axons and varicosities (green) and also serotonergic axons and varicosities (red). A: a noradrenergic varicosity within $5\mu\text{m}$ of the surface membrane of proximal dendrite. B: a noradrenergic varicosity in apposition with a proximal dendrite. C: indicates a noradrenergic varicosity within $5\mu\text{m}$ of the soma of the γ -motoneurone. A few yellow pixels can also be seen close to the arrowhead. This could misleadingly be interpreted as co-localisation of serotonin and noradrenaline. However, this interpretation is unreliable since this is projected image and the yellow colour is likely to be an artifact produced by the overlap of serotonergic and noradrenergic varicosities in different optical section. D: a noradrenergic varicosity in apposition with the soma of the γ -motoneurone. Scale bar = $150\mu\text{m}$.

3.3 Appositions

3.3.1 Cell bodies

All the labelled γ -motoneurones cell bodies were found to have appositions from DBH immunoreactive and serotonergic nerve terminals. Examples of their distribution are shown in figure 18 *A-D*. The majority of the apposing varicosities were small, their diameters being typically less than 5 μ m. On all γ -motoneurones, over 60% of DBH immunoreactive varicosities were small and over 60% of the serotonergic immunoreactive varicosities on five out of eight γ -motoneurones were small. However, cell 1 did have an unusually high proportion of large serotonergic immunoreactive varicosities apposing the cell body (Fig.18*A* and 18*C*), and cell 2 had the highest proportion of large DBH immunoreactive varicosities (Fig. 18*B* and 18*D*). Interestingly, this variation in size distribution of apposing varicosities on the γ -motoneurone 1 and 2 was not reflected in the proportions of the different sizes of varicosity in the immediate vicinity of the somata (see later).

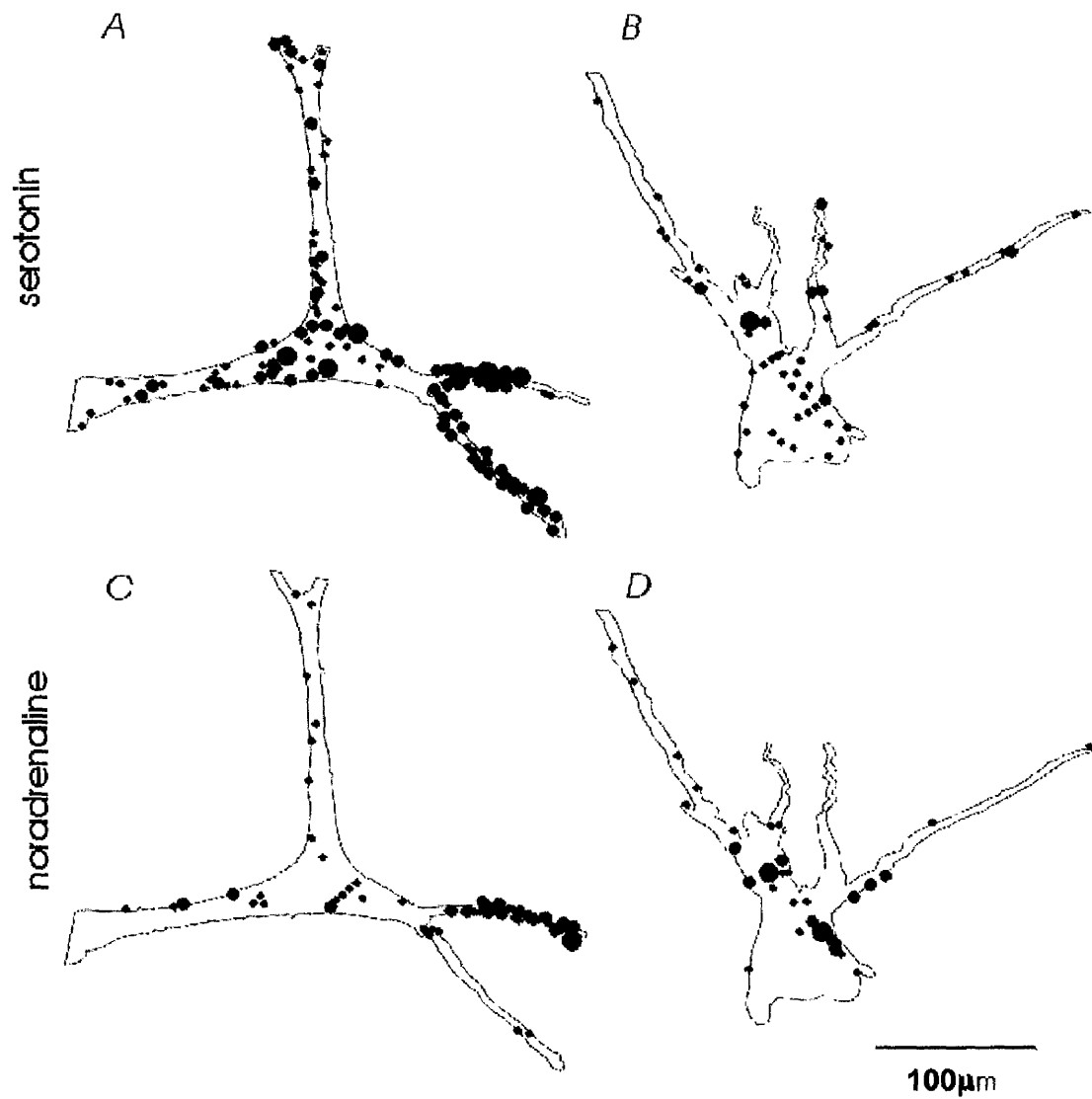


Figure 18. Distribution of serotonin and DBH immunoreactive varicosities in apposition to the cell bodies and proximal parts of the dendrites of γ -motoneurons 1 and 2 of Table 1. Note that appositions of all three size categories (small, intermediate and large, indicated by three sizes of filled circles) were present on both somata and dendrites. Also, note the clustering of serotonergic appositions on the two proximal dendrites on the right side of cell 1, in A, and of noradrenergic appositions on the upper of these dendrites in C

The mean density of noradrenergic appositions was 0.60 ± 0.10 per $100\mu\text{m}^2$ and of serotonergic appositions was, 1.12 ± 0.11 per $100\mu\text{m}^2$ soma cell membrane (see Table 4). There was little variation in these values between γ -motoneurons. In fact, the highest and lowest densities of varicosities in apposition with the γ -motoneurone soma, only differed by a factor of two. The only exception was the very low density of DBH immunoreactive appositions on cell 6 from the LGS motor nucleus. This was ten times less than that of the γ -motoneurone with the highest density. The *mean* number of serotonergic appositions found on the somata was 18.7 ± 4.0 (range 7-38 per cell). However, since the entire surface areas could not be reliably analysed in every case (see section 2.4) the count of appositions *underestimates* the total number. Estimates of the total number of appositions were made from the actual number of contacts per $100\mu\text{m}^2$ somata membrane that were present in the confocal images. These results were then extrapolated when an estimate of the total surface areas of the γ -motoneurone was calculated from the mean diameters of the γ -motoneurons (see section 2.4). The estimated mean total number of serotonergic appositions per soma was 31.6 ± 3.25 (range 22-44, see Table 4). The mean number of DBH immunoreactive appositions was 9.3 ± 3.0 , range 1-25 per cell and the estimated mean total number was 15.1 ± 3.17 (range 2-25).

Table 4. Comparison of densities of serotonergic and noradrenergic appositions on somata and dendrites of 8 γ -motoneurones

		Individual γ -motoneurones								Total	
		Number / motor nucleus / conduction velocity (ms^{-1}) / varicosities in apposition								Mean or *average	S.E.M.
Fibre	Density of appositions- ($100\mu\text{m}^{-2}$) Motor nucleus----- conduction velocity----- (ms^{-1})	1	2	3	4	5	6	7	8		
		MG	MG	MG	MG	MG	LGS	FDL	FDL		
		28	29	34	25	23	31	24	26		
5-HT	Soma	1.2	1.5	0.7	1.5	0.9	1.4	1.0	0.8	1.12	0.11
	Dendrites 0-100 μm	1.1	1.0	0.6	0.9	1.5	0.7	1.2	1.0	0.99	0.11
	Dendrites 100-300 μm	1.3	1.1	0.8	-	-	0.6	0.6	1.1	0.90	0.11
	Dendrites >300 μm	0.58	0.59	-	-	-	-	-	-	*0.58	-
NA	Soma	0.85	0.72	0.59	0.36	0.75	0.08	0.39	0.83	0.59	0.10
	Dendrites 0-100 μm	0.5	0.8	0.6	0.6	0.4	0.5	0.9	0.7	0.61	0.06
	Dendrites 100-300 μm	0.5	0.8	0.6	-	-	0.6	0.4	0.5	0.57	0.05
	Dendrites >300 μm	0.26	0.36	-	-	-	-	-	-	*0.31	-

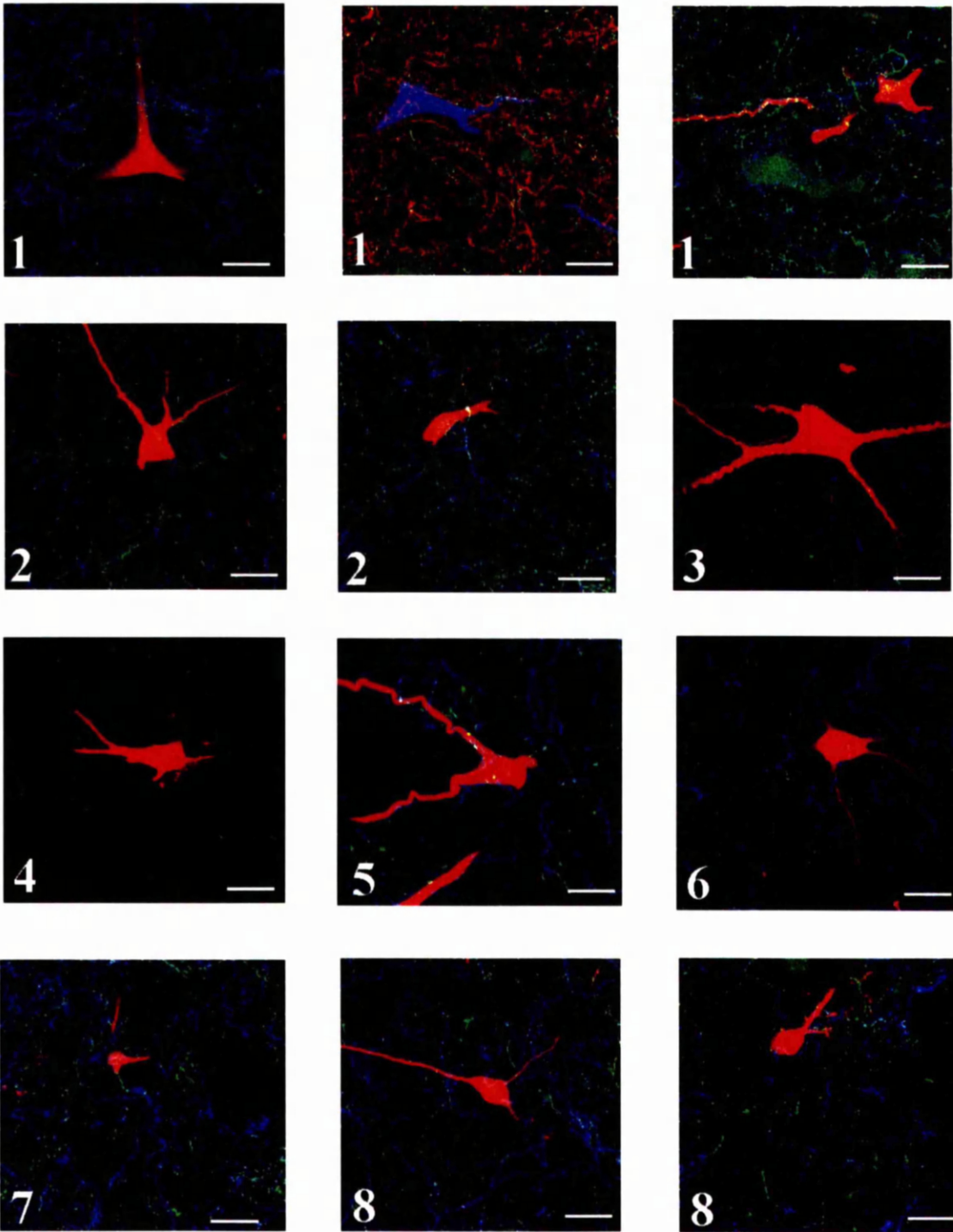


Figure 19.

Figure 19 shows confocal images of γ -motoneurons and their associated serotonergic and DBH immunoreactive fibres. With the exception of the upper middle image, all structure shown in red are γ -motoneurone, all structures in green are DBH immunoreactive and all structures shown in blue are serotonergic immunoreactive. In the upper middle image all blue structures are γ -motoneurone, all red structures are serotonergic and all green structures are DBH immunoreactive. Scale bar = 50 μ m.

1- γ -motoneurone 18, medial gastrocnemius, conduction velocity (cv) = 28 ms^{-1}

2- γ -motoneurone 8, medial gastrocnemius, cv = 29 ms^{-1}

3- γ -motoneurone 10, medial gastrocnemius, cv = 34 ms^{-1}

4- γ -motoneurone 6, medial gastrocnemius, cv = 25 ms^{-1}

5- γ -motoneurone 16, medial gastrocnemius, cv = 23 ms^{-1}

6- γ -motoneurone 7, lateral gastrocnemius/soleus, cv = 31 ms^{-1}

7- γ -motoneurone 10, flexi digitorum longus, cv = 24 ms^{-1}

8- γ -motoneurone 11, flexi digitorum longus, cv = 26 ms^{-1}

3.3.2 Dendrites

Noradrenergic and serotonergic appositions occurred with the dendrites of every γ -motoneurone studied. However there was no discernible relationship between them. In some dendritic segments both noradrenergic and serotonergic appositions were present in close proximity (Fig. 20 C and D). In other areas serotonergic appositions were present almost exclusively (Fig.20 E and F). Only rarely were there predominantly DBH immunoreactive appositions on a dendrite (Fig. 20 G and H). The clustering of appositions is also illustrated by the mapping of appositions on the dendrites to the right of the reconstruction of cell 18 (Fig.18 A and C). The lower right dendrite has dense serotonergic but sparse noradrenergic appositions, but the reverse is true of the distal part of the upper right dendrite. This tendency for clustering of appositions resulted in a marked variability in the densities of appositions for individual segments of dendrite.

The average densities of serotonergic and DBH immunoreactive terminals in apposition to the two best labelled γ -motoneurones remained fairly constant within a 300 μ m radial distance from the somata. However this density decreased at distances further than 300 μ m from the soma (figure 21E and F, and Table 4). In both cases this decrease in density was statistically significant. For the whole sample of γ -motoneurones, the mean density of serotonergic appositions with dendrites was 0.91 ± 0.07 per 100 μ m², and the value for noradrenaline was 0.56 ± 0.04 which is 62% of the mean for serotonergic appositions. Average densities of appositions for each of the 8 γ -motoneurones studied are given in Table 4. The total numbers of serotonergic immunoreactive varicosities designated as appositions in each of the radial distances studied (0-100, 100-200, 200-300 and >300 μ m from the soma see figure 22) were 280, 189, 123 and 126 respectively. The corresponding numbers of DBH appositions were 178, 140, 47 and 54 respectively.

The *total number* of serotonergic varicosities in apposition to dendrites was *estimated* to be 157-843. This was calculated from the mean number of appositions over the first 300 μ m ($11.8 \text{ } 100 \text{ } \mu\text{m}^{-1}$), and mean total lengths of 13,296 and 71,421 μ m of dendrites of small

and large γ -motoneurons (according to Moschovakis *et al.* 1991). The total number of DBH immunoreactive varicosities in apposition was estimated in the same way to be 103-552, taking into account the mean number of appositions over the first 300 μ m of 7.73/100⁻¹ μ m.

The majority of serotonergic immunoreactive varicosities in contact with dendrites were small, as was the case with those in apposition to the somata. When the percentages of the different sizes of serotonergic varicosities at the four distances from the somata were compared for all the γ -motoneurons, it was found that a minimum of 50% of serotonergic appositions were small in size, and for noradrenergic varicosities a minimum 65% were small. The percentage of small appositions tended to rise with increasing distance from the γ -motoneurone soma. At a distance of over 300 μ m from the soma, practically all appositions were small.

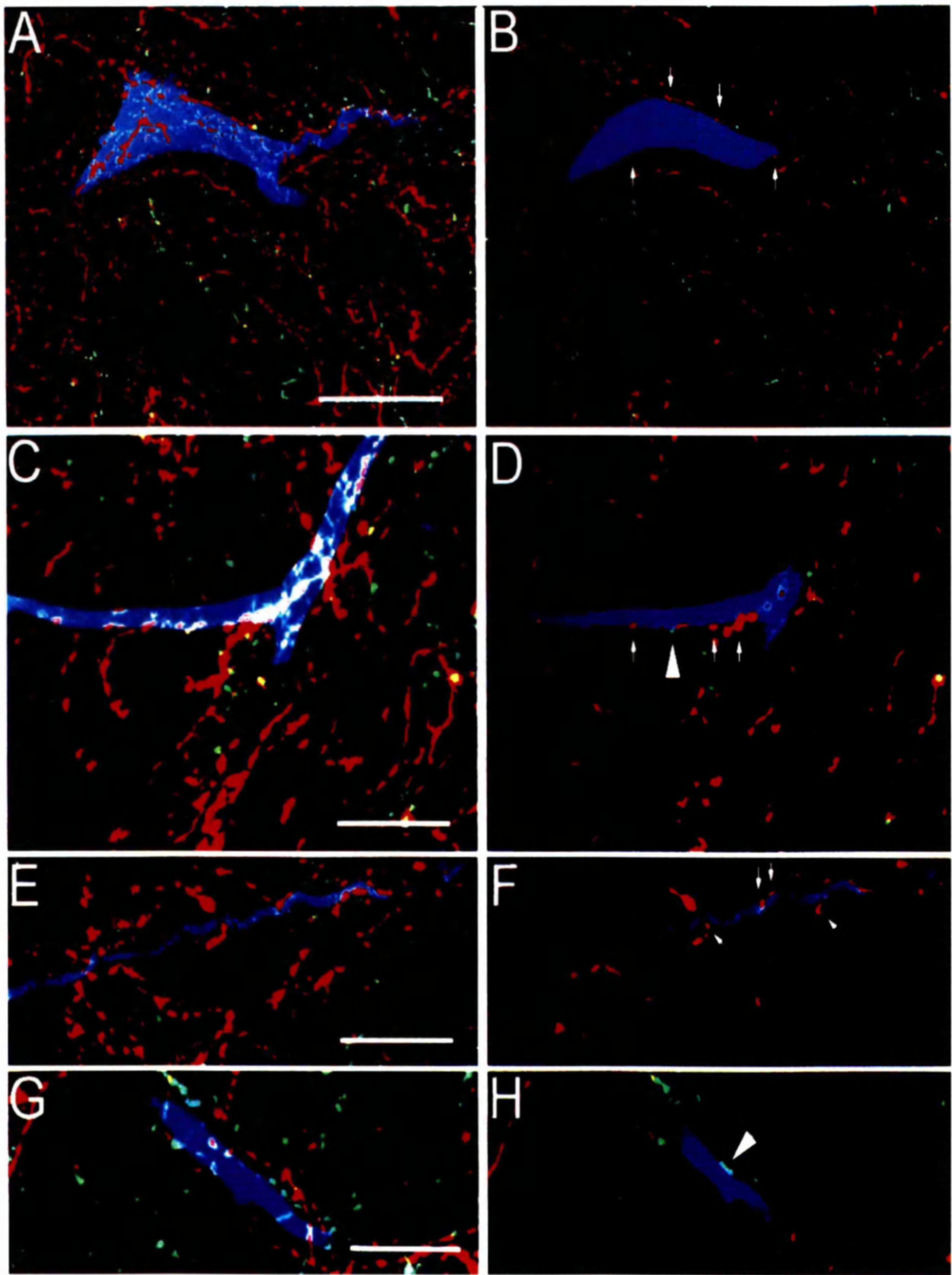


Figure 20

Figure 20 (Previous page). Examples of appositions between serotonergic (red) and DBH immunoreactive fibre terminals and a rhodamine-dextran-labelled γ -motoneurone. A: a projected image (21 optical sections) showing part of the soma and the most proximal parts of dendrites of a γ -motoneurone (cell 1) in planes across as well as just above and just below the neurone. B: appositions between serotonergic varicosities (arrows) and the soma shown in a single optical section across the neurone from the projected series illustrated in A. C: a projected image of part of one of the dendrites of the same γ -motoneurone (200-300 μ m from the soma; 15 optical sections). D: one of the optical sections from the projected series C showing appositions between this dendrite and serotonergic axons (arrows) and a single small DBH varicosity (arrowhead). E: a projected image of a distal part of the same dendrite as in C (>300 μ m) from the soma; 18 optical sections). F: a single optical section from the projected series in E showing appositions between serotonergic axons (arrows). G: a projected image of a dendrite of another γ -motoneurone (cell 1) 200-300 μ m from the soma (20 optical sections). H: a single optical section from the series shown in G. It shows appositions between DBH varicosities and dendrites (arrowheads). Scale bar = 50 μ m for A and B and 20 μ m for C, D, E, F, G and H.

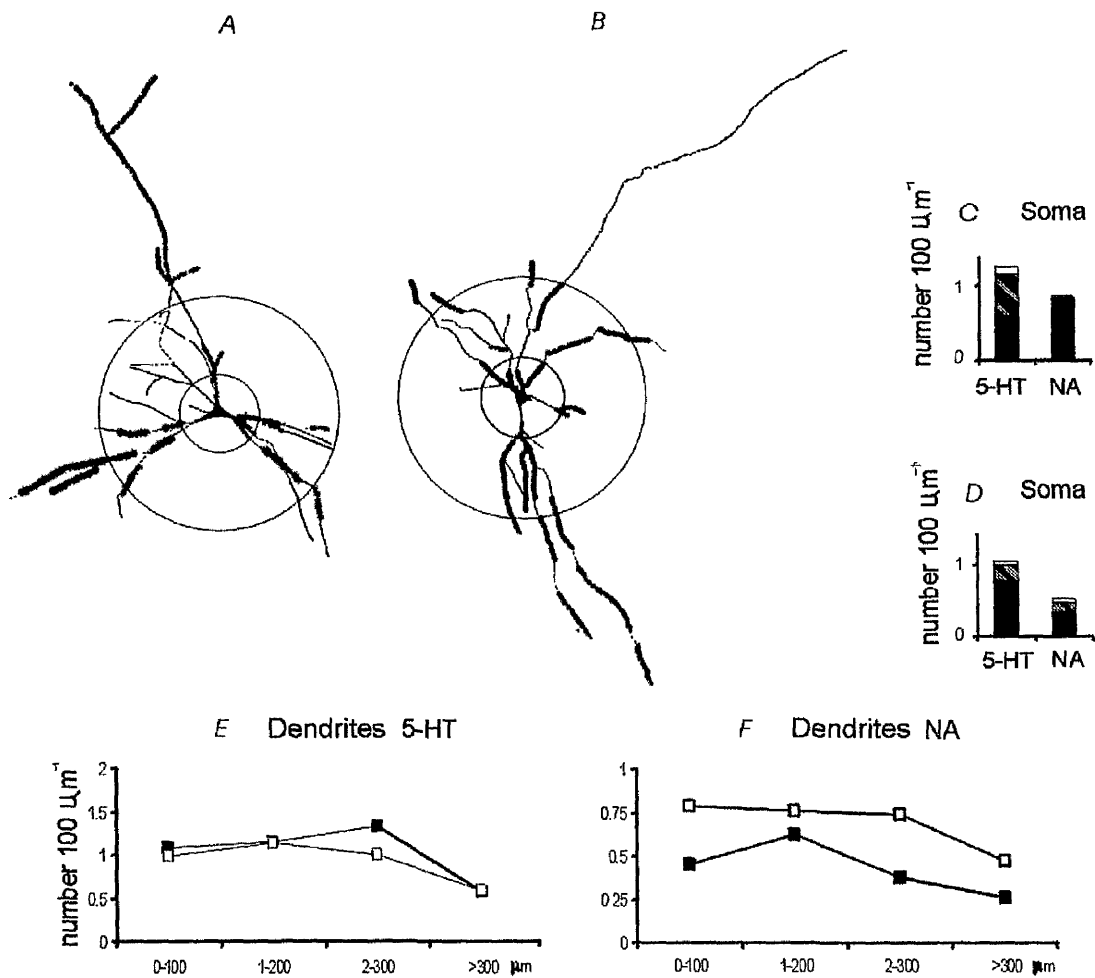


Figure 21. Comparison of the density of appositions of serotonin and DBH immunoreactive fibres with soma and with dendrites at different distances from the somata. A and B. Stick diagrams of the dendritic trees of the neurones illustrated in as contour diagrams in Figure 18 (cells 1 and 2); the segments of dendrites analysed are indicated with black thickened stippling. These were constructed from the original vibratome sections using light microscopy and Neurolucida. The circles indicate 100 and 300 μm distances from the soma. C and D: density of appositions of serotonin and of DBH immunoreactive fibres with the somata of the cells shown in A and B expressed in the number per $100\mu\text{m}^2$. The proportions of varicosities are indicated in the histograms to the right; small (black), medium (cross hatched) and large (white). It can be seen that the relative proportions for both cell are very similar. E and F: packing densities of 5-HT and DBH immunoreactive fibres with distance from the soma shown for cell 1 by black symbols and for cell 2 by grey symbols. See figure 21 for a montage of cell 1 made up of projected confocal images.

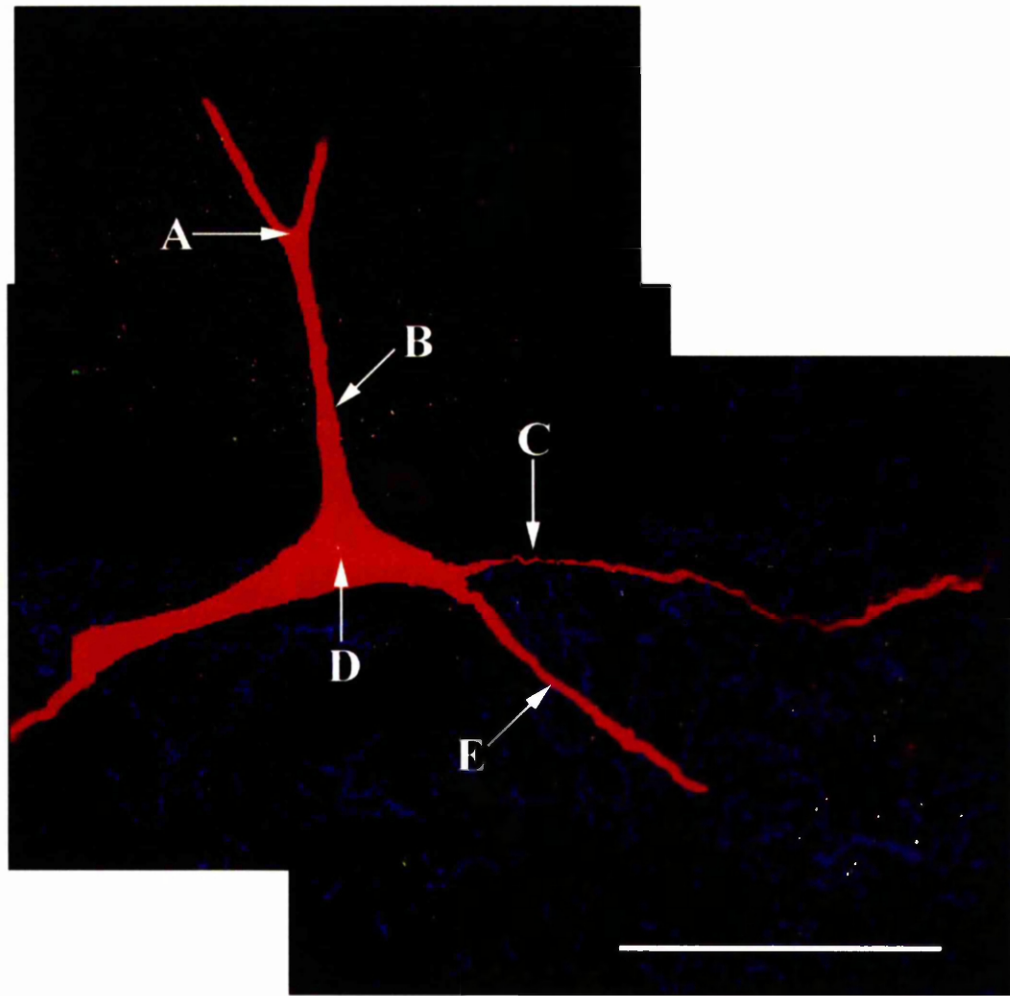


Figure 22. This shows a montage of five pseudocolour projected confocal images depicting γ -motoneurone 1. All structures coloured red are γ -motoneurone, those coloured blue are serotonergic axons and those coloured green are DBH-immunoreactive axons. These axons were not necessarily coloured in every confocal image, which accounts for their absence in some areas of the montage. Arrow A indicates where the large dendrite (B) bifurcates. Arrow C indicates where a thin dendrite undulates along its course toward the left. Arrow D indicates the soma of the γ -motoneurone, and arrow E indicates another slightly thicker dendrite. The scale bar is approximately 150 μ m.

3.4 Varicosities in the surround of dendrites

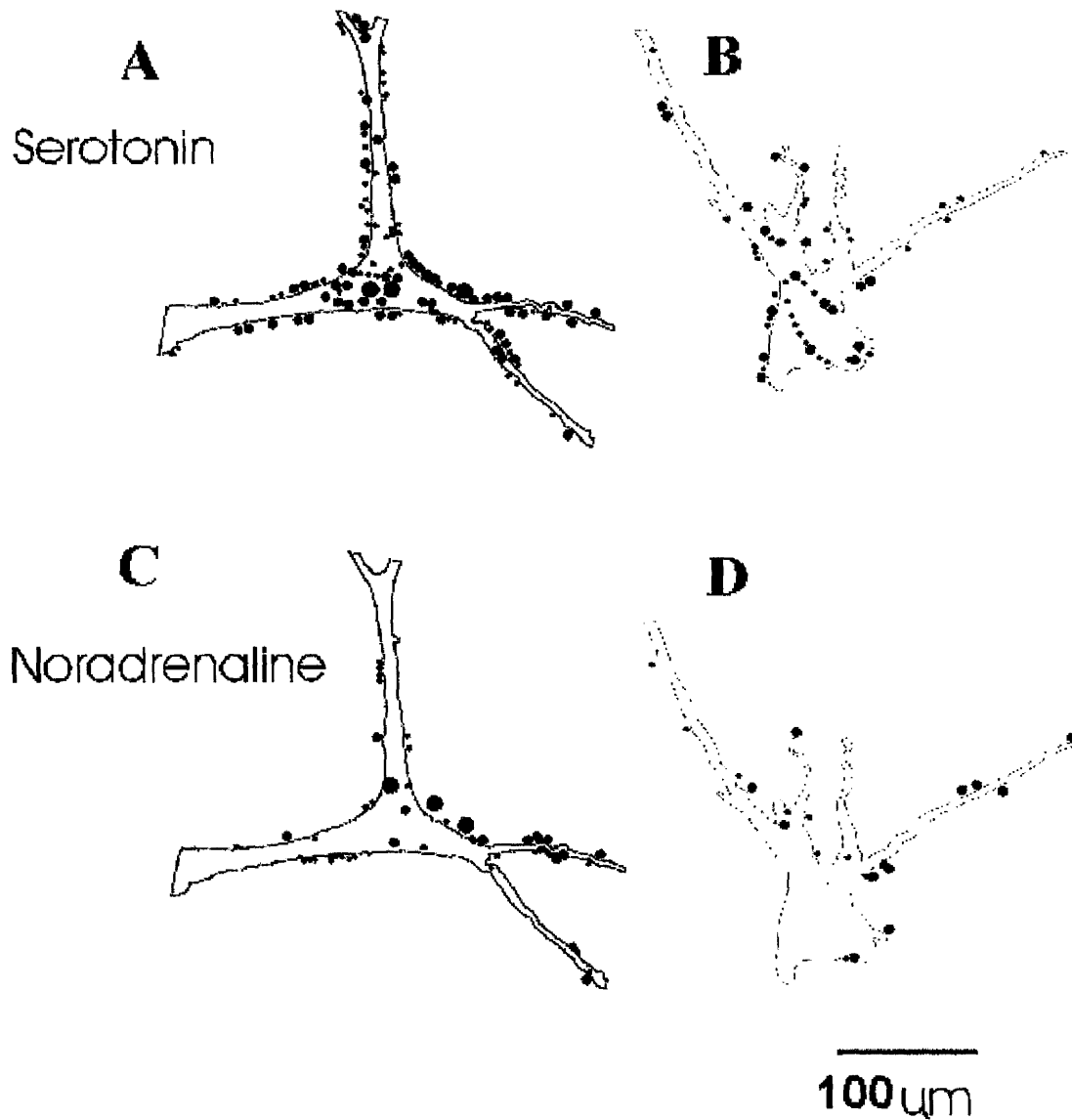


Figure 23 shows the distribution of serotonergic and noradrenergic varicosities in a 5 μm shell around the soma and proximal dendrites of γ-motoneurons 1 and 2. When compared to figure 19 which shows the actual appositions, a quite different distribution can be seen. Also note the density of the varicosities around the two dendrites to the right of cell 1 (A and C) is much less than the density of the appositions, even though the volume of the sector is greater.

It can be seen from figure 23 that many serotonergic and DBH immunoreactive varicosities were present within a few micrometers of the surface of the labelled γ -motoneurons in addition to those apposing the somata and dendrites. In order to determine whether the density of appositions with dendrites merely reflected the density of varicosities in the surrounding area, a comparison was made with the density of varicosities in a $5\mu\text{m}$ wide volume immediately surrounding each dendrite. If the monoaminergic varicosities were distributed evenly, and the axons reached the dendritic surfaces by chance, the numbers on the dendritic surface would reflect the numbers that would have occurred in the space occupied by the dendrites had the axons not been impeded by the dendritic surfaces. For this comparison the numbers of varicosities in apposition with dendrites were expressed in terms of their volume rather than surface area since the dendrites occupy a certain volume whereas the surface area is a two dimensional value. This whole volume could be occupied by a varicosity if the dendrite was not present. In every case, had the varicosities on the surface actually been present in the volume occupied by the dendrites (Figure 26A and B, closed symbols) their density would have been greater than that of varicosities in the immediate surround (open symbols). The densities for the dendrites were increased by a mean factor of 13.8 ± 0.4 for serotonin and 10.6 ± 1.5 for noradrenaline. Factors for individual sections of dendrites are shown in Figure 26C and D. Figure 24A and B also show that the density of serotonergic and noradrenergic varicosities in the immediate surround of the dendrites was similar in the three motor nuclei (MG, FDL and LGS, indicated by different symbols). Taking together the volumes of the $5\mu\text{m}$ surround of all the dendrites investigated from all the γ -motoneurons, and the total numbers of serotonergic and DBH immunoreactive varicosities in that space, their densities were estimated to be 798 and 585 mm^{-3} respectively.

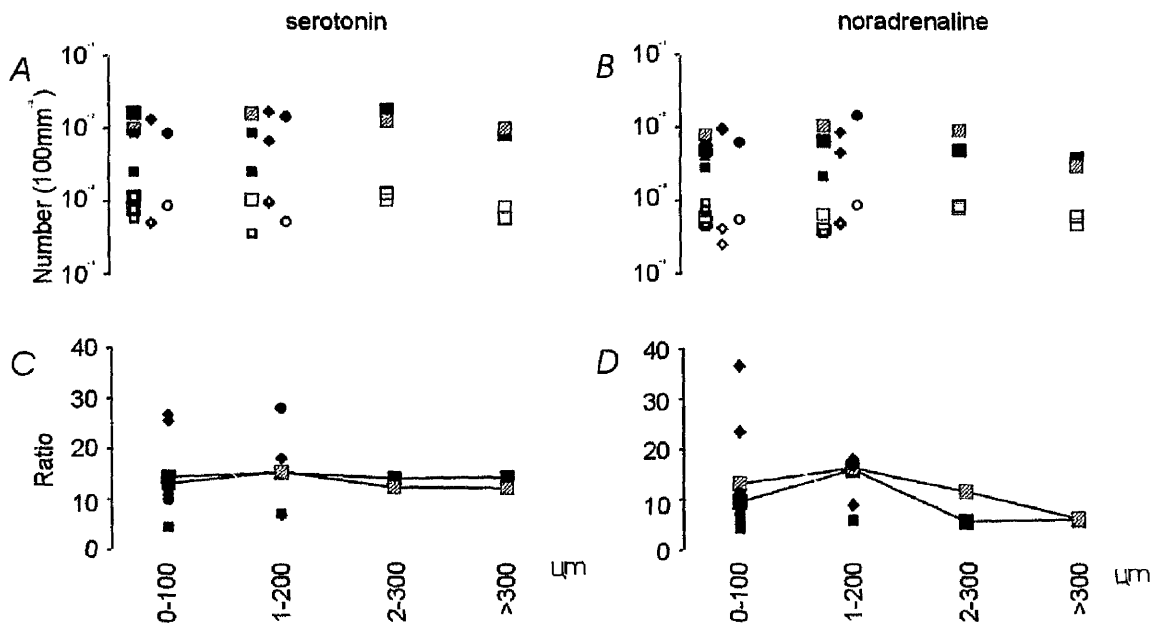


Figure 24. Comparison of the densities of serotonergic and DBH immunoreactive varicosities in the immediate surround of the dendrites and those in apposition with distance from the soma. A and B: open symbols: the density of varicosities in the 5 μ m wide surround of the dendrites; closed symbols: the density of varicosities in apposition expressed as if they were distributed throughout the volume of the dendrite. Squares: MG γ -motoneurones; large black squares: cell 1; large grey squares: cell 2. Diamonds: FDL γ -motoneurones. Circles: LG γ -motoneurone. Note that the density in the surround was always less. C and D: ratios of the densities of varicosities shown in A and B – an indication of the affinity of the dendrites for serotonergic (C) and noradrenergic (D) axons.

3.5 Spines, beads and thread-like processes

Occasionally spines, beads and threadlike processes as described by Ulfhake and Cullheim (1981) were encountered on the dendrites of γ -motoneurones. No appositions were observed with spines or thread-like processes, but both serotonergic and DBH appositions were found on beads.

3.6 The effects of Fentanyl

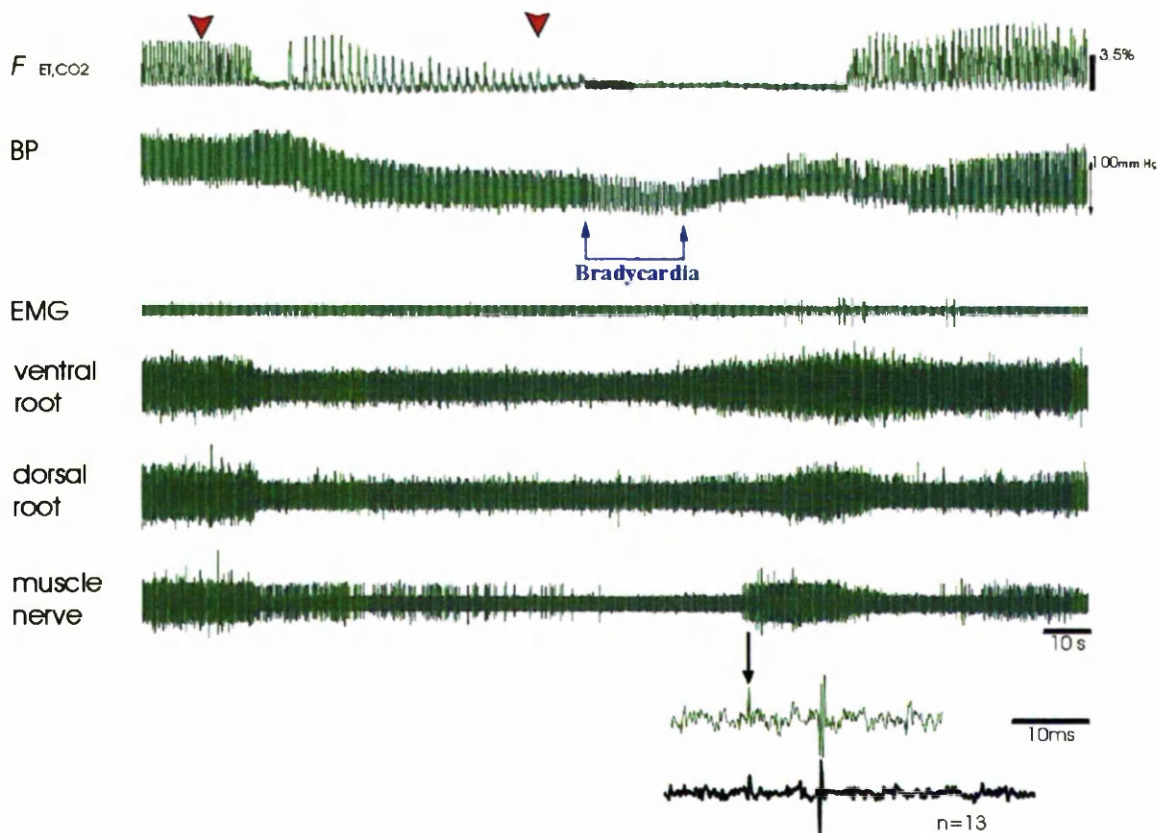


Figure 25 shows the effects of fentanyl upon the end tidal CO₂ (F_{ETCO_2}), the blood pressure (BP), the electromyographic activity of the muscle (EMG) and the neural activity in the ventral root and muscle nerve. The upper traces at the bottom right are expansions of the trace areas indicated by the arrow. It shows two large spikes preceded by a small spike indicated by the arrow. The lower trace (black) is an average of 13 large spikes from this part of the muscle nerve recording. The large spike is preceded by a small spike at constant latency. This is the 'driving' phenomenon and shows that a static γ -motoneurone was responsible for these afferent responses (see text for further explanation).

In figure 25, the first dose of fentanyl was administered ($30-90\mu\text{g kg}^{-1}$ intravenously) at the point indicated by the first arrowhead. After 12 seconds, the fractional end tidal carbon dioxide (F_{ETCO_2}) abruptly fell, indicating the cessation of respiration. This was accompanied by a marked decrease in the frequency of the action potentials in the ventral, dorsal and muscle nerve. The blood pressure (BP) also gradually fell. After about 20 seconds the respiratory effort began again albeit at a reduced rate. A second dose of fentanyl was therefore administered at the time indicated by the

second arrowhead. The respiration therefore ceased about 10 seconds after this. Approximately 20 seconds after fentanyl administration, a sudden increase can be seen in the electrical activity of the ventral and dorsal roots, in the muscle nerve and increased EMG activity. This reached a maximum in both the ventral roots and the muscle nerve until the ventilator was started some 50 seconds after the second fentanyl dose. This caused a fall in the discharge in all the neural records. The BP remained at a low level until the ventilator was started and after 30 seconds it had returned to normal levels. Closer inspection of activity in the muscle nerve revealed two sizes of spike with the initial deflection of the smaller spikes in the opposite direction to that of the larger spikes. This indicates the action potentials were crossing the electrode from different directions. The large spikes were identified as afferent because they could be elicited by stretching the muscle slip. Sometimes the small spikes were followed by large spikes with a fixed latency. The spike indicated by the arrow shows such an instance. The lowest trace in the diagram is an average, triggering on thirteen of these small spikes. The fixed latency indicates that this spike originated in a static γ -axon because the afferents are being 'driven' by the efferent. The driving effect arises because some static γ -axons innervate chain fibres, which have fast twitch contractions. The twitches briefly extend the primary sensory ending, each extension eliciting an afferent spike. This record is representative of results obtained in 49 rats on administration of fentanyl (see also Gladden *et al.* 2000).

3

3.7 The effects of reflexes on blood pressure, ventral and dorsal root and muscle nerve activity

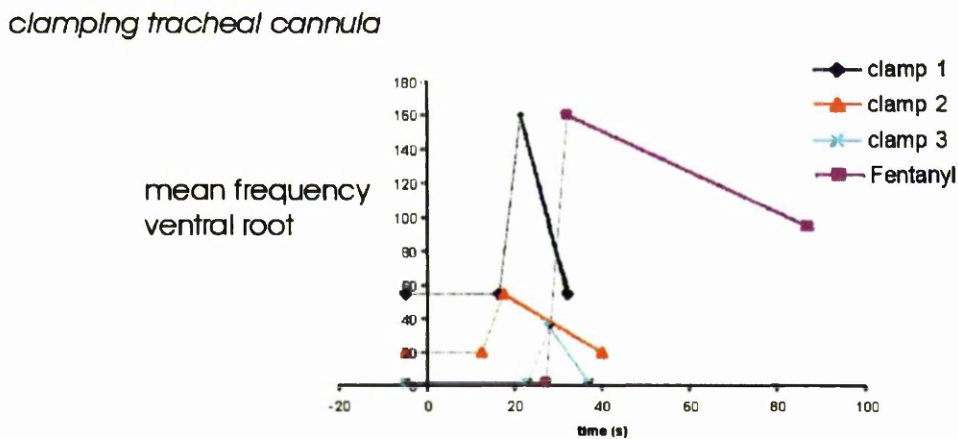
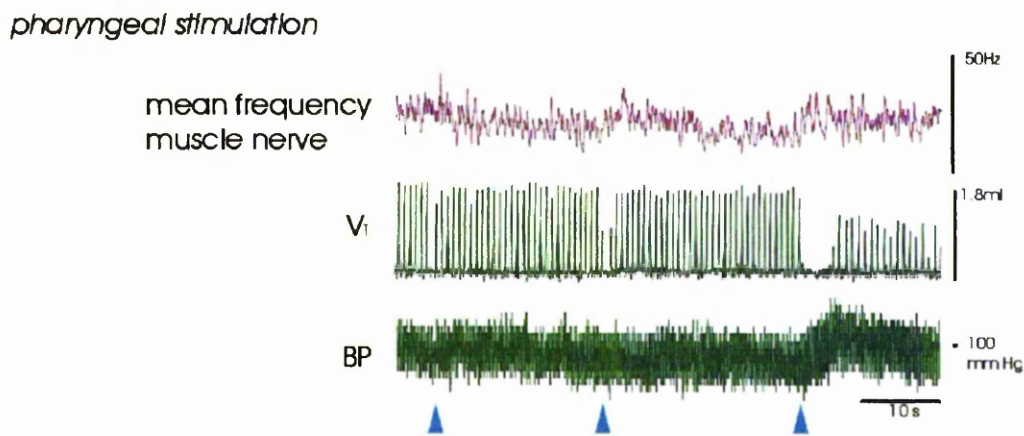
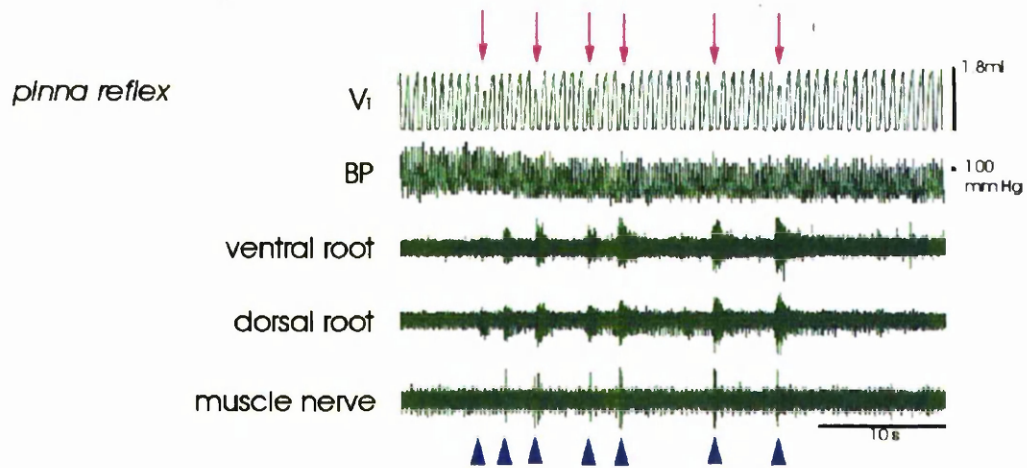


Figure 26. Traces taken from a typical experiment. See below for a full explanation.

3.7.1 The Pinna Reflex

The classical pinna reflex (Sherrington 1917; Granit *et al.* 1952) could be easily elicited in the urethane anaesthetised rats before they were given fentanyl (figure 26). When a plastic probe was gently rubbed against the walls of the auditory meatus (purple arrowheads), the rats displayed a rapid to and fro rolling of the head as if shaking a foreign body from the ear even though they were quite deeply anaesthetised. An increase in activity could be recorded from the ventral and dorsal roots and muscle nerves which coincided with the head shaking. It can be seen that there is a small but persistent decrease in BP during this reflex and also transient dips in the tidal volume (V_T).

3.7.2 The Pharyngeal Reflex

A blunt glass probe was slipped into the pharynx of the rat via its mouth to stimulate the pharyngeal wall (Figure 26, blue arrowheads). In contrast to the pinna reflex, there were very small and variable responses recorded in the ventral root, but there was a definite pause in the breathing cycle (Figure 26, pink arrows). Changes in BP were not always recorded. In the instance shown in figure 26, there is a definite rise in BP toward the end of the trace.

3.7.3 Clamping the Tracheal Cannula

The graph in figure 26 shows the mean frequency of spikes in the ventral root in response to clamping the tracheal cannula and thus arresting the normal breathing cycle. This was performed three times before administering fentanyl, each time allowing a five-minute recovery period between clamping. It can be seen that each successive test began at a lower mean frequency of spontaneous discharge, indicating deterioration in the physiological state of the animal. In each test the clamp was applied at time zero on the graph. Before the first clamping (black trace, diamond symbols) the spontaneous discharge was approximately 56Hz. After a latency of 18 seconds the mean discharge rate increased to 160Hz over about 2-3 seconds. At this

point the clamp was released and the firing rate rapidly decreased. Before the second clamping (orange trace, triangular symbols) the spontaneous discharge rate had already fallen to 20Hz. After a shorter latency (12-13 seconds) there was a small rise to only 55Hz over 5 seconds. The frequency immediately fell to the same value as before the clamping but after five minutes there was no spontaneous discharge. After clamping the trachea for the third time there was a response after approximately 22 seconds. The frequency rose to 39Hz over some 8 seconds but there was no spontaneous discharge after a further 7-8 seconds. However, after the administration of fentanyl ($30-90\mu\text{g kg}^{-1}$ intravenously) at time zero on the graph, and an apnoea lasting for 28 seconds, there was a large increase in discharge rate (up to 160Hz) over approximately 3-4 seconds. Although there was a decrease in discharge rate after the ventilator was started at 32 seconds, it remained at a higher value than before any intervention with the animals respiration.

3.8 The effects of apnoea on ventral and dorsal root and muscle nerve activity

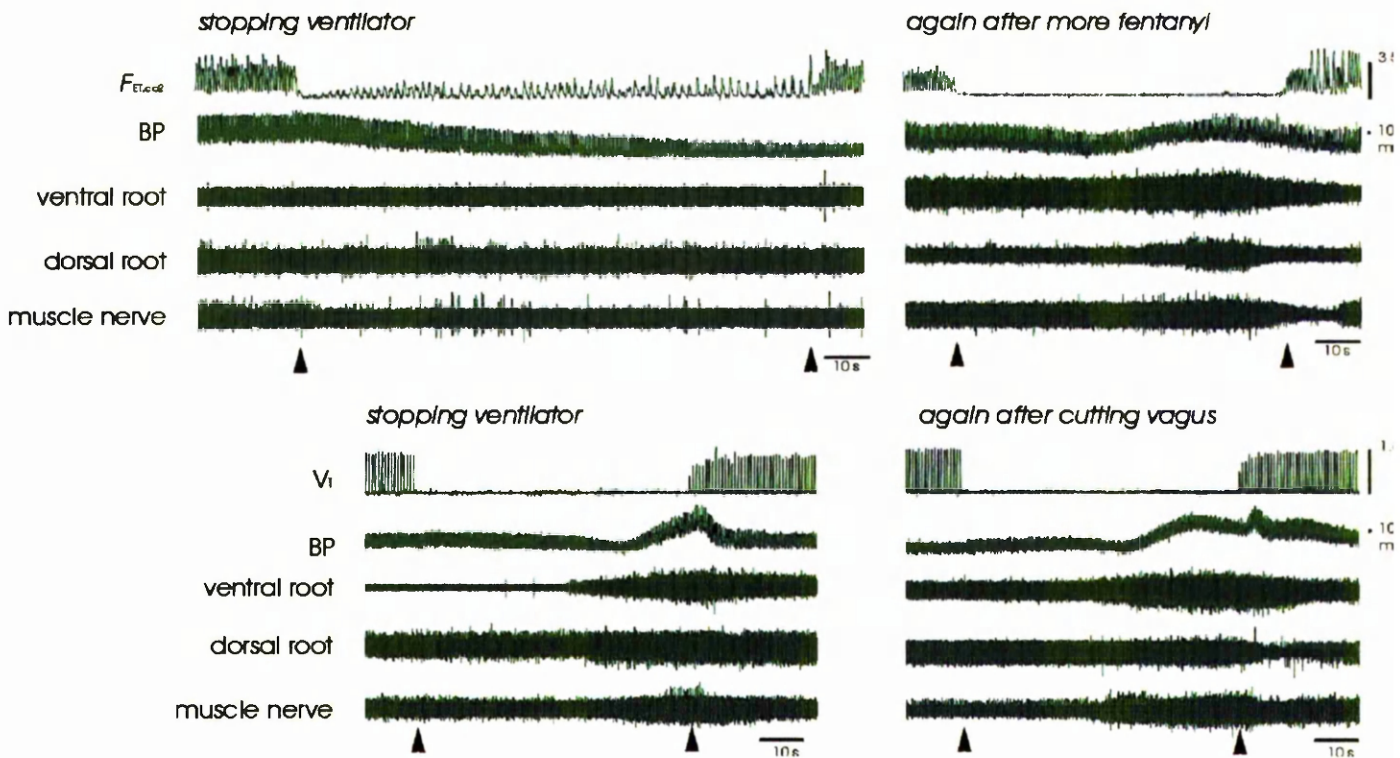


Figure 27. Apnoea seems necessary for the surge of γ -motoneurone activity. For description see text below.

Figure 27 shows the effects of apnoea after the administration of fentanyl (30-90 μ g/100g). The top left panel shows the effects when a dose of fentanyl was insufficient to cause complete apnoea. After the ventilator was stopped (starting and stopping of ventilator is indicated by the black arrowheads), a feeble respiratory effort is still present which does increase slightly. There is little change in activity in the ventral and dorsal roots or in the muscle nerve, and the BP steadily decreases throughout this period i.e., there was no neural or cardiovascular response although the rat's respiration must have been insufficient for its metabolic requirements. The rat was then given more fentanyl and after a recovery period of a few minutes the ventilator was again stopped. The effects of the apnoea are shown in the top right panel. After the ventilator was turned off, there was the usual response to apnoea - following a

period of about 30 seconds there was a surge of activity in the all three neural records and a rise in BP. When the ventilator was restarted, this activity falls back to normal levels and the BP returned to normal levels. This demonstrated that the surges in neural activity and rise in blood pressure after stopping the ventilator were not due to the development of hypoxia or hypercapnoea. This point was confirmed by administering various gas mixtures (see Methods, section 2.8.10) while continuing respiratory movements with the ventilator. In all cases tested ($n = 5$), administration of hypoxic, hypercapnoeic or hypoxic and hypercapnoeic gas mixtures failed to induce any increase in neural activity comparable to changes seen after the cessation of respiratory movements (Gladden and Sahal, 2000). It was therefore presumed that the cessation of the rhythmic input from stretch receptors could have triggered the neural response.

The bottom left panel in figure 27 shows the effects of stopping the ventilator after administration of fentanyl on tidal volume (V_T), BP, ventral and dorsal root and muscle nerve with an intact vagus. When tested again after the vagus had been bilaterally cut ($n = 3$) it can be seen there is little difference (bottom right panel). This indicates that the response is not mediated by the *lung* stretch receptors.

4 DISCUSSION

4.1 Appositions and synaptic contacts

This work does not claim that the all monoaminergic varicosities judged to be apposed to γ -motoneurons were synaptic contacts. Careful and time consuming electron microscopic studies of appositions with the γ -motoneurone would be required to verify a true synapse. However, the suggestion that there is a serotonergic and noradrenergic innervation of γ -motoneurons is strongly supported by analysis of their distribution. Observations in agreement with some selective innervation of γ -motoneurons by serotonergic and noradrenergic axons are as follows.

1. The appositions were unevenly distributed. Clustering of appositions of both types was evident especially on proximal dendrites. However this clustering did not necessarily mirror the density of varicosities in the immediate vicinity of the γ -motoneurone. When these data were mapped on the contour diagram of the cells, the pattern of distribution was quite different (figures 18 and 23). On more distal dendrites, the uneven distribution of varicosities was less obvious to the eye. However, this distribution was indicated by large variations in the density of appositions on different segments of dendrites, even though the average densities remained fairly constant with increasing radial distance from the soma (Fig.21E & F).
2. The distribution of appositions of different sizes changed with distance from the soma. There were very few medium sized, and no large varicosities in apposition with distal dendrites, although larger appositions *were* present in the surrounding areas.
3. The most compelling evidence was obtained when comparing the densities of appositions with the density of varicosities in the immediate surround of the dendrite. If the varicosities judged to be on the surface of the dendrites were distributed throughout the volume occupied by the dendrites, they would be considerably more

densely packed than varicosities found in a 5 μ m wide shell around the dendrites. It was estimated that the density would be 14 times greater on average for serotonergic varicosities, and 11 times for noradrenergic varicosities. This suggests that the dendrites of γ -motoneurons were being preferentially targeted by monoaminergic axons. It was important to make the comparison with the density of varicosities in the immediate surround of the dendrites since axons coursing through this space have potential access to the surface of the γ -motoneurone. Furthermore, had a comparison been made with the density of varicosities in a randomly chosen cube of ventral horn, the cellular content of the cube would have been unknown. For example, had this cube contained the soma of a large α -motoneurone, the density of varicosities would have been severely underestimated.

4. Evidence for selective innervation of γ -motoneurons by monoaminergic axons does not, however, rule out the possibility that the physiological effects of the monoamines may occur by volume transmission as well as synaptically. However it does suggest that the monoaminergic systems have more precise control of γ -motoneurons than would be possible with volume transmission alone.

4.2 Comparison of the density and distribution of serotonergic and noradrenergic varicosities

4.2.1 Somata

The ratio of densities of serotonergic to noradrenergic varicosities in apposition to the somata of the different γ -motoneurons studied was very variable (from 1:1 to 17:1. For values of densities see Table 4). In the immediate surround of the somata this ratio showed an even greater variation. A proportion of this variation may be explained by sampling problems since all areas of the somata could not be accessed. However there may be *actual* differences. For the two cells with the most fully explored surfaces, the density of DBH immunoreactive appositions was 68% and 36% of the density of serotonergic immunoreactive appositions, but the corresponding percentages in the immediate surround were 48% and 19%. These wide variations in the proportions of serotonergic and

noradrenergic appositions may reflect functional differences seen in records from individual γ -motoneurons. When the effects of locally applied noradrenaline were tested on γ -motoneurons (Jankowska *et al.* 1998), the effects on background spikes were variable, although noradrenaline depressed transmission from group II afferents to all γ -motoneurons tested. It should also be remembered that the γ -motoneurons in this study could be static or dynamic – tests to identify the functional types could not be carried out because it was necessary for the animals to be paralysed for intracellular recording. However it is likely that most of the studied γ -motoneurons were static because the proportion of dynamic γ -motoneurons is usually less than 30%, but even the static category are probably not functionally homogeneous (see Dickson *et al.* 1993; Taylor *et al.* 1998).

4.2.2 Dendrites

The overall lower density of DBH immunoreactive varicosities compared with serotonergic immunoreactive varicosities followed a similar pattern in all the motor nuclei studied. The density of noradrenergic axons in motor nuclei was generally found to be lower than of serotonergic fibres although in some nuclei it has been reported to be similar (Zhan *et al.* 1989). In the 5 μ m wide shell around the dendrites, the density of DBH immunoreactive varicosities was 66% of the density of the serotonergic immunoreactive varicosities. However, the overall percentage for appositions with the dendrites was lower (56%). The mean densities of monoaminergic appositions calculated for the whole sample of γ -motoneurons fell with radial distance from the somata (Table 4). Nevertheless, there was a trend in some cells for the densities of serotonergic or DBH immunoreactive appositions to be higher on dendrites between 100 and 200 μ m radially distant from the somata than on proximal dendrites (up to 100 μ m radially from somata) (Figure 21E & F and Table 4). It could be speculated that the monoaminergic appositions would have greater effects if they were strategically placed to modulate transmission in specific pathways. If this were the case, these regional accumulations of varicosities could indicate the location of incoming ‘traffic’. Since serotonin and noradrenaline both modulate the synaptic actions of group II muscle afferents, the location of direct connections of these

afferents on γ -motoneurons (and indirect connections via group II interneurons) may be primarily on the intermediate (100-200 μ m from somata) and distal dendrites of the γ -motoneurons. Thus it is interesting to compare with the distribution of group Ia contacts on α -motoneurons; relatively few contacts were found on or near the somata by Burke & Glenn (1996). It is unlikely that monoaminergic axons make *presynaptic* connections with group II afferents because these axons have not been found to make axo-axonic contacts with fibres that synapse with α -motoneurons (Ulfake *et al.* 1987), nor other types of spinal neurone see Maxwell *et al.* 2000).

Table 5. Comparison of the distribution of contacts between monoaminergic fibres on γ -motoneurons, α -motoneurons and premotor group II interneurons

Fibre	Mean numbers	γ -motoneurons	α -motoneurons	group II premotor interneurons
5-HT	Soma total number	18.7 (31.6**)	52	6.2
	Soma $100 \mu\text{m}^{-2}$	1.12 ± 0.111	0.27-1.12*	0.130
	Dendrites (<500 μm) $100 \mu\text{m}^{-2}$	0.97 ± 0.084	0.81 ± 0.25	0.29 ± 0.05
	Proximal dendrites $100\mu\text{m}^{-1}$	14.5	no data	3.1
	Intermediate dendrites $100\mu\text{m}^{-1}$	11.3	no data	4.0
	Distal dendrites $100\mu\text{m}^{-1}$	4.8	no data	3.8
NA	Soma total number	9.4 (21.7**)	no data	2.0
	Soma $100 \mu\text{m}^{-2}$	0.59	no data	0.052
	Dendrites (<500 μm) $100 \mu\text{m}^{-2}$	0.6 ± 0.01	no data	0.082 ± 0.03
	Proximal dendrites $100\mu\text{m}^{-1}$	9.2	no data	0.87
	Intermediate dendrites $100\mu\text{m}^{-1}$	7.6	no data	1.05
	Distal dendrites $100\mu\text{m}^{-1}$	2.3	no data	0.81

Table 5 shows the comparison of the distribution of appositions between monoaminergic fibres on γ -motoneurons, α - motoneurons (Alvarez *et al.* 1998) and premotor group II interneurons (Maxwell *et al.* 2000). The values denoted by an asterisk were obtained by relating the mean number of appositions per soma (52 per cell) found by Alvarez *et al.* (1998) to the mean surface area of 19113 and 4657 μm^2 , calculated for extremes of mean soma diameters (78 and 38.5 μm) of α -motoneurons according to Burke *et al.* (1977) Values for γ -motoneurons denoted by two asterisks were obtained by scaling the actual observed numbers by the ratio between explored area and the calculated total area of the soma.

4.3 Comparison of distribution and density of contacts of serotonergic fibres on α - and γ - motoneurones

Electron microscopic analysis of contacts of serotonergic immunoreactive varicosities on α -motoneurone have been demonstrated in several studies (Takeuchi *et al.* 1983; Ulfhake *et al.* 1987; Holtman *et al.* 1990; Alvarez *et al.* 1998). The distribution over both the soma and dendrites of α -motoneurones was investigated systematically (Alvarez *et al.* 1998). It is interesting, therefore, to compare the results of this study with those of Alvarez *et al.* (1998). However, they counted the total number of the apparent serotonergic contacts with the somata of α -motoneurones by light microscopy and not by confocal microscopy as in this study. In order to accommodate the data derived by different approaches, it was necessary to make some assumptions (see Table 5). Nevertheless the mean density and the number of serotonergic varicosities found in apposition to the somata of γ -motoneurones, whether actual or estimated, fall within the values published by Alvarez *et al.* (1998). They noted a wide variation in the numbers of varicosities contacting the somata – their range was 11-211. The packing density of appositions with dendrites of γ -motoneurones (about $1/100\mu\text{m}^2$) is also within their range of values (see Table 5).

It is interesting that Alvarez *et al.* (1998) estimated the number of serotonergic contacts with α -motoneurones to be in excess of the number of synapses by Ia afferents. Serotonin has facilitatory effects on α -motoneurones. The particular importance of the serotonergic input to α -motoneurones is indicated by the fact that the ability of α -motoneurones to generate plateau potentials depends on continued activity in the serotonergic pathway from the midbrain (Hounsgaard *et al.* 1988). Although serotonin has a facilitatory effect on γ -motoneurones, there have been no reports of plateau potentials in them.

4.4 Comparison with noradrenergic contacts on α -motoneurones

Synaptic contacts formed by noradrenergic fibres on presumed γ -motoneurones have been identified in some motor nuclei using electron microscopy (Holstege & Bongers 1991; Rajoafetra *et al.* 1992), but there has not been a systematic analysis of their distribution. It is therefore impossible to make any comparisons of the distribution of noradrenergic contacts on γ -motoneurones as presented in this thesis with published data for α -motoneurones since these data do not exist. All that can be said is that noradrenergic fibres appear to make appositions with both somata and dendrites in both types of neurone. However, Rosin *et al.* (1996) reported α_{2C} -adrenergic receptor-like immunoreactivity in the ventral horn at all spinal levels in rats, and stressed that the labelling was restricted to a fraction of large motoneurones. It may be possible to demonstrate more significant structural correlates of the different effects of noradrenaline on the responsiveness of α - and γ -motoneurones once the various receptor subtypes can be localised more reliably.

4.5 Possible explanation for the richer monoaminergic innervation of γ -motoneurones compared with premotor interneurones with input from group II afferents

The last column of Table 5 shows data for premotor interneurones (Maxwell *et al.* 2000). These interneurones are likely to be interposed in pathways from group II muscle spindle afferents to both α - and γ -motoneurones. The actions of the monoamines on these interneurones are similar to their actions on γ -motoneurones. As with γ -motoneurones, noradrenaline powerfully depressed transmission from group II muscle spindle afferents to these interneurones. However, serotonin *depressed* transmission in about half of those studied and facilitated it in the rest (Jankowska *et al.* 2000). Table 5 shows that there are some common features in the coupling of monoaminergic fibres with these interneurones and with γ -motoneurones. For example they both share a higher density of serotonergic appositions than noradrenergic appositions, and a greater number of these appositions are upon the dendrites than upon the somata. However, the density of serotonergic and noradrenergic appositions is strikingly less on somata and dendrites than on γ -motoneurones or indeed α -motoneurones. These intermediate zone interneurones are, nevertheless more richly innervated by the serotonergic and noradrenergic axons than

some types of dorsal horn interneurons which have scarcely any monoaminergic contacts (Stewart & Maxwell, 1999).

The premotor interneurons are smaller cells with less extensive dendritic trees than γ -motoneurons, and far less than those of α -motoneurons. However, this difference in scale cannot explain the markedly lower density of appositions upon them. Nonetheless, it could be an indication of fewer interaction sites along their dendrites. It could also be related to their input. In anaesthetised preparations, group II interneurons respond readily to muscle stretch but have hardly any resting discharges (in contrast to non-anaesthetised decerebrate preparations, see Shefchyk *et al.* 1990). On the other hand very deep anaesthetic levels are required to silence all γ -motoneurons, and they are likely to be activated by a greater number of descending systems. A larger number of contacts between the modulatory noradrenaline and serotonin releasing neurones and γ -motoneurons may thus be needed to adjust the rate of their discharge.

4.6 Is fusimotion contributing to integrated responses?

In man, γ -motoneurons become excited in arousal and stress (see Ribot-Ciscar *et al.* 2000) and in these situations activation of the serotonergic projection to the motor nuclei from the raphe nuclei is expected. The increased γ -activity recorded in these conditions may in fact originate from the raphe nuclei that lie in the medulla (the raphe, pallidus and obscurus nuclei). If this is correct the increased fusimotor activity would be part of an integrated alerting response which includes lowering the threshold for activating α -motoneurons, autonomic changes and analgesia (see Lovick, 1997). The role of the fusimotor activity would be to increase the input to the spinal cord and into control centres from muscle spindle afferents. This should have a priming effect, increasing the readiness for action.

The pinna reflex elicited in the anaesthetised cat is thought of as a γ -reflex *par excellence*, but this work has shown autonomic and respiratory effects in addition (see results figure 26). The pinna reflex is likely to be an 'alerting' response to the

presence of foreign bodies in the auditory canal - which is a prime site for allowing parasite entry, or for obstructions to hearing which is a vital monitor for changes in the environment. However it is not known whether serotonergic pathways are involved in the pinna reflex. By contrast to the pinna reflex, it was found that mechanical stimulation of the pharynx only slightly excited γ -motoneurons although it caused apnoea. The much smaller involvement of γ -motoneurons is appropriate in this reflex which is regarded as co-ordinating the defence against aspiration of solids and liquids into the lungs, and is implicated in diving responses. (see de Bugh Daly, 1998). Cold or mechanical stimulation of the face or stimulation of the pharynx by the sudden aspiration of cold water causes the cessation of respiratory efforts, thus minimising the risk of any further aspiration of water.

Taken together, these observations do suggest that the fusimotor system can act as a co-ordinating link between somatic and autonomic responses.

4.7 Opiate-induced rigidity

This phenomenon was investigated because noradrenaline has opposite effects on α - and γ -motoneurons (Jankowska *et al.* 1998). Opiates strongly inhibit the noradrenergic cells of the locus coeruleus (Guyenet, 1980). Since noradrenaline has a *facilitatory* action on α -motoneurons, the effect of inhibiting the noradrenergic cells would be to disfacilitate the α -motoneurons. Although α -motoneurons could not have been *directly* excited when opiates were applied to the locus coeruleus, Lui *et al.* (1989) nevertheless showed that the application caused rigidity. Could α -motoneurons be excited indirectly by removing the inhibitory effects of noradrenaline on γ -motoneurons? If γ -motoneurons thus became excited the increased spindle feedback would excite the α -motoneurons.

This work has shown that the administration of the potent opiate fentanyl caused a remarkable surge in γ -activity within a minute of the onset of apnoea. The γ -activity

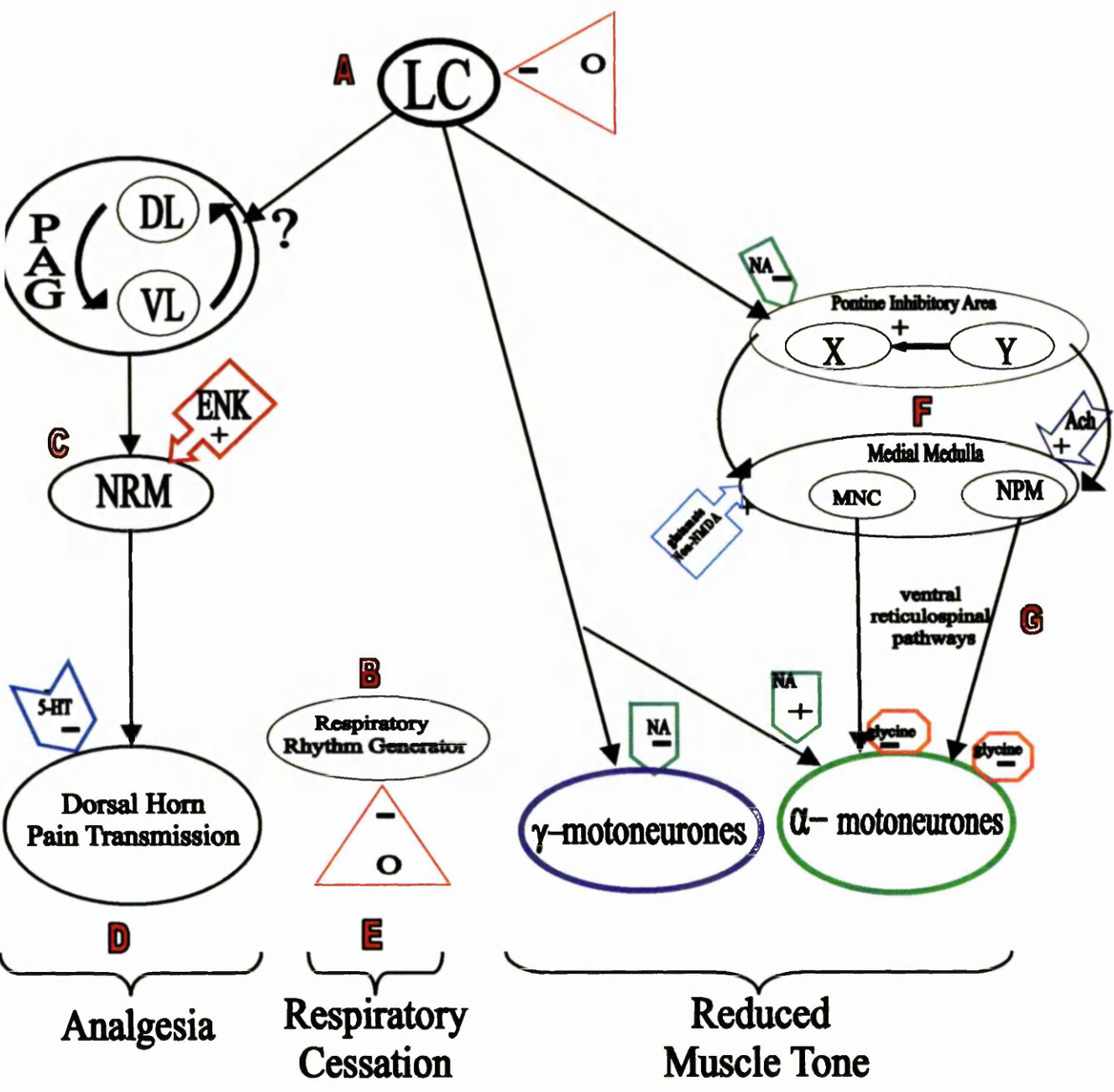
excited muscle spindle afferents. The preparations used were already deeply anaesthetised with urethane before the opiate was given. In these preparations there was sometimes no α -motoneurone activity detectable at all and in other preparations any α -activity occurred later than the large surge in γ -activity (see figure 27). It is therefore proposed that α -activity in opiate rigidity occurs secondarily to the γ -excitation of muscle spindle afferents - that is, opiate-induced rigidity is a γ -rigidity (see 1.23 and figure 10). However, since this is a controversial claim, it would be an advantage to obtain further supportive evidence concerning the state of the γ -motoneurones. For future studies, the sucrose gap technique (see Roberts and Wallis, 1978), applied to a caudal ventral root in the rat, could be used to monitor the EPSPs in a population of α -motoneurones. This would provide a much more sensitive monitor of the excitation of α -motoneurones than recording EMG activity. The activity of the γ -motoneurones could be monitored contralaterally by recording from the corresponding muscle nerve.

4.8 Parallels between the sequence of events after the onset of apnoea in opiate anaesthesia and the defence reaction

In figure 27 it was shown that although clamping the trachea excites γ -motoneurones in an anaesthetised preparation, repeated clamping decreased the response and increased its latency. After administration of the opiate, however, stopping respiration elicited a much more impressive and robust response - it could be repeated many times so long as circulating opiate levels were maintained. At the same time as the surge in γ -activity, there was an increase in blood pressure and a marked exophthalmia. There appears to be a parallel between this response modulation and the final struggle of an animal trying to escape the jaws of a predator, firmly closed around its throat. Similarly animals sometimes 'play dead' and hold their breath in order to escape detection by a predator. Respiratory movements are eventually made to avoid asphyxiation. At this point the animal must either flee or fight its assailant.

Endogenous opiates are involved in this response. The behavioural responses are known to be mediated by a switch between two areas of the periaqueductal grey matter in the midbrain, the ventrolateral and dorsolateral areas (see Introduction for references). The initial quiescent phase of the sequence (mediated by the ventrolateral area) is paralleled by the fall in neural activity, blood pressure and a bradycardia after stopping respiration in the opiate-mediated state. The struggle, fight or flight (mediated by the dorsolateral area) is paralleled by the increased neural activity, raised blood pressure and exophthalmia. It is proposed that the mechanisms responsible for the defence reaction are the same as those leading to opiate-induced rigidity.

Figure 28 shows the suggested mechanism for the initial phase of the opiate response after the onset of apnoea. In this figure, the well known pathway for the suppression of the transmission of pain pathways (on the left) is brought together with Siegal's (2000) proposed pathway for the reduction of muscle tone in REM sleep involving the locus coeruleus (on the right).



LC= Locus coeruleus
PAG= Periaqueductal grey (DL=dorsolateral area, VL=ventrolateral area)
NRM= Nucleus raphe magnus
X= Dorsal part of nucleus pontis centralis oralis and subcoeruleus
Y=pedunculopontine tegmental nucleus and laterodorsal tegmental nucleus
NMC= Nucleus magnocellularis
NPM= Paramedian reticular nucleus
NA=Noradrenaline
5-HT= Serotonin
O = Opioids
 Figure 28.

4.8.1 The switch from quiescence to activity

When the response to apnoea in opiate anaesthesia was first recorded, it was assumed that the switch to an increased neural output and the increase in blood pressure was initiated by hypoxia. However these effects could not be triggered by hypoxia when ventilatory movements continued. The lung stretch receptors are an obvious source of information regarding respiratory movements. However the neural response and increase in blood pressure following apnoea, continued after vagotomy (Results figure 27). It is not known, at present, how the switch is triggered, although it may be suggested that it is mediated by the prolonged cessation of rhythmic activity of the respiratory and abdominal muscles.

4.9 Possible pathways involved in the excitation of γ -motoneurones in opiate-induced rigidity

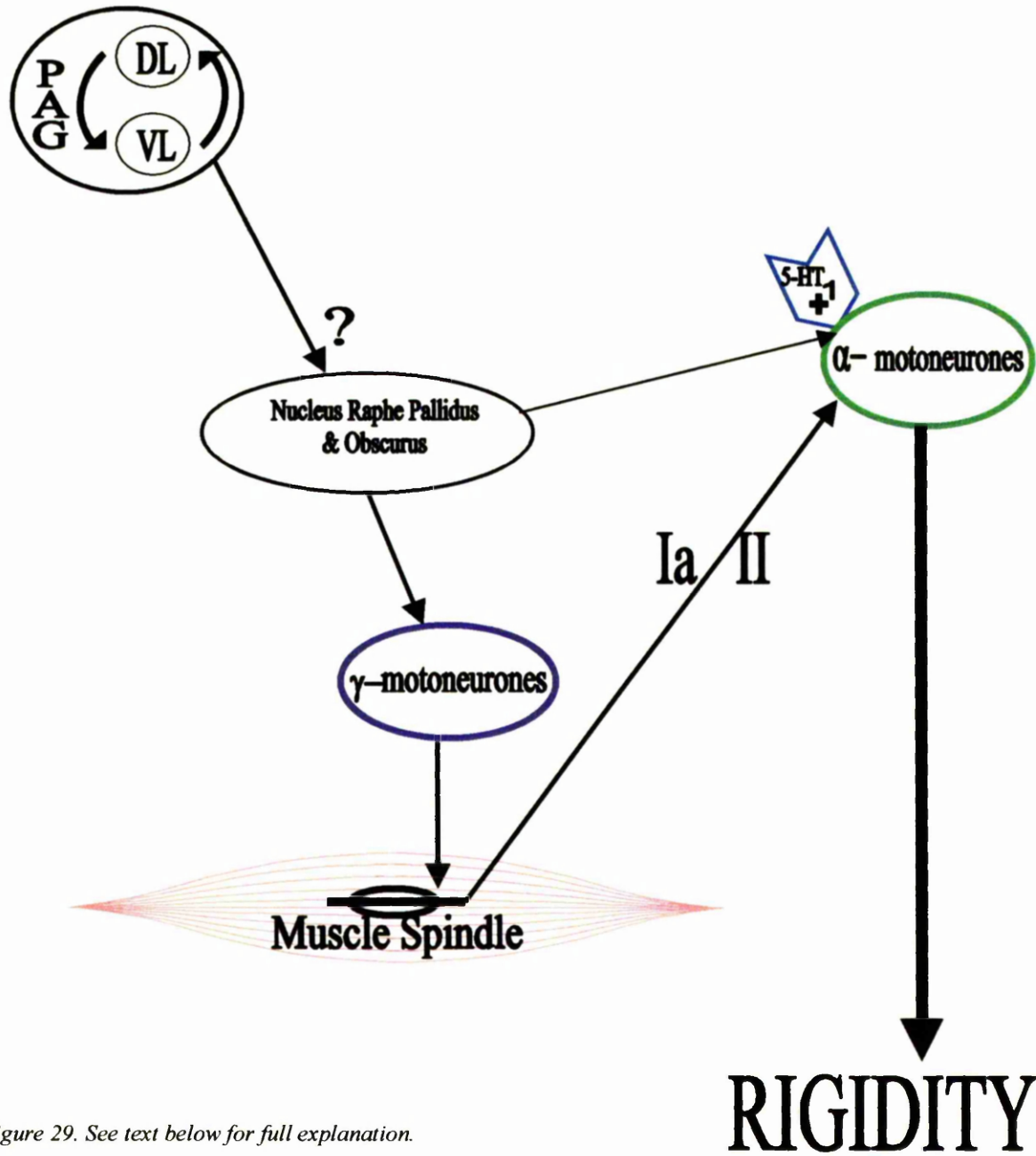


Figure 29. See text below for full explanation.

It is proposed that the surge in γ -activity, occurring after a lag in apnoea when opiates are present, is initiated by a switch in activity from the ventrolateral area in the periaqueductal grey (responsible for quiescence in the defence reaction) to the dorsolateral area which coordinates physiological responses required for fight or flight. There does not appear to be evidence in the literature that the raphe nuclei (pallidus and obscurus) are activated from the dorsolateral region of PAG. However, opiate-induced rigidity does not occur if serotonin antagonists are administered (Widdowson *et al.* 1986; Blasco *et al.* 1986; Weinger *et al.* 1991). It therefore seems likely that the raphe nuclei *are* involved. The serotonergic excitation of γ -motoneurons will excite the muscle spindle afferents which in turn will excite the α -motoneurons, leading to muscle rigidity. Serotonin also has a direct facilitatory effect on the α -motoneurons via their 5-HT₁ receptors although this is insufficient to excite them. The proposed pathway is shown diagrammatically in figure 29. The inhibitory effects of noradrenaline on the γ -motoneurons will be removed by the strong inhibition of the noradrenergic cells of the locus coeruleus by the opiates.

In summary it is proposed that modulation of γ -activity by monoamines is responsible for opiate-induced rigidity. Increased serotonin release has a facilitatory action on γ -motoneurons and there is also disinhibition of noradrenergic pathways. The facilitatory effect of serotonin is not only acting on excitatory pathways to γ -motoneurons from group II afferents but also by excitation of α -motoneurons by group Ia afferents.

5 References

- Ahlman H, Grilner S and Udo M. (1971). The effect of 5-HTP on the static fusimotor activity of an extensor muscle. *Brain Research* **27**, 393-396.
- Aldrich MS. (1990). Narcolepsy. *New England Journal of Medicine* **323**, 389-394.
- Alvarez FJ, Pearson JC, Harrington D, Dewey D, Torbeck L & Fyffe RE. (1998). Distribution of 5-hydroxytryptamine-immunoreactive boutons on alpha-motoneurons in the lumbar spinal cord of adult cats. *Journal of Comparative Neurology* **393**, 69-83.
- Anden NE, Lundberg A, Rosengren E & Vyklicky L. (1963). The effects of DOPA on spinal reflexes from the FRA. *Experientia* **19**, 654-655.
- Anden NE, Jukes MG & Lundberg A. (1964). Spinal reflexes and monoamine liberation. *Nature* **202**, 1222-1223.
- Anden, N.E., Jukes, M.G. & Lundberg, A., (1966a). The effect of DOPA on the spinal cord. A Pharmacological analysis. *Acta Physiol Scand* **67**, 387-397.
- Anden NE, Jukes MG, Lundberg A & Vyklicky L. (1966b). The effects of DOPA on the spinal cord. 1. Influence on transmission from primary afferents. *Acta Scandia* **67**, 373-386.
- Aston-Jones G, Ennis M, Pierbone VA, Nickell WT and Shipley MT. (1986). The Brain Nucleus Locus Coeruleus: Restricted Afferent Control of a Broad Efferent Network. *Science* **234**, 734-737.
- Aston-Jones G & Bloom FE. (1981). Activity of norepinephrine-containing locus coeruleus neurones in behaving rats anticipates fluctuations in the sleep-waking cycle. *Journal of Neuroscience* **1**, 876-886.
- Barbeau H & Rossignol S.(1991). Initiation and modulation of the locomotor pattern in adult chronic spinal cats by noradrenergic, serotonergic and dopaminergic drugs. *Brain Research* **546**, 250-260.

- Barker D, Emont-Denand F, Laporte Y, Proske U and Stacey MJ. (1973). *J. Physiol. (London)* **230**, 405-427.
- Basbaum AI, Clanton CH, and Fields HL. (1976). Opiate-and stimulus-produced analgesia: functional anatomy of medullospinal pathway. *Proc. Natl. Acad. Sci. USA* **73**, 4685-4688.
- Basbaum AI. Fields HL (1979). The origin of descending pathways in the dorsolateral funiculus of the spinal cord of the cat and rat: Further studies on the anatomy of pain modulation. *Journal of Comparative Neurology*. **187(3)** 513-531.
- Bennett DJ, De Serres SJ & Stein RB. (1996). Regulation of soleus muscle spindle sensitivity in decerebrate and spinal cats during postural and locomotor activities. *Journal of Physiology* **495**, 835-850.
- Benthuysen JL, Smith NT, Sandford TJ, Head N & Dec-Silver H. (1986). Physiology of Alfentanil-induced Rigidity. *Anesthesiology* **64**, 440-446.
- Bergmans J & Grillner S. (1968). Changes in dynamic sensitivity of primary endings of muscle spindle afferents induced by DOPA. *Acta Physiologica Scandinavica* **74**, 629-36.
- Blasco, T.A., Lee,D., Amalric, M., Swerlow,N.R., Smith, N.T. & Koob, G.F. (1986). The role of the nucleus raphe pontis and the caudate nucleus in alfentanil rigidity in the rat. *Brain Research*, **386 (1-2)** 280-286.
- Bowker RM, Reddy VK, Fung SJ, Chan JYH & Barnes CD. (1987). Serotonergic and non-serotonergic raphe neurons projecting to the feline lumbar and cervical spinal cord: a quantitative horseradish peroxidase-immunocytochemical study. *Neuroscience Letters* **75**, 31-37.
- Boyd IA. Trends in Neuroscience. Special Issue: The Control of Movement Vol. 3 no. **11**, 1980 [29].
- Brodal A, Walberg F and Taber E. (1960). The raphe nuclei of the brain stem in the cat. III. Afferent connections. *J. Comp. Neurol.* **114**, 261-279.

- Bunin MA & Wightman RM. (1998). Quantitative evaluation of 5-hydroxytryptamine (serotonin) neuronal release and uptake: an investigation of extrasynaptic transmission. *Journal of Neuroscience* **18**, 4854-4860.
- Bunin MA, Prioleau C, Mailman RB, Wightman RM. (1998). Release and uptake rates of 5-hydroxytryptamine in the dorsal raphe and substantia nigra reticulata of the rat brain. *Journal of Neurochemistry* **70** (3), 1077-1087.
- Burke, R.E., Strick, P.L., Kanda, K., Kim, C.C. & Walmesley, B. (1977). Anatomy of medial gastrocnemius and soleus motor nuclei in cat spinal cord. *Journal of Neurophysiology*, **40**, 667-680.
- Burke RE & Glenn LL. (1996). Horseradish peroxidase study of the spacial and electrotonic distribution of group Ia synapses on type-identified ankle extensor motoneurons in the cat. *Journal of Comparative Neurology* **372**, 465-485.
- Carlsson A, Falck B, Fuxe K, Hokfelt T. (1966). Histochemical and biochemical effects of diethyldithiocarbamate on tissues catecholamine. *J.Pharm. Pharmacol* **18**, 60-62.
- Carr PA, Noga BR, Nance DM & Jordan LM. (1994). Intracellular labelling of cat spinal cord neurons using a tetramethylrhodamine-dextran amine conjugate. *Brain Research Bulletin* **34**, 447-451.
- Clark FM & Proudfit HK. (1991). The projection of locus coeruleus neurons to the spinal cord in the rat determined by anterograde tracing combined with immunocytochemistry. *Brain Research* **538**, 231-245.
- Chazal G, Ralston HJ III (1987). Serotonin-containing structures in the nucleus raphe dorsalis of the cat: An ultrastructural analysis of dendrites, presynaptic dendrites, and axon terminals. *Journal of Comparative Neurology*. **259**(3) 317-329.
- Coates EL, Li A & Nattie EE. (1993). Widespread sites of brain stem ventilatory chemoreceptors. *Journal of Applied Physiology* **75**, 5-17.
- Commissiong JW, Hellstrom SO and Neff NH. (1978). A New Projection from the Locus Coeruleus to the Spinal Ventral Columns: Histochemical and Biochemical Evidence. *Brain Research*, **148**, 207-213.

- Conway BA, Hultborn H, Kiehn O & Mintz I. (1988). Plateau potentials in alpha-motoneurons induced by intravenous injection of L-DOPA and clonidine in the spinal cat. *Journal of Physiology* **405**, 369-384.
- Cordo P, Inglis JT, Vershueren S, Collins JJ, Merfeld DM, Rosenblum S, Buckley S & Moss F. (1996). Noise in human muscle spindles. *Nature* **383**, 769-770.
- Dalström A and Fuxe K. (1964). Evidence for the existence of monoamine-containing neurons in the central nervous system. I: Demonstration in the cell bodies of the brainstem neurons. *Acta Physiol. Scand* **62**, (suppl. 232) 1-55.
- Daly M de B. (1998). Physiological and pathophysiological modifications of cardiorespiratory control in mammals. *Journal of Physiology* **509P**, 20s.
- Destombes J, Horcholelle-Bossavit G, Thiesson D and Jami L. (1992). Alpha and Gamma Motoneurons in the Peroneal Nuclei of the Cat Spinal Cord: An Ultrastructural Study. *J. Comp. Neurology* **317**, 79-90.
- Dickson M, Emonet-Dénand F, Gladden MH, Petit J & Ward J. (1993). Incidence of non-driving excitation of Ia afferents using ramp frequency stimulation of static γ -axons in cat hindlimbs. *Journal of Physiology* **460**, 657-673.
- Duggan AW, Morton CR, Johnson SM, Zhao ZQ, (1984). Opioid antagonists and spinal reflexes in the anaesthetized cat. *Brain Research*. **297(1)** 33-40.
- Eccles RM & Lundberg A. (1959). Synaptic actions in motoneurons by afferents which may evoke the flexion reflex. *Archives Italiennes de Biologie* **97**, 199-221.
- Elam M, Yao T, Thorén P & Svensson TH. (1981). Hypercapnia and hypoxia: chemoreceptor-mediated control of the locus coeruleus neurons and splanchnic, sympathetic nerves. *Brain Research* **222**, 373-381.
- Ellaway PH & Trott JR. (1975). The Mode of Action of 5-Hydroxytryptophan in Facilitating a Stretch Reflex in the Spinal Cat. *Experimental Brain Research* **22**, 145-162.

- Foote SL, Bloom FE & Aston-Jones G. (1983). Nucleus locus coeruleus: new evidence of the anatomical and physiological specificity. *Physiological Reviews* **63**, 844-914.
- Fuxe K & Agnati LF. (1991). Two principal modes of electrochemical communication in the brain: volume versus wiring transmission. *In Volume transmission in the brain: novel mechanisms for neural transmission*, ed. Fuxe K & Agnati LF, pp 1-9. Raven Press, New York.
- Gladden, M.H., Jankowska, E. & Czarkowska-Bauch, J. (1998). New observations on coupling between group II muscle afferents and feline γ -motoneurons. *J. Physiol.* **512.2** 507-520.
- Gladden, M.H. & Sahal, A. (2000). Gamma motoneurons, asphyxia and opiates. *J. Physiol.* **531.P**, 144P.
- Gladden, M.H., Sahal, A. & Matsuzaki, H. (2000). Responses of γ -motoneurons to apnoea. *J. Physiol.* **531.P**, 144P.
- Giroux N, Rossignol S & Reader TA. (1999). Autoradiographic study of alpha1- and alpha2-noradrenergic and serotonin1A receptors in the spinal cord of normal and chronically transected cats. *J. Comp. Neurol.* **406**, 402-414.
- Granit R, Job C & Kaada BR. (1952). Activation of Muscle Spindles in Pinna Reflex. *Acta phys.Scandinav.* **27**, 163-168.
- Grillner S, Hongo T and Lundberg A. (1967). The effect of DOPA on the spinal cord. Reflex activation of static gamma-motoneurons from the flexor reflex afferents. *Acta Physiologica Scandinavica Suppl.* **70**, 403-411.
- Grillner S. (1969). Supraspinal and segmental control of static and dynamic gamma-motoneurons in the cat. *Acta Physiologica Scandinavica Suppl* **327**, 1-34.
- Guyenet G.G. (1980). The coeruleospinal noradrenergic neurons: Anatomical and electrophysiological studies in the rat. *Brain Research* **189**, 121-133.
- Holstege JC & Bongers CM. (1991). Ultrastructural aspects of the coeruleo-spinal projection. *Progress in Brain Research* **88**, 143-156.

- Holtman JR Jr, Vascik DS & Maley BE. (1990). Ultrastructural evidence for serotonin-immunoreactive terminals contacting phrenic motoneurons in the cat. *Experimental Neurology* **109**, 269-272.
- Hornby PJ, Rossiter CD, White RL, Norman WP, Kuhn DH & Gillis RA. (1990). Medullary raphe: A new site for vagally mediated stimulation of gastric motility in cats. *American Journal of Physiology - Gastrointestinal & Liver Physiology* **258** (4 21-4), 637-647.
- Houngaard J, Hultborn H, Jespersen B & Kiehn O. (1984). Intrinsic membrane properties causing a bistable behaviour of alpha-motoneurons. *Experimental Brain Research* **55**(2), 391-394.
- Houngaard J, Hultborn H, Jespersen B & Kien O. (1988). Bistability of α -motoneurons in the decerebrate cat and in the acute spinal cat after intravenous 5-hydroxytryptophan. *Journal of Physiology* **405**, 345-367.
- Hultborn H, Wigstrom H & Wängberg B. (1975). Prolonged activation of soleus motoneurons following a conditioning train in soleus Ia afferents-a case for a reverberating loop? *Neuroscience Letters* **1**, 147-152.
- Jacobs BL & Azmitia EC. (1992). Structure and function of the brain serotonin system. *Physiological Reviews* **72**, 165-229.
- Jacobs BL, Gannon PJ & Azamitia EC. (1984). Atlas of serotonergic cell bodies in the cat brainstem: an immunocytochemical analysis. *Brain Res. Bull.* **13:1**, 1-31.
- Jacobs BL, Fornal CA. (1993). 5-HT and motor control: A hypothesis. *Trends in Neurosciences* **16**(9), 346-352.
- Jankowska E, Hammar I, Djouhri L, Heden C, Szabo-Lackberg Z & Yin XK. (1997a). Modulation of responses of four types of feline ascending tract neurons by serotonin and noradrenaline. *European Journal of Neuroscience* **9**, 1375-1387.
- Jankowska E, Hammar Simonsberg I & Chojnicka B. (1998). Modulation of information forwarded to feline cerebellum by monoamines. *Annals of New York Academy of Sciences* **860**, 106-109.

- Jankowska E, Gladden MH & Czarkowska-Bauch J. (1998). Modulation of responses of feline gamma motoneurons by noradrenaline, tizanidine and clonidine. *Journal of Physiology* **512**, 521-531.
- Jankowska E, Hammar I, Chojnicka B & Hedén CH. (2000). Effects of monoamines on interneurons in four spinal reflex pathways from group I and/or group II muscle afferents. *European Journal of Neuroscience* **12**, 701-714.
- Jankowska E. (2001). Spinal interneuronal systems: identification, multifunctional character and reconfigurations in mammals. *Journal of Physiology* **553.1**, 31-40.
- Jurna I & Lundberg A. (1966). The influence of an inhibitor of dopamine-beta-hydroxylase on the effect of dopa on transmission in the spinal cord. *In Fourth international meeting of neurobiologists*, ed. Editor00469-472. Pergamon Press, Oxford & New York, Place.
- Kausz M. (1986). Distribution of neurones in the lateral pontine tegmentum projecting to thoracic, lumbar and sacral spinal segments in the cat. *J. Hirnforsch* **5**, 485-493.
- Kausz M. (1991). Arrangement of neurons in the medullary reticular formation and raphe nuclei projecting to thoracic, lumbar and sacral segments of the spinal cord in the cat. *Anat. and Embryol.* **183**, 151-163.
- Kilduff TS & Peyron C. (2000). The hypocretin/orexin ligand-receptor system: implications for sleep and sleep disorders. *Trends in Neuroscience* **23**, 359-365.
- Kiss JP, & Vizi ES. (2001). Nitric Oxide: a novel link between synaptic and nonsynaptic transmission. *Trends in Neuroscience* **24 (4)**, 211-215.
- Krowicki ZK & Hornby PJ. (1995). Pancreatic polypeptide, microinjected into the dorsal vagal complex, potentiates glucose-stimulated insulin secretion in the rat. *Regulatory Peptides* **60(2-3)**, 185-192.
- Kupfermann I. (1979). Modulatory actions of neurotransmitters. *Annu. Rev. Neurosci.* **2**, 447-465.

- Lovick TA. (1997). The medullary raphe: a system for integration and gain control in autonomic and somatomotor responsiveness? *Experimental Physiology* **82**, 31-41.
- Lui P-W, Tsen L-Y, Fu M-J, Yeh C-P, Lee T-Y, Chan SHH, (1995). Inhibition by intrathecal prazosin but not yohimbine of fentanyl-induced muscular rigidity in the rat. *Neuroscience Letters*. **201(2)** 167-170.
- Lui P-W, Lee TY & Chan HH. (1989). Involvement of locus coeruleus and noradrenergic neurotransmission in fentanyl-induced muscular rigidity in the rat. *Neuroscience Letters* **96**, 114-119.
- Lui P-W, Lee TY & Chan HH. (1990). Involvement of coeruleospinal noradrenergic pathway in fentanyl-induced muscular rigidity in rats. *Neuroscience Letters* **108**, 183-188.
- Maeda T, Arai R & Kitahama K. (1989a). Extrinsic and Intrinsic Aminergic Inputs to Noradrenaline Neurones in the Locus Coeruleus of the Rat: an Electron microscope study by Monoamine Oxidase Enzyme Histochemistry. *Biomed. Res.* **10** (Suppl. 3), 259-268.
- Maeda T, Kojima Y, Arai R, Fujimiya M, Kimura H, Kitahama K and Geffard M. (1991). Monoaminergic Interaction in the Central Nervous System: A Morphological Analysis in the Locus Coeruleus of the Rat. *Biochem. Physiol.* **Vol. 98C** No.1, 193-202.
- Engberg, I. & Marshall, K.C. (1971). Mechanism of noradrenaline hyperpolarization in spinal cord motoneurons of the cat. *Acta Physiol Scand* **83**, 142-144.
- Maxwell DJ, Riddell JS & Jankowska E. (2000). Serotonergic and noradrenergic axonal contacts associated with premotor interneurons in spinal pathways from group II muscle afferents. *European Journal of Neurosciences* (in press).
- Millhorn DE. (1986). Stimulation of raphe (obscurus) nucleus causes long-term potentiation of phrenic nerve activity in cat. *Journal of Physiology* **381**, 169-179.
- Moschovikas AK, Burke RE and Fyffe REW. (1991). The Size and Dendritic Structure of HRP-Labeled Gamma Motoneurons in the Cat Spinal Cord. *J. Comp. Neurology* **311**, 531-545.

- Neguss SS, Pasternak GW, Koob GF & Weinger MB. (1993) Antagonistic effects of betafunaltrexamine and naloxonazine on alfentanil-induced antinociception and muscle rigidity in the rat. *J. Pharmacol. Exp. Ther.* **264**, 739-745.
- Oliveras J-L, Redjemi F, Guildbaud G & Besson JM. (1975). Analgesia induced by electrical stimulation of the inferior centralis nucleus of the raphe in the cat. *Pain* **563**, 139-145.
- O'Connor JJ, Kruk ZL. (1992). Pharmacological characteristics of 5-hydroxytryptamine autoreceptors in rat brain slices incorporating the dorsal raphe or the suprachiasmatic nucleus. *British Journal of Pharmacology* **106(3)**, 524-532.
- Oyamada Y, Ballantyne D, Mückenhoff K & Scheid P. (1998). Respiratory-modulated membrane potential and chemosensitivity of the locus coeruleus in the *in vitro* brainstem-spinal cord of the neonatal rat. *J. Physiol.* **513.2**, 381-398.
- Parent A, Desscarries L and Beaudet A. (1981). Organization of ascending serotonergic systems in the adult rat brain. A radioautographic study after intraventricular administration of [³H] 5-HT. *Neuroscience* **6**, 115-138.
- Pasternak GW. (1993) Pharmacological mechanisms of opioid analgesics. *Clinical Neuropharmacology* **1**, 1-18.
- Pazos A & Palacios JM. (1985). Quantitative autoradiographic mapping of the serotonin receptors in the rat brain. I. Serotonin-1 receptors. *Brain Research* **346**, 205-230.
- Pazos A, Cortes R & Palacios JM. (1985). Quantitative autoradiographic mapping of serotonin receptors in the rat brain. II. Serotonin-2 receptors. *Brain Research* **346**, 231-249.
- Pompeiano, O. (1995). Noradrenergic locus coeruleus influences on posture and vestibulospinal reflexes. In: *Alpha and Gamma Motor Systems*. Ed. A. Taylor, M.H. Gladden & R Durbaba. Plenum Press, New York.
- Rajaofetra N, Ridet J-L, Poulat P, Marlier L, Sandillon F, Geffard M and Privat A. (1992). Immunocytochemical mapping of noradrenergic projections to the rat spinal cord with an antiserum against noradrenaline. *J. Neurocytology* **21**, 481-494.

- Ribot-Ciscar E, Rossi-Durand C & Roll J-P. (2000). Increased muscle spindle sensitivity to movement during reinforcement manoeuvres in relaxed human subjects. *Journal of Physiology* **523**, 271-282.
- Roberts MHT, Davies M, Girdlestone D, Foster GA. (1988) Effects of 5-hydroxytryptamine agonists and antagonists on the responses of rat spinal motoneurons to raphe obscurus stimulation. *British Journal of Pharmacology* **95(2)**, 437-448.
- Roberts MHT & Wallis DI. (1978). Dorsal and ventral root potentials recorded in vivo by the sucrose-gap method. *Journal of Physiology* **277**, 42P .
- Rosin DL, Talley EM, Lee A, Stornetta RL, Gaylinn BD, Guyenet PG and Lynch KR. (1996). Distribution of α_2 -adrenergic receptor-like immunoreactivity in the rat central nervous system. *Journal of Comparative Neurology* **372**, 135-165.
- Rossignol S, Giroux C, Chau C, Marcoux J, Brustein E & Reader TA. (2001). Pharmacological aids to locomotor training after spinal injury in the cat. *J. Physiol.* **533.1**, 65-74.
- Sahal A, Maxwell DJ, Jankowska E & Gladden MH. (1998). Relationships between noradrenaline and serotonin-immunoreactive axons and gamma-motoneurons. *Journal of Physiology* **509P**, 172P.
- Scanman FL. (1983). Fentanyl-O₂-N₂O rigidity and pulmonary compliance. *Anesth. Analg.* **62**, 232-334.
- Schenberg LC & Lovick TA. (1995). Attenuation of the midbrain-evoked defense reaction by selective stimulation of medullary raphe neurons in rats. *American Journal of Physiology - Regulatory Integrative & Comparative Physiology* **269(638-6)**, 1378-1389.
- Shefchyk S, McCrea D, Kriellaars D, Fortier P & Jordan L. (1990). Activity of interneurons within the L4 spinal segment of the cat during brainstem-evoked fictive locomotion. *Experimental Brain Research* **80**, 290-295.
- Sherrington CS. (1917). The integrative action of the nervous system. New York-London:Yale Univ. Press 1906/1947 – Reflexes elicitable in the cat from the pinna, vibrissae and jaws. *J.Physiol. (Lond.)* **51**, 404-431.

- Siegal JM. (2000). Narcolepsy. *Sci. Am.* **282**, 76-81.
- Shik ML, Severin FV, Orlovsky GN. (1966). Control of walking and running by means of electrical stimulation of the mid-brain. *Biophysics* **11**, 756-765.
- Shiple M, Fu L, Ennis M, Lui W-L & Aston-Jones G. (1996). Dendrites of locus coeruleus neurons extend preferentially into two pericoerulear zones. *J. Comp. Neurol.* **365**, 56-68.
- Simmons RM & Jones DJ. (1988). Binding of [3H]prazosin and [3H]p-aminoclonidine to alpha-adrenoceptor in the rat spinal cord. *Brain Research* **445**, 338-349.
- Skagerberg G, Bjorklund A, Lindvall O & Schmitt RH. (1982). Origin and Termination of the Diencephalospinal Dopamine System in the Rat. *Brain Res. Bull.* **9**, 237-244.
- Stanley TH, Philbin DM, Coggins CH. (1979). Fentanyl-oxygen anaesthesia for coronary artery surgery: Cardiovascular and antidiuretic hormone responses. *Can. Anaesthetic Soc. J.* **26**, 168-172.
- Stewart W & Maxwell DJ. (1999). A population of lamina III/IV neurokinin-1-immunoreactive cells are targeted by serotonin-immunoreactive axons in the rat dorsal horn. *Journal of Physiology* **518.P**, 166P.
- Stone TW. (1995). Neuropharmacology. From *Biochemical and Medicinal Chemistry Series*. Published by W.H.Freeman, Spektrum, Oxford, New York, Heidelberg.
- Swanson, L.W. (1998). Brain Maps: Structure of the Rat Brain. Published by Elsevir Amsterdam, Lausanne, New York, Oxford, Shannon, Singapore, Tokyo.
- Takeuchi Y, Kojima M, Matsuura T & Sano Y. (1983). Serotonergic innervation on the motoneurons in the mammalian brainstem. Light and electron microscopic immunohistochemistry. *Anatomy and Embryology* **167**, 321-333.
- Taylor A, Ellaway PH & Durbaba R. (1998). Physiological signs of the activation of bag₂ and chain intrafusal muscle fibres of gastrocnemius muscle spindles in the cat. *Journal of Neurophysiology* **80**, 130-142.

- Todd AJ & Millar J. (1983). Receptive fields and responses to ionophoretically applied noradrenaline and 5-hydroxytryptamine of units recorded in laminae I-III of the cat dorsal horn. *Brain Research* **288**, 159-167.
- Ulfhake B and Cullheim S. (1981). A Quantitative Light Microscopic Study of the Dendrites Cat Spinal γ -Motoneurons After Intracellular Staining With Horseradish Peroxidase. *J. Comp. Neurology* **202**, 585-596.
- Ulfhake B, Arvidsson U, Cullheim S, Hökfelt T, Brodin E, Verhofstad A & Visser T. (1987). An ultrastructural study of 5-hydroxytryptamine-, thyrotropin-releasing hormone- and substance P-immunoreactive axonal boutons in the motor nucleus of spinal cord segments L7-S1 in the adult cat. *Neuroscience* **23**, 917-929.
- Veasey SC, Fornal CA, Metzler CW, Jacobs BL. (1995). Response of serotonergic caudal raphe neurons in relation to specific motor activities in freely moving cats. *Journal of Neuroscience* **15(7 II)**, 5346-5359.
- Vizi ES. (1980). Modulation of cortical release of acetylcholine by noradrenaline released from nerves arising in the rat locus coeruleus. *Neuroscience* **5**, 2139-2144.
- Weinger, M.B., Smith, N.T. , Blasco, T.A., & Koob, G.F. (1991). Brain sites mediating opiate-induced rigidity in the rat. *Brain Research*, **544(2)**, 181-190.
- Westbury DR. (1982). A Comparison of the Structures of α - and γ - Spinal motoneurons of the Cat. *J. Physiol.* **325**, 79-91.
- Westlund KN, Bowker RM, Ziegler MG and Coulter JD. (1983). Noradrenergic Projections to the Spinal Cord of the Rat. *Brain Research* Vol **263 (1)**, 15-31.
- Widdowson, P.S., Griffiths, E.C. & Slate, P.(1986). The effects of the opioids in the periaqueductal grey region of the rat brain and on hind-limb muscle tone. *Neuropeptides*, **7 (3)** 251-258.
- Wiklund,L., Leger,.L. & Persson M. (1981). Monoamine cell distribution in the cat brainstem: a fluorescence histochemical study with quantification of indolaminergic and locus coeruleus cell groups . *J.Comp. Nerol.* **203**, 613-647.

Williams JT, North RA, Shefner SA, Nishi S & Egan TM. (1984). Membrane properties of rat locus coeruleus neurones. *Neuroscience* **13**, 137-156.

Willis, W.D. (1984). The Raphe-spinal system. In: *Brainstem control of spinal cord function*. Ed. Charles D. Barnes, Academic Press, New York.

Wu M-F, Gulyani SA, Yau E, Mignot E, Phan B, Siegel JM. (1999). Locus coeruleus neurons: Cessation of activity during cataplexy. *Neuroscience* **91**(4), 1389-1399.

Zhan WZ, Ellenberger HH & Feldman, JL. (1989). Monoaminergic and GABAergic terminations in phrenic nucleus of rat identified by immunohistochemical labeling. *Neuroscience* **31**, 105-113.

